STUDIES ON ROBUST MULTIVARIABLE DISTILLATION CONTROL

by

Petter Lundström

A Thesis Submitted for the Degree of

Dr. Ing.

University of Trondheim

The Norwegian Institute of Technology

Trondheim, July 1994

ACKNOWLEDGEMENTS

First of all I want to thank my supervisor Professor Sigurd Skogestad, who has inspired, guided and encouraged me through this work. Sigurd has a remarkable ability to extract the essential parts and bits from sometimes rather chaotic results. He also has a remarkable patience. (It has been a long time Sigurd, and you have helped me a lot.)

I also want to thank Professor Manfred Morari for his supervision during the seven months I spent with his group at Caltech in 1990. It was a great experience and I am indebted to both Manfred and Sigurd for making this stay possible. Chapter 5 of this thesis is a direct result from this stay, and the other chapters are strongly affected of the μ-influence from Manfred and John Doyle.

Thanks also to Zi-Qin Wang for his contributions to chapters 2 and 3 of this thesis.

The number of Ph.D. students at the Chemical Engineering Department in Trondheim has been very high during the years I have spent there. In particular, Sigurd has had a large group of students. This means that there has always been a number of people to discuss research issues with (also late Saturday nights), and occasionally we have had a beer, or two, together. For these discussions (and beers) I want to thank, in particular, Elling W. Jacobsen, Per Christian Lund, Morten Hovd, Knut W. Mathisen, Bernd Wittgens, Eva Sørensen and Erik A. Wolff.

There are also three former Caltech students (presently professors or almost professors) who I want to thank; Jay H. Lee, Francis J. Doyle III and Richard D. Braatz. Jay for guiding me into the Model Predictive Control world, and for his contributions to chapter 5. Frank for inviting me to Joshua Tree National Park and to parties at Newport Beach. Richard for numerous fruitful discussions, both in the US and in Norway during his two visits here. In particular, our discussions concerning chapter 3 of this thesis, has been very useful to me.

I also want to thank Professors John D. Perkins and Geoff W. Barton who introduced me to process modelling, simulation and control, in 1986 when I spent a year at the University of Sydney in Australia. John and Geoff are in a sense responsible for initiating this thesis.

When I left Sweden for Norway, to commence the work with this thesis, I expected a *few* years of hard work. Now, *several* years later, the work is finished. In the process I have not only learned a lot, but also I have become a married man and a father, two results of this Dr. Ing. study that I did not expect when starting off on this trek. So, finally I want to thank Angela for her courage to marry me and carry our son Joakim.

Financial support from the Royal Norwegian Council for Scientific and Industrial Research (NTNF), the Nordic Industry Fund and the Sweden America Foundation is gratefully acknowledged. I also want to thank the Chemical Enginering Department (Institutt for Kjemiteknikk) for financial support in form of employment as "vitenskapelig assistent".

ABSTRACT

Robust Control and Model Predictive Control have been two of the main areas of interest within the process control community during the last decade. This thesis is a study on how these two control concepts may be applied to Distillation Control. A simple distillation model is used as an example process throughout the thesis.

The structured singular value (SSV, μ) framework is used to define and assess robustness in this work. The thesis presents guidelines for how to transform (approximate) a control problem formulated in physical terms into frequency dependent weights defining a problem suitable for μ-analysis and synthesis.

Two different approaches to performance weight selection are presented and studied. The first approach considers direct bounds on important transfer functions, the second approach considers the output response to sinusoidal disturbances, setpoints and noise. Both approaches has their strong sides and it is often fruitful to use both.

Gain and delay uncertainty is commonly used to quantify plant model mismatch in process control. This parametric uncertainty description cannot be directly used in the μ-framework. The thesis presents a thorough study on how to obtain tight approximations of gain and delay uncertainty on linear fractional form, suitable for the μ-framework. Both complex and real perturbations are considered, in combination with both rational and irrational weighting functions. It is shown that a *non-optimistic* and *non-conservative* approximation of the gain and delay uncertainty can be derived, however, from a practical point of view, a less tight approximation is preferred for most applications.

The design of a two degree of freedom controller, for a benchmark problem from the literature, is used to demonstrate how a given control problem may be approximated into a μ-problem, and solved by DK-iteration (μ-synthesis). The obtained controller satisfies all objectives specified in the benchmark, and thereby outperforms several other controllers proposed in the literature.

Model Predictive Control (MPC) provides means to deal with constraints, a very valuable property for process control applications. In the thesis one of the most popular MPC algorithms, Dynamic Matrix Control (DMC), is examined and three inherent limitations with this algorithm are highlighted. The thesis also demonstrates how to modify the DMC algorithm in order to avoid these limitations.

Finally, opportunities and difficulties with 5×5 distillation control is studied, *i.e.* control of levels, pressure and composition by one multivariable controller. The distillation model used in this chapter is much more detailed than what is usual in control studies. Both MPC and μ-methods are applied in the design of the 5×5 controller. It is demonstrated that multivariable interactions can be counteracted with a 5×5 controller, however, the main advantage is constraint handling which requires on-line optimization, as in MPC. It is also shown that weights and D-scales from $\mathcal{H}_\infty/\mu$ controller design yields useful guidelines for robust tuning of an MPC controller.

Contents

1 Introduction **1**
1.1 Distillation Control 1
1.2 Robust Control 2
1.3 Model Predictive Control 3
1.4 Thesis overview 3
References 5

2 Performance Weight Selection for H-infinity and μ-control Methods **9**
2.1 Introduction 10
2.2 Model uncertainty and the structured singular value 13
2.3 Performance weights 15
2.3.1 Performance approach A. Weights on transfer functions (Loop shaping) 17
2.3.2 Performance approach B. Frequency by frequency sinusoidal signals 18
2.3.3 Combining performance weights (going from Approach B to A). 19
2.3.4 Performance approach C. Power signals - Power spectrum weights 21
2.4 Fixed or adjustable weights 22
2.5 Skogestad et al. (1988) example revisited 23
2.5.1 Original problem formulation (Performance approach A) 23
2.5.2 Alternative controller designs (Approach A) 26
2.5.3 Other performance weights (Approach A) 27
2.5.4 Performance approach B 28
2.6 Some comments on μ-synthesis 30
2.7 Conclusions 33
Nomenclature 33
References 34
Appendix 1 36
Appendix 2 38

3 Models of Gain and Delay Uncertainty for the Structured Singular Value Framework **39**
3.1 Introduction 40
3.2 The μ-framework 42

3.3 Uncertainty Models . . . 44
3.3.1 The gain and delay uncertainty set . . . 45
3.3.2 Complex uncertainty, irrational weight . . . 45
3.3.3 Complex uncertainty, rational weight . . . 48
3.3.4 Real uncertainty, irrational weight . . . 51
3.3.5 Real uncertainty, rational weight . . . 53
3.4 Distillation Example . . . 55
3.4.1 Problem definition . . . 55
3.4.2 Analysis . . . 56
3.5 Discussion . . . 56
3.6 Conclusions . . . 58
Nomenclature . . . 58
References . . . 59

4 Two Degree of Freedom Controller Design for an Ill-conditioned Plant Using μ-synthesis 61
4.1 Introduction . . . 62
4.2 CDC problem definition . . . 63
4.2.1 Plant model . . . 63
4.2.2 Design specifications . . . 63
4.3 The μ-framework . . . 65
4.4 Design procedure . . . 67
4.5 Controller design . . . 67
4.5.1 ODF-controller for "original" specifications . . . 68
4.5.2 TDF-controller for "original" specifications . . . 71
4.5.3 Weight selection for CDC specifications . . . 73
4.5.4 TDF-controller for CDC specifications; Alt.1 . . . 77
4.5.5 TDF-controller for CDC specifications; Alt.2 . . . 78
4.6 Discussion . . . 82
4.7 Conclusions . . . 83
References . . . 83

5 Limitations of Dynamic Matrix Control 85
5.1 Introduction . . . 87
5.2 Model Predictive Control . . . 88
5.2.1 Dynamic Matrix Control . . . 88
5.2.2 DMC with general state space model . . . 91
5.2.3 Observer Based Model Predictive Control . . . 92
5.3 Limitations of Dynamic Matrix Control . . . 95
5.3.1 Limitation 1: Good performance may require an excessive number of step response coefficients . . . 95
5.3.2 Avoiding limitation 1 . . . 96
5.3.3 Limitation 2: Poor response for ramp-like disturbances . . . 98

5.3.4 Avoiding limitation 2 . . . 99
5.3.5 Limitation 3: Poor response for interactive MIMO plants . . . 100
5.3.6 Avoiding limitation 3 . . . 104
5.4 Discussion . . . 108
5.5 Conclusions . . . 111
Nomenclature . . . 111
References . . . 113

6 Opportunities and Difficulties with 5×5 Distillation Control 114
6.1 Introduction . . . 115
6.2 5×5 Distillation Model . . . 116
6.3 Controllability analysis . . . 119
6.3.1 Scaling . . . 120
6.3.2 Relative gain array (RGA) . . . 120
6.3.3 RHP-zeros . . . 122
6.3.4 Input saturation . . . 123
6.3.5 Decentralized control . . . 123
6.4 $\mathcal{H}_\infty/\mu$ control . . . 124
6.4.1 Weight selection . . . 124
6.4.2 Setpoint tracking with no uncertainty . . . 128
6.4.3 Including model uncertainty . . . 128
6.4.4 Setpoint tracking with input uncertainty . . . 129
6.4.5 Including disturbances and output uncertainty . . . 130
6.4.6 Final remarks . . . 131
6.5 Model Predictive 5×5 control . . . 131
6.6 Discussion . . . 135
6.7 Conclusions . . . 136
References . . . 136

7 Final Discussion and Conclusions 138
7.1 Discussion . . . 138
7.2 Conclusions . . . 139
7.3 Directions for Future Work . . . 140
7.3.1 Tuning of MPC . . . 140
7.3.2 μ synthesis . . . 140
7.3.3 Implementation of μ-controller . . . 141
7.3.4 5×5 control . . . 141
References . . . 141

Chapter 1

Introduction

Robust Control and Model Predictive Control have been two of the main areas of interest within the process control community during the last decade. In this thesis these two control concepts are applied to Distillation Control.

The thesis consists of this introductory chapter, five self contained chapters each in form of a separate paper, and finally a chapter where the overall conclusions from the work are presented.

The purpose of this introductory chapter is to briefly present each of the three sub-topics of this thesis

- Distillation Control
- Robust Control
- Model Predictive Control

and to present a short overview of each of the chapters.

1.1 Distillation Control

Distillation is used to separate a binary- or multi-component feed stream into two or more product streams with different compositions. It is one of the most common operations in refineries, petrochemical and chemical industries. In refineries crude oil is separated into heavy oil, light oil, gasoline etc., by distillation. In petrochemical and chemical industries distillation is the most common technique used to separate desired products from bi-products and unreacted raw material.

The physical principle for separation in a distillation column is the difference in volatility of the separated components. The separation takes place in a vertical column where heat is added to a reboiler in the bottom and removed from a condenser in the top. A stream of vapor, produced in the reboiler, rises through the column and is forced into contact with a liquid stream, from the condenser, flowing downwards in the column. The volatile (light) components are enriched in the vapor phase and the less

volatile (heavy) components are enriched in the liquid phase. A product stream taken from the top of the column will therefore mainly contain light components, while a stream taken from the bottom will contain heavy components.

Composition control of distillation columns has been studied for several years and by a large number of researchers, *e.g.* Boyd (1946) and Rijnsdorp (1965). Despite this fact there are still sides of this topic to unravel. In their 500 pages long book Buckley, Luyben and Shuta (1985) formulate it like this: "A truly definitive treatment of composition control, even for simple binary distillation, has not yet been published – and the reader will not find one here."

There are many reasons for the large interest in distillation control. From an academic point of view distillation control is an interesting multivariable problem, and from an industrial point of view improved distillation control has a potential to substantially increase profit. The major benefits with improved composition control are:

1. Reduced energy consumption.
2. Increased yield.
3. Higher throughput.

In industry most columns are operated by single input single output (SISO) controllers and usually only one composition is automatically controlled (one-point-control). This leads to waste of valuable products and excessive use of energy. However, automatic control of both compositions may be very difficult to obtain due to strong interaction between top and bottom compositions. Skogestad *et al.* (1988) showed that in particular high purity columns, *i.e.* columns where both top and bottom compositions are very pure, suffer from strong interaction which makes the system very sensitive to inaccuracies in the manipulated variables (input uncertainty). Without a rigorous method for dealing with uncertainty it may be practically impossible to tune a two-point-controller for a system with strong interaction. This may in fact be one of the reasons to why one-point-control is so commonly used.

The development of robust control theory during the last decade provides a rigorous framework to address uncertainty issues. Skogestad (1987) was one of the first to apply these new methods to distillation control. This thesis is to some extent continuing parts of Skogestad's work. The thesis mainly deals with two-point composition control, but in chapter 6 a controller used to control levels, pressure and compositions is considered.

1.2 Robust Control

"Robust Control" is a novel control field, however, robustness has always been of major importance for feedback control, since any control strategy has to be robust in order to become successful.

In this thesis we use the structured singular value (SSV, μ) (Doyle, 1982) to define and assess robustness. Other branches of robust control also exist, but are not considered here. In the μ-framework performance is defined using the $\mathcal{H}_\infty$-norm. This norm

provides a direct generalization of classical SISO Bode-plot design methods to MIMO systems. Historically the $\mathcal{H}_\infty$-norm was introduced because of its ability to deal with non-parametric uncertainty, however, now $\mathcal{H}_\infty$-methods are used also for parametric uncertainty.

This thesis does not contribute to the theoretical development of $\mathcal{H}_\infty/\mu$ methods, but focus on applications of these methods. Brief introductions to the μ-framework are presented in chapters 2,3 and 4 of this thesis, more detailed presentations of μ can be found in articles referred to in these three chapters.

Robust control is one of the most active areas of control research. An overview of the most recent developments within this field is available in the January 1993 number of Automatica, which is a special issue on robust control. This special issue also contains a bibliography on robust control by Dorato *et al.* (1993).

Several books on the topic have also been published the last years (see Dorato *et al.*, 1993). Computer software for robust analysis and design is also readily available through two 'toolboxes' for MATLAB (Balas *et al.*, 1991; Chiang and Safonov, 1992).

1.3 Model Predictive Control

The optimal operating condition for a process is almost always at a limiting constraint. This is true both for distillation columns and for other process. A constraint is a strong non-linearity and can generally not be effectively dealt with using a linear controller. However, a Model Predictive Controller which uses on-line optimization, can deal with constraints.

Model Predictive Control (MPC), or Receding Horizon Control as it is also called, emerged in the process industry in the late seventies, Richalet *et al.* (1978) and Cutler and Ramaker (1979). There are several different variants of MPC, known under names such as Dynamic Matrix Control, Model Algorithmic Control, Model Predictive Heuristic Control etc. The main idea for all of these methods is to optimize a control objective over a moving or receding horizon.

While robust control theory has been developed in a rigorous mathematical framework by academics, MPC has not had a solid fundamental basis until recently, *e.g.* Bitmead *et al.* (1990). However, several successful implementations of different variants of MPC has shown the strength of this control concept.

1.4 Thesis overview

The overall motivation for the research presented in this thesis is the fact that uncertainties and constraints are two central issues for process control. The effect of uncertainties can be rigorously analysed in the structured singular value framework, and constraints can be dealt with using MPC. However, in order to apply these methods in practice, guidelines for doing so are required. The purpose with the thesis is to derive and present such guidelines.

The backbone of the thesis are the five papers presented in chapters 2 to 6. These papers have all been presented at international conferences [18], [25], [24], [21] and [17]. Chapter 2 has also been published in an international journal [19].

A very simple distillation model proposed by Skogestad, Morari and Doyle (1988) called "column A" is used in some sense or another in all five papers. This model is not a very good representation of a distillation column, but it captures the interactions between top and bottom compositions and is an excellent model for studies concerning robustness to input uncertainty. Due to its simplicity this model has been used by several authors to illustrate different aspects of robust controller design. In fact this model was the basis for an entire session of the 1991 CDC at Brighton, U.K.

Chapter 2. This chapter presents different approaches to performance weight selection when the $\mathcal{H}_\infty$-norm is used to specify desired performance.

Upper bounds on important transfer functions are used to specify performance in the first approach. This approach is very similar to classical loop shaping techniques for SISO systems, however instead of specifying the desired open-loop transfer function, we specify an upper bound on the sensitivity function. The method can of course also be used to specify bounds on other important closed loop transfer functions. The main advantage with this method is that well understood criterions in terms of sensitivity, complementary sensitivity and other closed loop transfer functions can be employed.

The other method is a signal oriented approach. Here the maximum allowed 'size' of input and output signals of a system are specified by input and output weighting functions. This approach has a more direct connection of the induced norm interpretation of the $\mathcal{H}_\infty$-norm and is sometimes more appropriate for multivariable systems.

This chapter also presents an improved solution to the example problem from Skogestad, Morari and Doyle (1988). Several properties of this improved controller clearly indicates that it is very close to the true optimal controller.

The chapter is almost identical with the paper published in Transactions of the Institution of Measurements and Control [19] , however some minor correction have been made and Appendix 2 has been added. The nomenclature used in this chapter is slightly different from that used in the rest of the thesis. An early version of this paper was presented a the Symposium on "Robust Control System Design Using H-infinity and Related Methods" in Cambridge March 1991 and published as a chapter in the proceedings from this conference [18].

Chapter 3. This chapter deals with uncertainty modelling for controller analysis and design using the structured singular value framework. Most of the material presented here is from [25], but the uncertainty model based on a real perturbation and irrational weights (section 3.3.4) has not been presented elsewhere.

Four classes of linear fractional uncertainty models are presented: 1) Complex perturbation with rational weight, which is the most useful class from a practical engineering point of view and may be used for both analysis and synthesis; 2) Complex perturbation with irrational weight, which yield a tighter uncertainty model than 1 due to the irrational weight, but can only be used for analysis; 3) Mixed real/complex perturbation with rational weight, which yield a tighter model than 1 due to the real/complex

perturbation, but the real perturbation also complicates the computation of μ; and finally 4) Mixed real/complex perturbation with irrational weight, which yields a perfect match of the gain delay uncertainty up to a certain frequency.

Chapter 4. In this chapter a benchmark problem from the literature (Limebeer, 1991) is used to demonstrate the flexibility with the μ-framework for robust controller design. The controller designed and presented in this paper satisfies all performance requirements specified in the benchmark, and thereby it outperforms all other "solutions" to this problem presented in the literature.

Chapter 5. Limitations of "standard DMC" is highlighted in this chapter. The main problems with DMC are the model representation and the disturbance assumption employed by the algorithm. With these two problems identified, the paper also outlines how to avoid these problems.

This chapter presents results obtained during a stay at Manfred Morari's group at Caltech in 1990. The material presented in this chapter is strongly connected to the results presented in Lee, Morari and Garcia (1991) and in Morari and Lee (1991) where the examples from chapter 5 are used.

A short version of the chapter was presented at the 1st European Control Conference in Grenoble, France, 1991 [21]. Since then, further improvements of MPC has been suggested, *e.g.* Rawlings and Muske (1993) have demonstrated how a finite horizon problem may be reformulated as an infinite horizon problem. This modification yields an algorithm which guarantees Nominal Stability, which was not guaranteed with the standard finite horizon approach.

Chapter 6. This chapter is an updated and somewhat extended version of a paper presented at ADCHEM'94 [17]. Here we discuss opportunities and difficulties with a truly multivariable distillation control scheme, *i.e.* control of levels, pressure and compositions The ideas in the Model predictive part of the paper has previously been presented at the Annual AIChE meetings in Los Angeles 1991 [15] and Miami Beach 1992 [16].

Chapter 7. This chapter presents conclusions and suggestions for future work.

During the work with this thesis the author has participated in several projects which in all have resulted in 5 journal publications ([37], [32], [19], [38] and [40]) and 18 conference papers or presentations ([9], [11], [12], [15], [16], [17], [18], [20], [21], [22], [23], [24], [25], [31], [34], [35], [36] and [39])

References

[1] Balas, G.J, Doyle, J.C., Glover, K., Packard, A.K. and Smith, R. (1991). "The μ-Analysis and Synthesis Toolbox", The MathWorks Inc., Natick, MA.

[2] Bitmead, R.B., Gevers, M. and Wertz, V. (1990). *Adaptive Optimal Control*, Prentice Hall.

[3] Boyd, D.M. (1946). "Control of Fractionation Columns", *Petroleum Refiner*, **25**, 4, 147-151.

[4] Buckley, P.S., Luyben, W.L. and Shunta, J.P. (1985). *Design of Distillation Column Control Systems*, Instrument Society of America, Triangle Research Park, NC.

[5] Chiang, R.Y. and Safonov, M.G. (1992). "Robust-control toolbox for MATLAB. User's guide", The MathWorks Inc., Natick, MA.

[6] Cutler, C.R. and Ramaker, B.L. (1979). "Dynamic Matrix Control - A Computer Control Algorithm", *AIChE National Meeting*, Houston, TX; also *Proc. Joint Autom. Control Conf.*, San Francisco, CA, (1980), Paper WP5-B.

[7] Dorato, P., Tempo, R. and Muscato, G. (1993). "Bibliography on Robust Control", *Automatica*, **29**, 1, 201-214.

[8] Doyle, J.C. (1982). "Analysis of Feedback Systems with Structured Uncertainties", *IEE Proc.*, **129**, Part D, 242-250.

[9] Flatby, P., Skogestad, S. and Lundström, P. (1994). "Rigorous dynamic simulation of distillation columns based on UV-flash", *IFAC Symposium ADCHEM'94*, Kyoto, Japan.

[10] García, C.E., Prett, D.M. and M. Morari, M. (1989). "Model Predictive Control: Theory and Practice - a Survey", *Automatica*, **25**, 3, 335-348.

[11] Hovd, M., Lundström, P. and Skogestad, S. (1990). "Controllability Analysis Using Frequency-dependent Measures for Interactions and Disturbances", Poster 312j, *AIChE Annual Meeting*, Chicago, IL.

[12] Jacobsen, E.W., Lundström, P. and Skogestad, S. (1991). "Modelling and identification for robust control of ill-conditioned plants – a distillation case study", *Proc. Am. Control Conf.*, Boston, 242-248.

[13] Lee, J.H., Morari, M. and García, C.E. (1991). "State-Space Interpretation of Model Predictive Control", Submitted to *Automatica*.

[14] Limebeer, D.J.N. (1991). "The specification and purpose of a controller design case study", *Proc. IEEE Conf. Decision Contr.*, Brighton, England, 1579-1580.

[15] Lundström, P. and Skogestad, S. (1991). "Robust and Model Predictive Control of 5×5 Distillation Columns", *AIChE Annual Meeting*, Los Angeles, CA.

[16] Lundström, P. and Skogestad, S. (1992). "Robust Model Predictive Control of Distillation Columns", *AIChE Annual Meeting*, Miami Beach, FL.

[17] Lundström, P. and Skogestad, S. (1994). "Opportunities and difficulties with 5×5 Distillation Control", *IFAC Symposium ADCHEM'94*, Kyoto, Japan.

[18] Lundström, P., Skogestad, S. and Wang, Z.-Q. (1991). "Weight selection for H-infinity and mu-control methods – Insights and examples from process control", *Symposium on "Robust Control System Design Using H-infinity and Related Methods"*, Cambridge, UK.
Published in: Robust Control System Design Using H-infinity and Related Methods, P.H. Hammond (Ed.), Institute of Measurement and Control, London, UK, 139-157.

[19] Lundström, P., Skogestad, S. and Wang, Z.-Q. (1991). "Performance weight selection for H-infinity and μ-control methods", *Trans. Inst. MC*, **13**, 5, 241-252.

[20] Lundström, P., Skogestad, S. and Wang Z.-Q. (1991). "Uncertainty weight selection for H-infinity and mu-control methods", *Proc. IEEE Conf. Decision Contr.*, Brighton, England, 1537-1542.

[21] Lundström, P., Lee, J.H., Morari, M. and Skogestad, S. (1991). "Limitations of Dynamic Matrix Control", *Proc. European Control Conference*, 1839-1844, Grenoble, France.

[22] Lundström, P., Skogestad, S., Hovd, M. and Wang, Z.-Q. (1991). "Non-uniqueness of robust H_∞ decentralized control", *Proc. Am. Control Conf.*, Boston, 1830-1835.

[23] Lundström, P., Flatby, P. and Skogestad, S. (1993). "Effect of flow dynamics, energy balance and pressure dynamics on the overall response of distillation columns", *AIChE Annual Meeting*, St.Louis.

[24] Lundström, P., Skogestad, S. and Doyle, J.C. (1993). "Two degree of freedom controller design for an ill-conditioned plant using μ-synthesis", *European Control Conference*, Groningen, the Netherlands.

[25] Lundström, P., Wang, Z.-Q. and Skogestad, S. (1993). "Modelling of gain and delay uncertainty in the structured singular value framework", *Preprints IFAC World Congress on Automatic Control*, Sydney, Australia.

[26] Morari, M. and Lee, J.H. (1991). "Model predictive control: The good, the bad and the ugly". In Y. Arkun and W.H. Ray, editors, *Proceeding of Fourth International Conference on Chemical Process Control CPCIV*, South Padre Island, TX.

[27] Rawlings, J. and Muske, K. (1993). "The stability of constrained receding horizon control", *IEEE Trans. Autom. Control*, **38**, 1512-1516.

[28] Richalet, J.A., Rault, A., Testud, J.L. and Papon, J. (1978). "Model predictive heuristic control: Applications to an industrial process", *Automatica*, **14**, 413-428.

[29] Rijnsdorp, J.E. (1965). "Interactions in Two-Variable Control Systems for Distillation Columns, I-II", *Automatica*, **1**, 15-52.

[30] Skogestad, S. (1987). "Studies on Robust Control of Distillation Columns", Ph.D. Thesis, California Institute of Technology, CA.

[31] Skogestad, S., and Lundström, P. (1988). "Mu-optimal PID settings for Distillation Columns", Paper 126f, *AIChE Annual Meeting*, Washington DC.

[32] Skogestad, S. and Lundström, P. (1990). "Mu-optimal LV-control of distillation columns", *Computers chem. Engng.*, **14**, 4/5, 401-413.

[33] Skogestad, S., Morari, M. and Doyle, J.C (1988). "Robust Control of Ill-conditioned Plants: High-purity Distillation", *IEEE Trans. Autom. Control*, **33**, 12, 1092-1105. (Also see correction to μ-optimal controller in **34**, 6, 672).

[34] Skogestad, S., Jacobsen, E.W. and Lundström, P. (1989). "Selecting the Best Distillation Control Structure", *Preprints IFAC Symposium DYCORD'89*, 295-302, Maastricht, the Netherlands.

[35] Skogestad, S., Lundström, P. and Hovd, M. (1989). "Control of Identical Parallel Processes", Poster 167Ba, *AIChE Annual Meeting*, San Francisco, CA.

[36] Skogestad, S., Jacobsen, E.W. and Lundström, P. (1990). "Modelling Requirements for Robust Control of Distillation Columns", *Preprints IFAC World Congress*, Vol.11, 213-219, Tallinn, Estonia.

[37] Skogestad, S., Lundström, P. and Jacobsen, E.W. (1990). "Selecting the Best Distillation Control Configuration", *AIChE Journal*, **36**, 5, 753-764. Also: "Reply to comments by J. Riggs", *AIChE Journal*, **36**, 7, 1125-1126.

[38] Skogestad, S., Hovd, M. and Lundström, P. (1991). "Simple frequency-dependent tools for analysis of inherent control limitations", *MIC*, **12**, 4, 159-177.

[39] Skogestad, S., Hovd, M. and Lundström, P. (1991). "Towards Integrating Design and Control: Use of Frequency-dependent Tools for Controllability Analysis", *Proc. PSE 91*, III.3.1, Montebello, Canada.

[40] Wang, Z.-Q., Lundström, P. and Skogestad, S. (1994). "Representation of uncertain time delays in the H_∞ framework", *Int. J. Control*, **59**, 3, 627-638.

Chapter 2

Performance Weight Selection for H-infinity and μ-control Methods

Petter Lundström, Sigurd Skogestad and Zi-Qin Wang
Chemical Engineering
University of Trondheim, NTH
N-7034 Trondheim, Norway

Published in *Trans Inst MC, Vol 13, No 5, 1991*

Abstract

The paper discusses, from a process control perspective, different approaches to performance weight selection when using H-infinity objectives. Approach A considers direct bounds on important transfer functions such as sensitivity and complementary sensitivity. Approach B considers the output response to sinusoidal disturbances, setpoints and noise. We also give some insight into the practical use of H-infinity and μ methods. μ is the structured singular value (SSV) introduced by Doyle (1982). μ-synthesis is generally not a convex optimization problem and is presently not straightforward. We will discuss some of the problems we have encountered.

2.1 Introduction

One criticism against the traditional "optimal" control techniques which use a quadratic cost function (*e.g.*, LQG control, see Kwakernaak and Siwan (1972)), has been that the weights (cost matrices and covariance matrices) have a very indirect effect on the behavior of the closed-loop system. One can generalize the cost function by introducing frequency-dependent weights and use a more general H_2-norm minimization procedure, but even in this case one cannot specify directly important frequency-domain properties such as bandwidth and magnitude of resonance peaks on certain transfer functions. One natural extension is then to directly specify performance in the frequency domain by employing an H_∞-objective. For a stable transfer function $E(s)$ the H_∞-norm is given by

$$\|E\|_\infty = \sup_\omega \bar{\sigma}(E(j\omega)) \tag{2.1}$$

where $\sup_\omega$ denotes the peak value over all frequencies. The H_∞-norm may be viewed as a direct generalization of the frequency domain performance specifications used in classical control for single-input single-output (SISO) systems. For example, a very common performance objective is to minimize the weighted sensitivity function, and select $E = w_P S$ where $S = (I + GC)^{-1}$ (see the block diagram of a conventional feedback system in Fig. 2.1).

This paper is based on the paper on ill-conditioned plants by Skogestad, Morari and Doyle (1988), and the reader is referred to that paper for notation and background material. We shall use the same simplified distillation column (the LV-configuration) as our example. In the previous paper the effect of various uncertainty descriptions was studied, but here we use the example to discuss alternative choices for the performance weight.

Even though much progress has been made in terms of synthesizing H_∞-optimal controllers (e.g., Doyle *et al.*, 1989), the selection of appropriate performance weights is still very much an art. This may seem somewhat contradictory, as one of the motivations for introducing the H_∞-norm for performance has been to introduce weights which are more meaningful from a physical point of view. There are several reasons

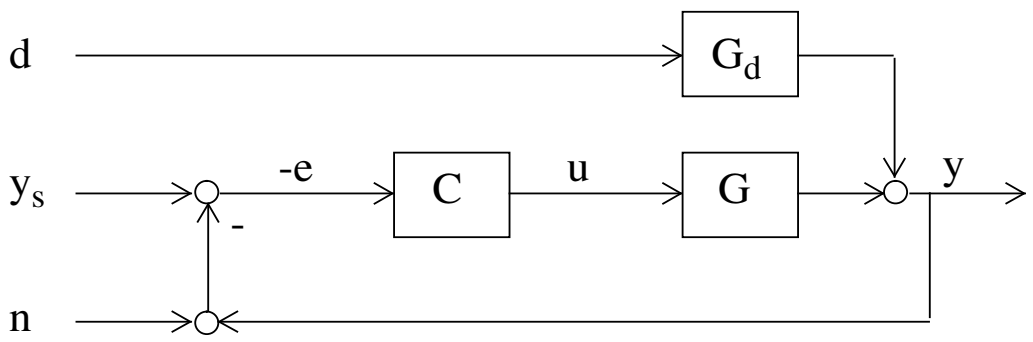

Figure 2.1: Block diagram of conventional feedback system.

for why weight selection is difficult:

- One obvious reason is that in most real design cases the specifications are not fixed before the design starts, and the weights are "knobs" which the engineer adjusts until he obtains a system which performs satisfactory.

- Another reason is that there are several ways of setting up the problem, and each of these yield different ways of adjusting the weights. There are several physical interpretations of the H_∞-norm (Doyle, 1987) which give rise to different procedures for selecting the performance weights. In this paper we will mainly discuss two of these procedures:

  Approach A) The transfer function or loop shaping approach. Here one considers direct bounds on important transfer functions such as S, $T = GCS$ and CS. Often several transfer functions are considered simultaneously and "stacked" on top of each other when evaluating the H_∞-norm. For example, Yue and Postlethwaite (1988) consider the transfer functions S and CS, and use the norm

  $$\left\| \begin{matrix} W_1 S W_1' \\ W_2 C S W_2' \end{matrix} \right\|_\infty \tag{2.2}$$

  Similarly, Chiang and Safonov (1988) and Chiang *et al.* (1990) consider the transfer functions S and T. In this case the first transfer function may be used to specify the bandwidth to achieve acceptable disturbance rejection, whereas the latter is used to avoid amplification of noise at high frequency. McFarlane and Glover (1990) use a direct loop-shaping approach.

  Approach B) The signal approach (e.g., Doyle *et al.*, 1987). Here one considers the response to sinusoidal signals. In this approach one cannot directly specify bandwidth, etc. However, this approach may be more appropriate for multivariable problems where a number of objectives must be taken into account simultaneously. Also, in such systems the concept of bandwidth is often difficult to use.

- There are different ways of handling model uncertainty. Above, we discussed nominal performance (NP). The ability to address also robust stability (RS) and robust performance (RP) in a consistent and rigorous manner is probably the most important reason for using the H_∞-norm for performance. However, there are at least two approaches for taking model uncertainty into account:

  1) The mixed NP-RS approach: Add the robust stability condition as an additional H_∞-objective to be minimized. One example is to try to optimize simultaneously nominal performance using $w_P S$ and robust stability with respect to relative output uncertainty of magnitude $|w_2(j\omega)|$ using $w_2 T$. These objectives are combined and the controller is designed to minimize the combined objective function

  $$\min_C \|N_{mix}\|_\infty; \quad N_{mix} = \begin{pmatrix} w_P S \\ w_2 T \end{pmatrix} \tag{2.3}$$

Note that this is the same objective as discussed by Chiang and Safonov (1988), but here the bound on T follows as a RS-condition and not as a condition for noise amplification. This follows since the same transfer function may be given both a performance and a stability interpretation. In practice, these considerations are often combined when selecting the weights, and Approach A for performance selection is usually combined with the mixed NP-RS approach for model uncertainty.

2) The RP-approach: Use the same H_∞-performance specification, but require that it is satisfied (or minimized) not only for the nominal plant, but for all plants as defined by the uncertainty description, that is, require robust performance. For example, when performance is measured in terms of w_pS, the robust performance objective with output uncertainty becomes (e.g., Skogestad *et al.*, 1988)

$$\min_C \sup_\omega \mu(N_{RP}); \quad N_{RP} = \begin{pmatrix} w_2T & w_2T \\ w_PS & w_PS \end{pmatrix} \tag{2.4}$$

Comment: For this particular case with both performance and uncertainty measured at the plant outputs there is almost no difference between the mixed NP-RS approach and the RP approach. (At each frequency $\mu(N_{RP})$ is by most a factor of $\sqrt{2}$ larger than $\bar{\sigma}(N_{mix})$). However, for ill-conditioned plants with uncertainty at the plant inputs (which is always present), this is not the case and the mixed approach may yield very poor RP. For example, this applies to the example studied by Skogestad *et al.* (1988) which is also studied in this paper.

The RP-approach is used in this paper. It is more rigorous than the mixed NP-RS approach, but it requires use of the structured singular value. This makes controller synthesis rather involved, but analysis is straightforward. A good design approach may be to synthesize controllers using the mixed approach, and analyze them using RP and μ. It may be necessary to iterate on the weights in order to obtain acceptable μ-values (Actually, as discussed in the next section, the presently used "D-K" iteration for μ-synthesis involves solving a series of H_∞-problems).

Software to synthesize H_∞-controllers has been available for some time, for example, through the Robust Control toolbox in MATLAB (Chiang and Safonov, 1988). Recently, a μ-toolbox for MATLAB has become available (Balas *et al.*, 1990). This toolbox includes alternative H_∞-software, and μ-analysis and synthesis is included as outlined above. All computations presented in this paper have been done employing this toolbox.

Some important terms:

Nominal stability (NS): The closed-loop system without uncertainty is stable.

Robust stability (RS): The system is stable for all defined uncertainty ("worst case is stable").

Nominal performance (NP): The system satisfies the performance requirements for the case with no uncertainty.

Robust performance (RP): The system satisfies the performance requirements for all defined uncertainty ("worst case satisfies performance requirement").

2.2 Model uncertainty and the structured singular value

The objective of this section is to give the reader a short introduction to model uncertainty and the structured singular value, μ. A more detailed introduction to μ is given by Doyle (1982; 1987) and Skogestad *et al.* (1988).

An important reason for selecting the H_∞-norm for performance, is that also model uncertainty may be readily formulated using this norm. In particular, this applies to uncertain or neglected high-frequency dynamics that are always present, and which cannot be modelled by parametric uncertainty in a state space model with fixed order. In the H_∞-framework the model uncertainty is modelled in terms of uncertain perturbations, Δ_i. Using weights they are normalized such that their H_∞-norm is less than 1.

$$\|\Delta_i\|_\infty < 1 \Leftrightarrow \bar{\sigma}(\Delta_i(j\omega)) < 1, \forall\omega \tag{2.5}$$

Unstructured uncertainty. In the simplest approach all the uncertainty is lumped into *one* perturbation matrix, Δ, for example at the output. This is an *unstructured* uncertainty description, and gives rise to robust stability conditions in terms of the singular value (H_∞-norm). For example, for input uncertainty of magnitude w_2, where also "cross-channel" uncertainty is allowed, Δ is a full matix, and the RS-condition becomes $\|w_2 T_I\| < 1$. However, this approach is generally conservative because it will include a lot of plant cases that cannot occur in practice. If cross-channel uncertainty does not occur in practice then the correct RS-condition is $\mu(w_2 T_I) < 1, \forall\omega$, where Δ is a diagonal matrix as given in Eq. 2.6 below.

Structured uncertainty. To model the uncertainty more tightly we must consider structured uncertainty, that is, use several perturbation blocks. Usually each of these blocks is related to a specific physical source of model uncertainty, for example a measurement uncertainty or an input uncertainty. For example, for the input uncertainty without cross-channel coupling we need one perturbation block for each input and we get for a system with n inputs

$$\Delta = \begin{bmatrix} \delta_1 & & 0 \\ & \delta_2 & \\ & & \ddots \\ 0 & & \delta_n \end{bmatrix} \tag{2.6}$$

Robust stability. To test for robust stability the system with the uncertainty blocks is rearranged such that N_{RS} (which includes the uncertainty weights) represents the interconnection matrix from the outputs to the inputs of the uncertainty-blocks, Δ. In

the following we assume that N_{RS} is stable. Using the small gain theorem, we know that robust stability will be satisfied if $\|N_{RS}\|_\infty < 1$, or equivalently

$$\text{RS} \quad \text{if} \quad \bar{\sigma}(N_{RS}) < 1; \quad \forall\omega \tag{2.7}$$

However, this bound is generally conservative unless the uncertainty is truly unstructured. First, the issue of stability should be independent of scaling. Thus, an improved robust stability condition is

$$\text{RS} \quad \text{if} \quad \min_{D(\omega)} \bar{\sigma}(DN_{RS}D^{-1}) < 1; \quad \forall\omega \tag{2.8}$$

where D is a real block-diagonal scaling matrix with structure corresponding to that of Δ, such that $\Delta D = D\Delta$. A further refinement of this idea led to the introduction of the structured singular value (Doyle, 1982, 1987). We have (essentially, this is the definition of μ)

$$\text{RS} \quad \text{iff} \quad \mu(N_{RS}) < 1; \quad \forall\omega \tag{2.9}$$

Thus $\min_D \bar{\sigma}(DMD^{-1})$ is an upper bound on $\mu(M)$. It is usually very close in magnitude. The largest deviation reported so far is about 10-15% (Doyle, 1982, 1987). Computationally tractable lower bounds for μ also exist and are in common use.

Robust Performance. An additional bonus of using the H_∞-norm both for performance and uncertainty is that the robust performance problem may be recast as a robust stability problem (Doyle, 1982), with the performance specification represented as a fake uncertainty block. To test for robust performance one considers the interconnection matrix N_{RP} from the outputs to the inputs of *all* the Δ-blocks, including the "full" Δ_P-block for performance. N_{RP} depends on the plant G, the controller C and on the weights used to define uncertainty and performance. The condition for robust performance within the H_∞-framework is (see Fig. 2.2)

$$\text{RP} \quad \text{iff} \quad \mu_{\tilde{\Delta}}(N_{RP}) < 1, \quad \forall\omega \quad , \tilde{\Delta} = \begin{bmatrix} \Delta & 0 \\ 0 & \Delta_P \end{bmatrix} \tag{2.10}$$

Analysis of robust performance for a given controller using μ is straightforward, but controller design using μ-synthesis is still rather involved. The present "D-K iteration" uses the upper bound on μ, and involves solving a number of "scaled" H_∞-problems. We will discuss this further in section 2.6.

Uncertainty weights. Since uncertainty modelling using the H_∞-framework is a worst-case approach, one should generally not include too many sources of uncertainty, since it otherwise becomes very unlikely for the worst case to occur in practice. One should therefore lump various sources of uncertainty into a single perturbation whenever this may be done in a non-conservative manner. On the other hand, one should be careful about excluding physically meaningful sources of uncertainty that limit achievable performance. From this it follows that selecting appropriate uncertainty weights is very problem-dependent, and it is important that guidelines for specific classes of problems be developed.

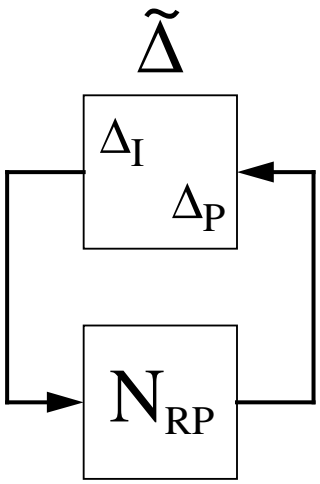

Figure 2.2: General block structure for μ analysis.

Sometimes one might use a smaller uncertainty set for robust performance than for robust stability. The idea is to guarantee stability for a large set of possible plants, but require performance only for a subset. This is to avoid very conservative designs with poor nominal performance.

For the example in this paper we only consider input uncertainty. The effect of output uncertainty, time constant uncertainty, and correlated gain uncertainty was studied by Skogestad *et al.* (1988). They found that these sources of uncertainty were less important than the input uncertainty for this particular ill-conditioned plant.

2.3 Performance weights

There are several different physical interpretations of the H_∞-norm of E (Doyle, 1987, Zhou *et al.*, 1990), and as mentioned in the introduction this gives rise to different methods for weight selection.

Approach A. Consider E as a transfer function. Since $||E||_\infty = \sup_\omega \bar{\sigma}(E(j\omega)$ the H_∞-norm may be viewed as a direct generalization of classical frequency-domain bounds on transfer functions (loop-shaping) to the multivariable case.

Approach B. Alternatively, consider $E(j\omega)$ as the frequency-by-frequency sinusoidal response. That is, for a unit sinusoidal input to channel j with frequency ω, the steady-state ouput in channel i is equal to $E_{ij}(j\omega)$. To consider all the channels combined, we use the maximum singular value, $\bar{\sigma}(E(j\omega))$, which gives the worst-case (with respect to choice of direction) amplification of a unit sinusoidal input of frequency ω through the system.

Approach C. The induced norm from bounded power spectrum inputs to bounded power spectrum outputs in the time domain is equal to the H_∞-norm.

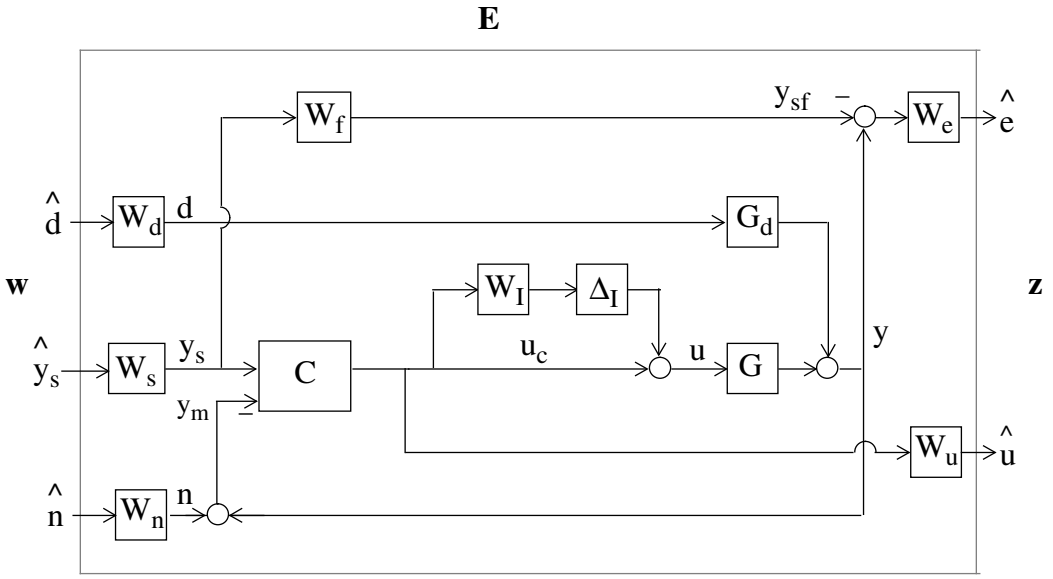

Figure 2.3: General feedback system with weights, a two-degree-of-freedom controller and input uncertainty. It is assumed that the outputs are measured directly. The transfer function E is used for H_∞-performance with Approach B.

There are also other interpretations of the H_∞-norm: It is equal to the induced 2-norm (energy) in the time domain. It is equal to the induced power-norm. It is also equal to induced norm in the time domain from signals of bounded magnitude to outputs of bounded power.

The following discussion is mostly relevant to approaches B and C. A general way to define performance within the H_∞-framework is to consider the H_∞-norm of the closed-loop transfer function E between the external weighted input vector w (disturbances d, setpoints y_s and noise n) and the weighted output vector z (may include $y - y_s$, manipulated inputs u which should be kept small, etc.). Weights are chosen such that the magnitude (in terms of the 2-norm) of the normalized external input vector is less than one at all frequencies, *i.e.* $\|w(j\omega)\|_\infty \leq 1$, and such that for acceptable performance the normalized output vector is less than 1 at all frequencies, *i.e.* $\|z(j\omega)\|_\infty < 1$. With $z = Ew$ the performance requirement becomes

$$\|E\|_\infty = \sup_\omega \bar{\sigma}(E(j\omega)) < 1 \tag{2.11}$$

Introducing the weights W_d, W_s, W_n, W_e and W_u into Fig. 2.1 yields the block diagram in Fig. 2.3 where E is given as shown by the dotted box. We also have introduced an "ideal response" W_f from y_s to y, and use a "two degree of freedom controller". Note that it is only the magnitude of these weights that matters; they should therefore be stable and minimum phase.

2.3.1 Performance approach A. Weights on transfer functions (Loop shaping)

Many performance specifications may be translated into an upper bound $1/|w_P|$ on the frequency plot of the magnitude of the sensitivity function $S = (I + GC)^{-1}$.

$$\bar{\sigma}(S(j\omega)) < 1/|w_P(j\omega)|, \quad \forall\omega \tag{2.12}$$

This is equivalent to (2.11) with $E = w_P S$ (weighted sensitivity). The concept of bandwidth, which is here defined as the frequency ω_B where the asymptote of $\bar{\sigma}(S)$ first crosses one, is closely related to this kind of performance specification, and most classical frequency domain specifications may be captured by this approach.

Classical frequency domain specifications. For example, assume that the following specifications are given in the frequency domain:

1. Steady-state offset less than A.
2. Closed-loop bandwidth higher than ω_B.
3. Amplification of high-frequency noise less than a factor M.

These specifications may be reformulated in terms of Eq. 2.12 using

$$w_P(s) = \frac{1}{M}\frac{\tau_{cl}s + M}{\tau_{cl}s + A}, \qquad \text{with } \tau_{cl} = 1/\,\omega_B \tag{2.13}$$

and the resulting bound $1/|w_P(j\omega)|$ is shown graphically in Fig. 2.4.

In many cases a steeper slope on S is desired at frequencies below the bandwidth to improve performance. For example, this may be the case if the disturbances are relatively slow as discussed below (Section 2.3.3).

Several transfer functions. As mentioned in the introduction one may define similar performance objectives in terms of other transfer functions, and consider the combined effect by stacking them together when computing the H_∞-norm.

Matrix valued weights. In the multivariable case the generalized weighted sensitivity is $W_P S W_P'$. For example, one may use different bounds on the sensitivity function for various outputs. Assume we want the response in channel 1 to be about 10 times faster than that in channel 2. Then we might use the performance specification

$$\|W_P S\|_\infty < 1; \qquad W_P = \begin{pmatrix} w_{P11} & 0 \\ 0 & w_{P22} \end{pmatrix} \tag{2.14}$$

with $\omega_{B11} = 10\omega_{B22}$. We shall later study the use of different weights in each channel for the distillation example.

Introducing matrix valued weights is necessary if the disturbances have strong directionality. However, the direct implications for the shape of the sensitivity function then become less clear, and it is then probably better to shift to the more general signal-oriented approach discussed next.

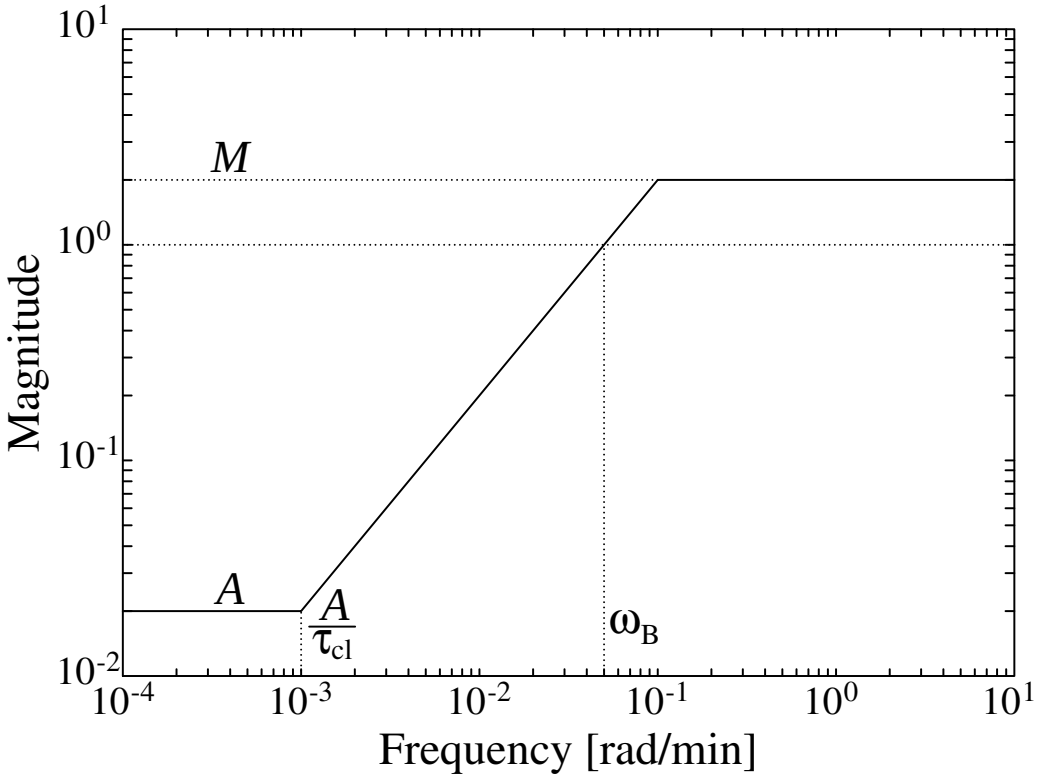

Figure 2.4: Asymptotic plot of $1/w_P = M\frac{\tau_{cl}s+A}{\tau_{cl}s+M}$ where $\tau_{cl} = 1/\omega_B$. $|S(j\omega)|$ should lie below $1/|w_P|$ to satisfy classical frequency-domain specifications in terms of A, M and ω_B.

2.3.2 Performance approach B. Frequency by frequency sinusoidal signals

In many cases it is not possible, or at least difficult, to directly specify appropriate weights on selected transfer functions. A sinusoidal signal-oriented approach is then more suitable. For example, this approach is used in the space shuttle application study by Doyle *et al.* (1987).

In this approach we consider the effect of persistent sinusoidal input signals of a given frequency. Consider again Fig 2.3, the signal weights W_d, W_s and W_n will be diagonal matrices which give the expected magnitude of each input signal at each frequency. Typically, the disturbance weight, W_d, and the setpoint weight, W_s, do not vary very much with frequency [1], while the noise weight, W_n, usually has its peak

[1] That is, in this approach B we should *not* add a integrator $(1/s)$ to the weight even if step changes in disturbances or setpoints are expected (however, in approach C this is correct). The reason is that in approach B we consider the response frequency-by-frequency and a step change cannot really be modelled very well, and certainly not as a slow-varying sinusoid of infinite magnitude. A more reasonable approach is to consider a range of sinusoids and use a nearly constant weight with the

value at high frequency. W_e is a diagonal matrix which at each frequency specifies the *inverse* of the allowed magnitude of a specific output error. If we want no steady-state offset the weight should include an integrator such that its magnitude is infinite at steady-state (we require offset-free response to slow-varying sinusoids) [2]. We let the weight (W_e) level off at high frequencies at a value $\frac{1}{M}W_s^{-1}$. The factor M limits the maximum peak of $\sigma(\bar{S})$ and is a way of including some loop-shaping ideas from Approach A. Often the value of M is about 2. The corner frequency for the weight W_w (where it levels off) should be approximately M/τ_{cle} where τ_{cle} is the maximum allowed closed-loop time constant for that output. The actuator penalty weight, W_u, is usually small or zero at steady-state [3]. W_u may be close to a pure differentiator (s) if we want to penalize fast changes in the inputs.

It is important to check that the various performance requirements are consistent. This may be done by evaluating their influence of the required loop shapes (approach A), in particular, at low and high frequencies. Alternatively, one may test if it is possible to get $\mu < 1$ for NP by performing a H_∞-synthesis with no uncertainty.

The approach described above tends to give a large number of weights, and this is an disadvantage. First, the dimension of the problem grows and the solution takes more time. Second, with too many independent sources of noise and disturbances it may become very unlikely for the worst case to occur in practice (note that the H_∞-norm represents a worst-case approach as the singular value picks out the worst direction). For example, if we have a large number of measurements (it may be possible to have 100 measurements in a distillation column), it will be very unlikely that the worst combination of measurement noise will ever occur in practice. Mejdell (1990) encountered this problem and found it necessary to reduce the number of independent noise directions.

2.3.3 Combining performance weights (going from Approach B to A).

There are of course cases where Approaches A and B are identical, but in general there is a significant difference between considering A) the shape of the transfer functions (e.g., in terms of its slope and frequency where it crosses one), and B) considering the magnitude of a specific output signal to sinusoidal disturbances.

To illustrate how specifications on setpoints and disturbance rejection (approach B) may be reformulated as bounds on the weighted sensitivity (approach A) consider Fig. 2.3 and evaluate the transfer function from normalized disturbances and setpoints

same magnitude as of the step.

[2] Note that we may not require offset-free response for $y - y_s$ if the measurement noise is nonzero at steady-state ($\omega = 0$). Therefore, to get a controller with integral action we should select W_n to be zero at $\omega = 0$. Alternatively, we may require no offset for $y_m - y_s$, where $y_m = y + n$ is the measurement.

[3] The use of actuators inputs of a certain magnitude is often unavoidable (independent of the controller) in order to reject slow-varying disturbances, and penalizing the inputs at low frequencies makes little sense in such cases.

to normalized errors. We have

$$z = \hat{e} = E \begin{pmatrix} \hat{d} \\ \hat{y}_s \end{pmatrix} = Ew \tag{2.15}$$

With conventional feedback control (one-degree of freedom), no setpoint filtering ($W_f = I$) and no uncertainty ($\Delta_I = 0$) we have (Fig. 2.3)

$$E = \begin{pmatrix} W_e S G_d W_d & W_e S W_s \end{pmatrix}. \tag{2.16}$$

The performance specification is $\|E\|_\infty < 1$, but we want to obtain a bound on $\bar{\sigma}(S)$. To this end we find a weight $w_P(j\omega)$ such that at each frequency $\bar{\sigma}(w_P S) = \bar{\sigma}(E)$. For the SISO (scalar) case we get $\bar{\sigma}(E) = |W_e S|\sqrt{|G_d W_d|^2 + |W_s|^2}$ and $\bar{\sigma}(w_P S) = |w_P S|$, and we have at each frequency

$$|w_P| = |W_e|\sqrt{|G_d W_d|^2 + |W_s|^2} \tag{2.17}$$

Consider the following special SISO case where we assume:
i) Outputs have been scaled such that for setpoints $W_s = 1$;
ii) G_d has been scaled such that disturbances $\hat{d}$ are less than 1 in magnitude, thus $W_d = 1$;
iii) Disturbance model $G_d = k_d/(1 + \tau_d s)$; and
iv) The errors, e, should be less than M in magnitude at high frequencies, and we want integral action and require a response time better than about τ_{cle}, i.e., $W_e = (\tau_{cle} s + M)/M\tau_{cle} s$.

With the exception of at most a factor $\sqrt{2}$ (at frequencies where $|G_d| \approx 1$) we may then use the following approximation for Eq. (2.17):

$$w_P(s) \approx W_e(s)\left(\frac{|k_d|}{1 + \tau_d s} + 1\right) = \frac{s + M/\tau_{cle}}{Ms}\frac{s + \frac{|k_d|+1}{\tau_d}}{s + 1/\tau_d} \tag{2.18}$$

Obviously, if the disturbance gain, $|k_d|$, is small compared to 1 (the magnitude of the setpoints), then $w_P(s) \approx W_e(s)$, and the disturbance does not affect the bound on $S(j\omega)$. However, in general the requirement of disturbance rejection may require a faster response than the response time, τ_{cle}, required by the weight W_e. The most important feature of the performance weight, $w_P(s)$, is it's bandwidth requirement, ω_B^*, which we define as the frequency where the asymptote of $w_P(s)$ crosses 1. Introduce the response time constant imposed by disturbances

$$\tau_{cld} = M\frac{\tau_d}{|k_d| + 1} \tag{2.19}$$

A closer analysis of (2.18) shows that $\omega_B^* = \max\{1/\tau_{cle}, 1/\tau_{cld}\}$. For $\tau_{cld} < \tau_{cle}$ the bandwidth requirement is determined by disturbance rejection. This is illustrated in Fig. 2.5 where we show the bound $1/|w_P|$ on $|S|$ as a function of frequency. The solid line shows the requirement for setpoint tracking only, whereas the various dotted lines

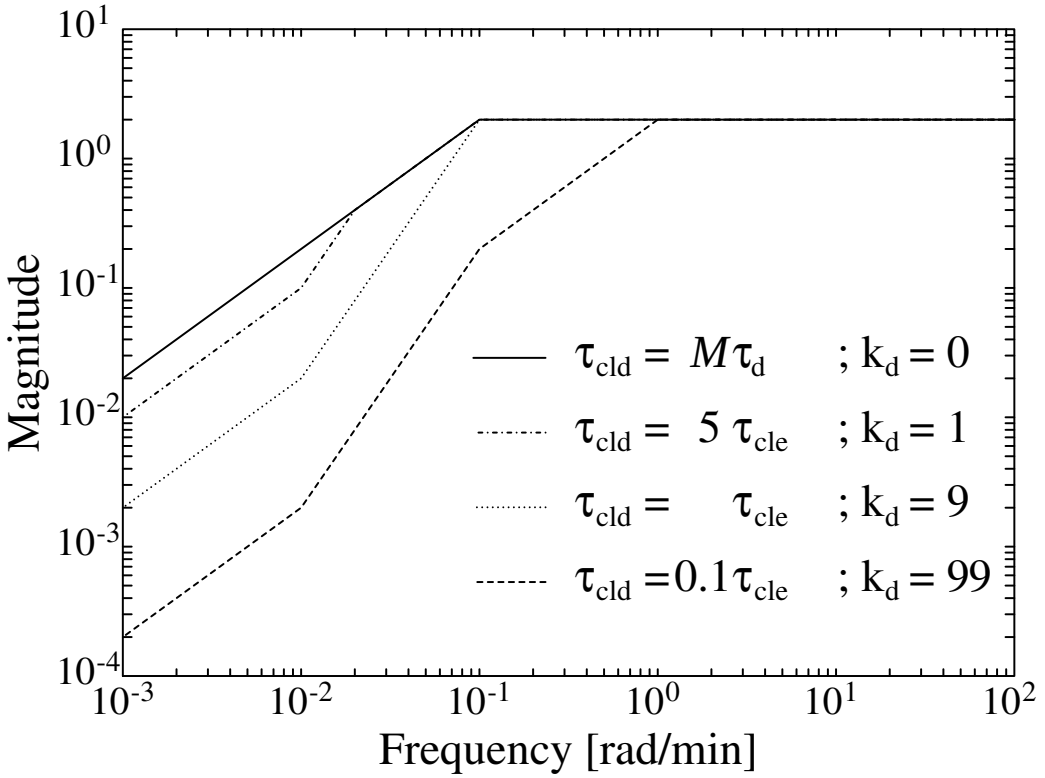

Figure 2.5: Asymptotic plot of $1/w_P$ (Eq. 2.18) for cases where $\tau_{cle} < \tau_d$ ($M = 2$, $\tau_{cle} = 20$ min and $\tau_d = 100$ min is used in the plot).

show the requirement for increasing magnitude of the disturbance. In this case with "slow disturbances" ($\tau_{cle}/M < \tau_d$) the weight in (2.18) has a region at low frequencies where $|w_P(j\omega)|$ has a slope of -2 on a log$|w_P|$-logω plot.

In the multivariable case we must use matrix-valued weights, and it is not possible to transform approach B into a scalar bound on S. Specifically, $\bar{\sigma}(SG_d(j\omega))$ may be significantly smaller than $\bar{\sigma}(S(j\omega))\bar{\sigma}(G_d(j\omega))$ when G_d is in the "good" direction corresponding to the large plant gains (see Skogestad *et al.*, 1988).

2.3.4 Performance approach C. Power signals - Power spectrum weights

This is not a frequency-by-frequency approach. Rather one must consider the entire frequency spectrum. One may think of the weights W_d, W_n and W_s as upper bounds on the power spectral density of the input signals, whereas W_e and W_u are equal to the inverse of the upper bounds on the power spectral density of the output signals. For example, if we allow for step changes of the setpoints, we may choose a weight $W_s = 1/s$ (but we will also allow a lot of other signals bounded by this spectral density). We will not discuss this approach any further, but just note that it compared to approach B

in many cases corresponds to shifting integrators from the output weights to the input weights.

2.4 Fixed or adjustable weights

One advantage with H_∞ or μ-optimal control is that it is relatively well-defined what an objective function with a value close to 1 means: The worst-case response will satisfy our performance objective. If μ at a given frequency is different from 1 then the interpretation is that at this frequency we can tolerate $1/\mu$ times more uncertainty and still satisfy our performance objective with a margin of $1/\mu$.

Controller synthesis almost always consists of a series of steps where the designer iterates between mathematical formulation of the control problem, synthesis and analysis. In μ-synthesis the designer will usually redefine the control problem by adjusting some performance or uncertainty weight until the final optimal μ-value is reasonably close to 1. In most cases this is done in an more or less *ad hoc* fashion, but it may also be done systematically. One attractive option is to keep the uncertainty weight fixed (of course, it must be possible to satisfy RS) and evaluate the achievable performance with this level of uncertainty, that is, adjust some performance weight to make $\sup_\omega \mu(N_{RP}) = 1$. There are two obvious options to adjust the performance weight:

1) Scale the performance frequency-by-frequency such that $\mu(N_{RP}) = 1$ at all frequencies, that is, at each frequency find a $k(\omega)$ which solves

$$\mu \begin{pmatrix} N_{RP_{11}} & N_{RP_{12}} \\ kN_{RP_{21}} & kN_{RP_{22}} \end{pmatrix} = 1 \tag{2.20}$$

This option is most attractive for analysis with a given controller. The numerical search for k is straightforward since μ increases monotonically with k, and since a solution always exists provided we have RS.

2) Adjust some parameter in the performance weight such that the peak value of $\mu(N_{RP})$ is 1. This option is most reasonable for μ-synthesis, that is, if the controller is not given. For example, with the performance weight (2.13) we may adjust the time constant τ_{cl} such that the optimization problem becomes

$$\min_{\tau_{cl},C} |\tau_{cl}| \,; \quad \text{s.t.} \quad \mu(N_{RP}(C,\tau_{cl})) \leq 1, \quad \forall\omega \tag{2.21}$$

Different plants may then be compared based on their maximum achievable bandwidth. A disadvantage with this approach is that it may be impossible to achieve $\mu(N_{RP}) = 1$ by adjusting τ_{cl} in the performance weight if, for example, the high-frequency specification (value of M) is limiting. Skogestad and Lundström (1990) have used this approach to compare alternative control structures for a distillation column example. An other approach is to keep τ_{cl} and M in the weight (2.13) fixed, and rather adjust the weight at *all* frequencies with the same constant. However, sometimes this does not make sense from a physical point of view since we cannot adjust the weight very much at high frequencies (since $S \approx I$ at high frequencies).

In this paper we do not employ these approaches, but use fixed weights only.

2.5 Skogestad et al. (1988) example revisited

We shall use the same plant as studied previously by Skogestad *et al.* (1988). The plant model is

$$G(s) = \frac{1}{75s+1}\begin{pmatrix} 0.878 & -0.864 \\ 1.082 & -1.096 \end{pmatrix} \tag{2.22}$$

which has a condition number of 141.7 and a RGA-value of 35.5 at all frequencies. The unit for time is minutes. This is a very crude model of a distillation column, but it is an excellent example for demonstrating the problems with ill-conditioned plants. Freudenberg (1989) and Yaniv and Barlev (1990) also used this model to demonstrate design methods for robust control of ill-conditioned plants.

In Skogestad *et al.* (1988) the following specifications were used:

1) The relative magnitude of the uncertainty in each of the two input channels is given by

$$w_I(s) = 0.2(5s+1)/(0.5s+1). \tag{2.23}$$

Thus the uncertainty is 20% at low frequencies and reaches 1 at a frequency of approximately 1 rad/min. Note that the corresponding uncertainty matrix, Δ_I, is a diagonal matrix since we assume that uncertainty does not "spread" from one channel to another (for example, we assume that a large input signal in channel 1 does not affect the signal in channel 2).

2) RP-specification (using performance approach A): The worst case (in terms of uncertainty) H_∞-norm of $w_P S$ should be less than 1.

$$w_P(s) = 0.5(10s+1)/10s \tag{2.24}$$

This requires integral action, a bandwidth of approximately 0.05 rad/min and a maximum peak for $\bar{\sigma}(S)$ of 2.

The resulting μ-condition for Robust Performance becomes (see Fig 2.2):

$$\mu_{\tilde{\Delta}}(N_{RP}) \leq 1, \quad \forall\omega \tag{2.25}$$

where

$$N_{RP} = \begin{bmatrix} -w_I CSG & w_I CS \\ wpSG & -w_P S \end{bmatrix}; \quad \tilde{\Delta} = \begin{bmatrix} \delta_1 & & \\ & \delta_2 & \\ & & \Delta_P \end{bmatrix} \tag{2.26}$$

In the following we shall keep the uncertainty description fixed, but consider alternative performance specifications.

2.5.1 Original problem formulation (Performance approach A)

Skogestad *et al.* (1988) used a software package based on the H_∞-minimization in Doyle (1985) (denoted "the 1984-approach" in Doyle et al., 1989) to design a "μ-optimal"

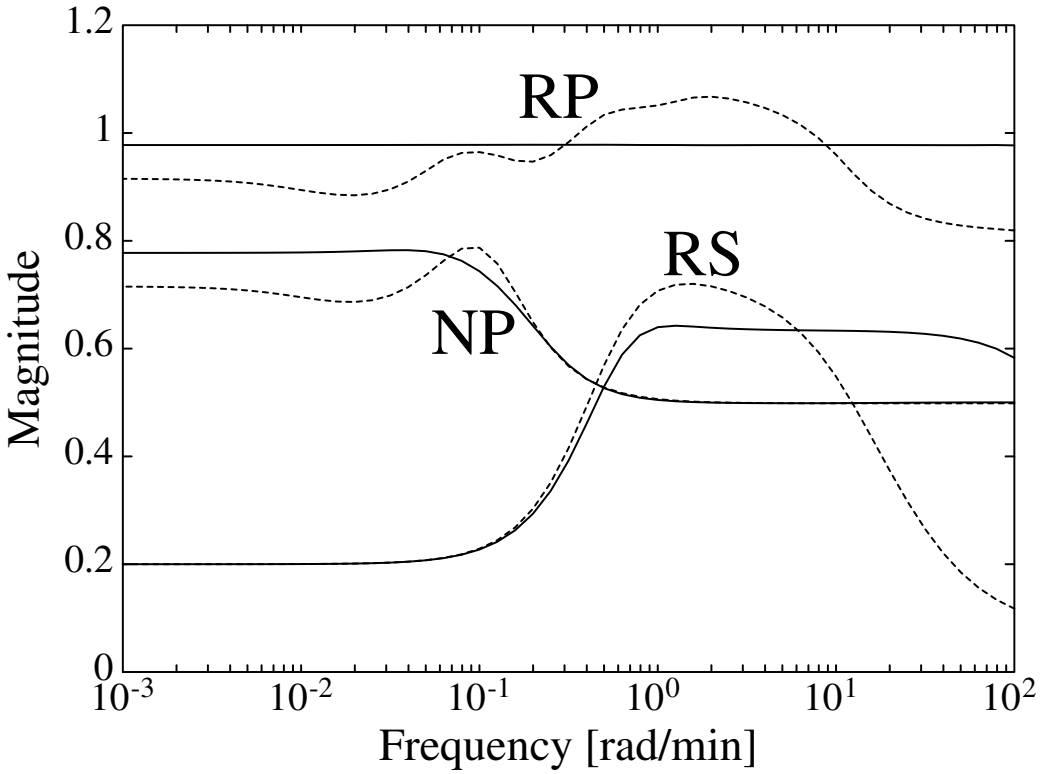

Figure 2.6: μ-plots for $C_{\mu new}$ (solid curves) and $C_{\mu old}$ (dashed curves).

controller. Their controller has six states and gives $\sup_\omega \mu(N_{RP}) = \mu_{RP}$=1.067 for both structured and unstructured Δ_I. We will denote this controller $C_{\mu old}$. Freudenberg (1989) used another design method and achieved a controller with five states giving μ_{RP}=1.054 for unstructured Δ_I. Yaniv and Barlev (1990) do not present a μ value for their design, but show some time responses[4].

New optimal design. With the new H_∞-software (Balas *et al.*, 1990) based on the state-space solution of Doyle *et al.* (1989), the μ-synthesis ("D-K iteration") performs better than with the 1984-approach. We were able to design a controller which, compared to $C_{\mu old}$, lowered μ_{RP} from 1.067 to 0.978. The new controller will be denoted $C_{\mu new}$. It has 22 states and a state space representation is given in Appendix 1.

Figure 2.6 shows μ for RP, NP and RS as a function of frequency for $C_{\mu new}$ (solid curves) and $C_{\mu old}$ (dashed curves). $\mu(N_{RP})$ for the new controller is extremely flat and the peak value, μ_{RP}, is substantially lower than for the old controller. The *nominal* performance is generally worse for the new controller, while robust stability is improved for some frequencies.

Fig. 2.7 shows the time response to setpoint changes for controller $C_{\mu new}$. The solid

[4]Based on the data in Yaniv and Barlev (1990) we obtained $\mu_{RP} = 1.97$ for their design. However, our time responses did not quite match those presented in their paper.

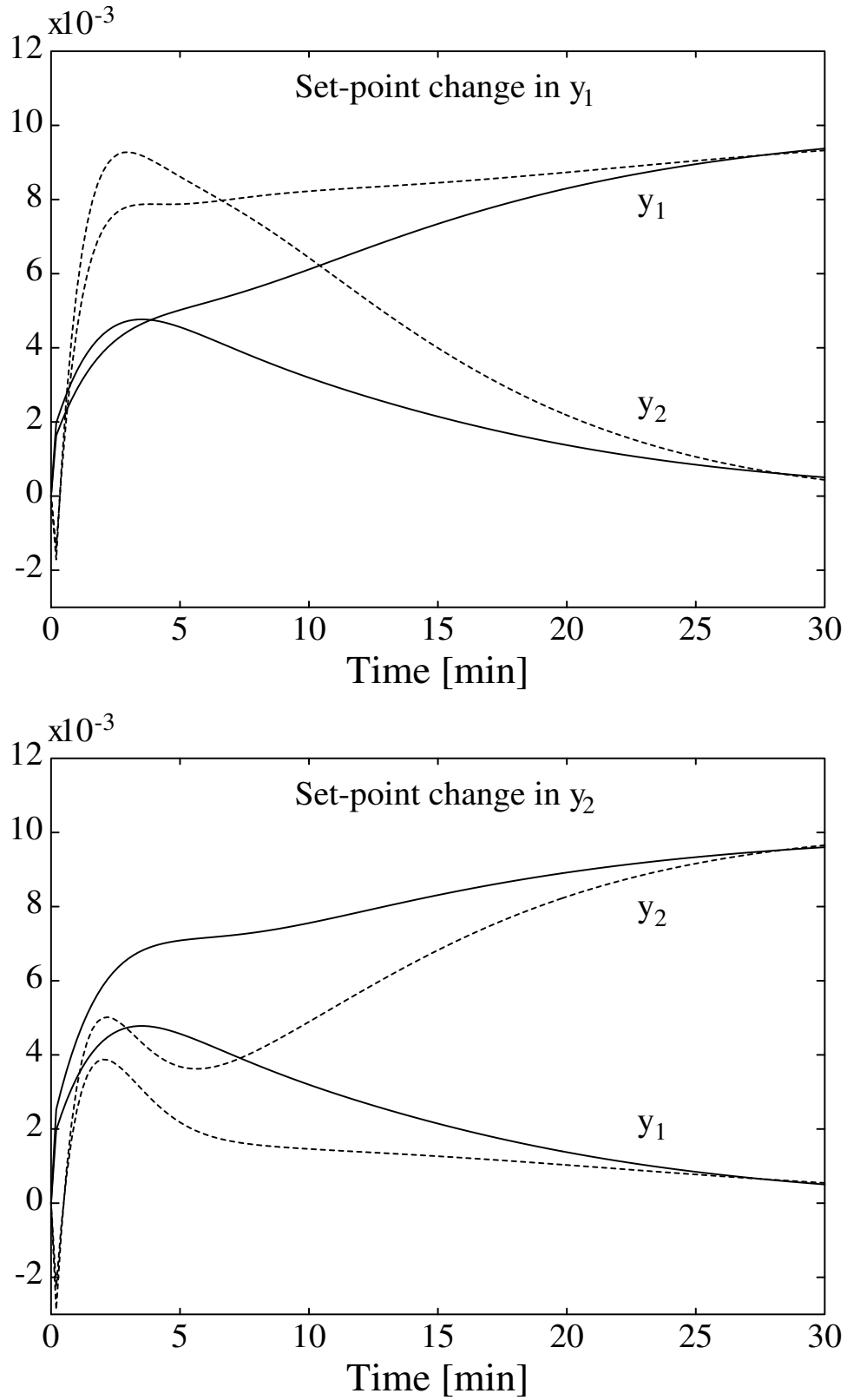

Figure 2.7: Simulation of setpoint changes using controller $C_{\mu new}$. Responses are shown both for nominal case (solid curves) and with input uncertainty given in Eq. 2.27 (dashed curves).

Table 2.1: Optimal μ_{RP}-values for the original problem formulation, Eq. 2.25–2.26, (Approach A).

Controller type	μ_{RP}	k_1	k_2	τ_{I1} min.	τ_{I2} min.	τ_{D1} min.	τ_{D2} min.
μ-ODF ($C_{\mu new}$)	0.978						
μ-TDF ($C_{\mu 2}$)	0.926						
PI	1.50	142	-25.6	64.4	1.35		
PID	1.32	163	-39.1	41.2	0.896	0.342	0.290

curves show the nominal response, and the dotted curves the response with model error. The specific model error we use is

$$u(s) = \begin{pmatrix} \frac{-0.5s+1.2}{0.5s+1} & 0 \\ 0 & \frac{-0.5s+0.8}{0.5s+1} \end{pmatrix} u_c(s) \tag{2.27}$$

where u is the true input signal and u_c the input signal computed by the controller.

This uncertainty is covered by the the uncertainty description, $w_I(s)$). By comparing the time responses to those presented for the controller $C_{\mu old}$ in Skogestad *et al.* (1988) we see that the difference is relatively small.

2.5.2 Alternative controller designs (Approach A)

Table 2.1 shows minimized μ-values obtained for different controller structures. μ-ODF is a One Degree of Freedom μ controller and μ-TDF is a Two Degree of Freedom μ controller. The second row shows that with a TDF controller we may reduce the μ-value for RP from 0.978 to 0.926. (To avoid numerical problems when obtaining this controller we had to introduce some measurement noise). In general, a TDF controller yields improved performance when we have simultaneous disturbance rejection and command following. In our case the model uncertainty in effect introduces disturbances (generated internally) and makes it advantageous to use a controller which shapes the setpoints differently.

In Table 2.1 we also show the results using two PI- or PID-controllers of the form below.

$$C(s) = \begin{pmatrix} c_{PID_1}(s) & 0 \\ 0 & c_{PID_2}(s) \end{pmatrix}; \quad c_{PID_i}(s) = k_i \frac{1+\tau_{I_i}s}{\tau_{I_i}s} \frac{1+\tau_{D_i}s}{1+0.1\tau_{D_i}s} \tag{2.28}$$

Optimal PI/PID tunings were obtained using a general-purpose optimization algorithm to minimize μ_{RP} with respect to the six parameters [5]. We obtained optimal μ_{RP}-values of 1.50 for PI-control and 1.32 for PID-control. Note that the optimal tunings are very

[5] We set up the problem as a min-max problem, $\min_c \max_\omega \mu(N_{RP})$, and used the routine "minimax" in the Optimization toolbox for MATLAB (Grace, 1990)

Table 2.2: Optimal μ_{RP}-values for different performance weights, Eq. 2.13, (Approach A).

Controller type	μ_{RP}	τ_{cl1} min.	τ_{cl2} min.	k_1	k_2	τ_{I1} min.	τ_{I2} min.	τ_{D1} min.	τ_{D2} min.
μ-ODF	0.978	20	20						
μ-ODF	0.970	40	10						
μ-ODF	0.937	80	5						
μ-ODF	1.098	20	10						
PID	1.32	20	20	163	-39.1	41.2	0.896	0.342	0.290
PID	1.15	40	10	98.4	-17.7	67.5	0.769	0.385	0.529
PID	1.09	80	5	56.2	-39.3	68.1	1.48	0.332	0.582
PID	1.33	20	10	164	-37.2	39.2	0.674	0.398	0.327

different for the two channels in spite of the fact that the problem formulation is nearly symmetric. This is probably caused by the fixed structure and limited number of states of PI/PID controllers. This issue is discussed in more detail by Lundström *et al.* (1991).

2.5.3 Other performance weights (Approach A)

Here we use the same problem formulation as in the previous section, except for using different performance weights in each output channel.

$$W_P(s) = \begin{pmatrix} w_{P_1} & 0 \\ 0 & w_{P_2} \end{pmatrix}; \quad w_{P_i}(s) = \frac{1}{M}\frac{\tau_{cl_i}s + M}{\tau_{cl_i}s} \tag{2.29}$$

Intuitively, we may reduce the "interactions" (this is a term which is relevant for single-loop control) in the system by having one channel with a fast response, and one channel with a slow response. Optimal μ-values for different choices of τ_{cl_1} and τ_{cl_2} are shown in Table 2.2. We keep the "average" response time constant by holding $\tau_{cl_1}\tau_{cl_2}$ constant. We see that the μ-values are somewhat lower when we allow different response times in the two channels (Of course, this is only true to a limited extent, since the response time of the fast channel is limited by the uncertainty weight which crosses one at a frequency of 1 rad/min). The fourth entry in Table 2.2 does not have the same "average" response time, but is included to illustrate that the μ_{RP}-value increases markedly if we require that one loop is made faster without relaxing the requirement of the other loop.

As expected, the reduced interaction becomes even more clear if we study single-loop (decentralized) control using PID controllers. The tuning parameters and μ_{RP} for different choices of performance weights are also given in Table 2.2. The last entry in the table shows that for these controllers we *can* increase the speed of one channel at almost no cost in terms of μ_{RP}.

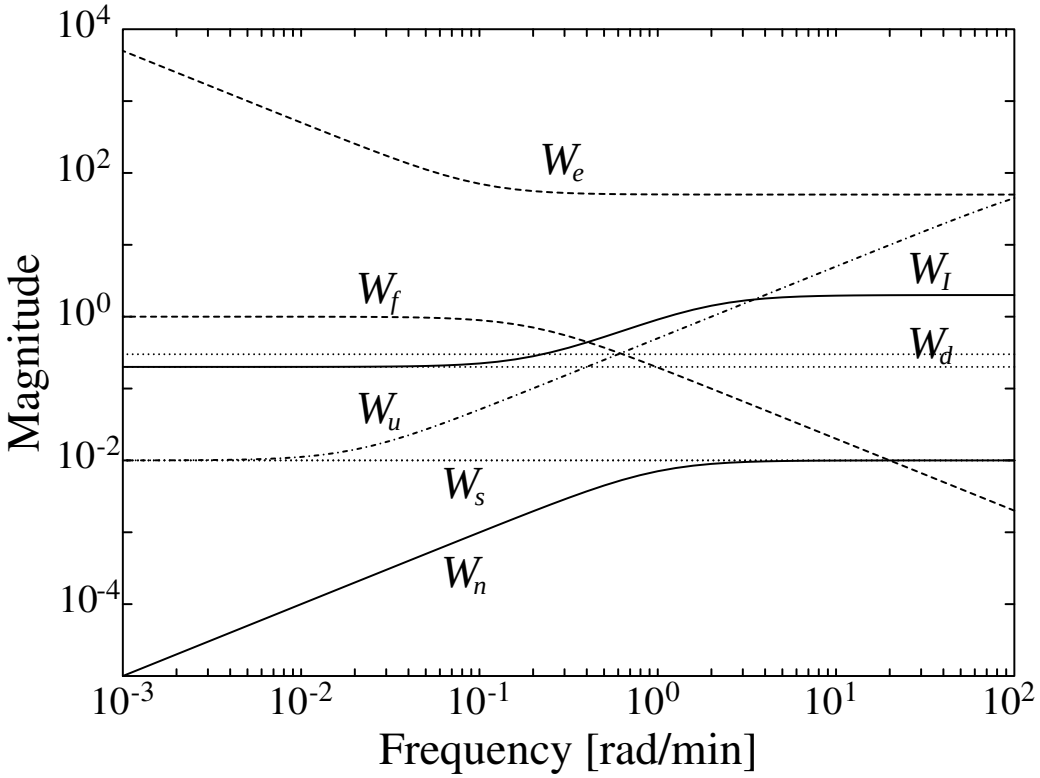

Figure 2.8: Frequency plot of the weights used in Approach B in section 2.5.4.

2.5.4 Performance approach B

Consider a revised problem that includes disturbance rejection as shown in the block diagram in Fig. 2.3. We shall design a two-degree-of- freedom controller using approach B. The plant G is given in Eq. 2.22. G_d describes the effect of disturbances (feed flow, F, and feed composition, z_F) on the two controlled variables (top and bottom composition, y_D and x_B).

$$G_d(s) = \frac{1}{75s+1}\begin{pmatrix} 0.394 & 0.881 \\ 0.586 & 1.119 \end{pmatrix} \tag{2.30}$$

We use the following weights to define the problem:

$$W_d(s) = \begin{pmatrix} 0.3 & 0 \\ 0 & 0.2 \end{pmatrix} \quad ; \qquad W_s(s) = 0.01 I_{2x2} \quad ; \qquad W_n(s) = 0.01\frac{s}{s+1} I_{2x2} \tag{2.31}$$

$$W_f(s) = \frac{1}{5s+1} I_{2x2} \quad ; \qquad W_I(s) = 0.2\frac{5s+1}{0.5s+1} I_{2x2} \tag{2.32}$$

$$W_e(s) = \frac{100}{2}\frac{20s+2}{20s} I_{2x2} \quad ; \qquad W_u(s) = 0.01\frac{50s+1}{0.0005s+1} I_{2x2} \tag{2.33}$$

These weights are plotted in Fig. 2.8.

G and G_d were found by linearizing a non-linear model at an operating point where $y_D = 0.99, x_B = 0.01, F = 1.0$ and $z_F = 0.5$ (Skogestad and Morari, 1987). W_d shows that we are expecting up to 0.3/1=30% variation in F and 0.2/0.5=40% in z_F. Similarly, W_s specifies the setpoint variations, $0.98 \leq y_{Dsp} \leq 1.00$ and $0.00 \leq x_{Bsp} \leq 0.02$. These weights reflect the relative importance of the external inputs, i.e. we consider 30% variation in F to be comparable to a setpoint variation of 0.01 kmol/kmol. The noise at high frequency is allowed to be of magnitude 0.01. We see from the weight W_e that the allowed output error $y - ys$ is 2/100=0.02 at high frequencies and the required response time $\tau_{cle} = 20$ min. The factors 0.01 and 100 in the weights for W_s, W_n and W_e correspond to an output scaling, and could alternatively have been accomplished by multiplying the elements in G and G_d by 100.

The optimal controller, $C_{\mu B}$, gives a μ_{RP} value for this problem definition of 1.04, whereas the controller $C_{\mu new}$ (with input $y_s - y_m$), which is essentially tuned for setpoints only, gives a value of 1863 at high frequencies and 1.75 at low frequencies. The reason for the extremely high μ-value is that $C_{\mu new}$ is tuned without any direct penalty on manipulated inputs, while in the new formulation (Approach B) such a penalty (W_u) is included. Conversely, when applied to the original problem definition, $C_{\mu B}$, gives $\mu_{RP} = 1.18$, whereas $C_{\mu new}$ gives 0.978.

Recall the analysis of Eq. 2.17 where we analyzed the relative importance of disturbance and setpoint tracking on performance. If in this example we look at the disturbance rejection from a scalar point of view, the performance time constants, τ_{cld} in Eq. 2.19, for the effect of the two disturbances in F and z_F on output x_B are about $2 \cdot 75/(0.3 \cdot 58.6 + 1) = 8.0$ min and $2 \cdot 75/(0.2 \cdot 111.9 + 1) = 6.4$ min, respectively, whereas τ_{cle} for setpoints is 20 min. However, this does not take into account the *direction* of the disturbances. In our cases the disturbance condition number (Skogestad *et al.*, 1988) for the two disturbances are 11.5 and 1.8, respectively, whereas the "disturbance" condition number for the two setpoints are 111 and 89 (Skogestad and Morari, 1987). Thus, the disturbances are in the "good" directions of the plant, and the bandwidth requirements imposed by the disturbances are not as hard as computed above. However, the disturbances do put tighter restrictions at lower frequencies (the "slope two" requirement) than the setpoint requirement. This is also clear from the simulations discussed next.

In Fig. 2.9 controller $C_{\mu new}$ and $C_{\mu B}$ are compared with respect to disturbance rejection. The disturbances are in F (+30%) at time $t = 0$ and in z_F (+40%) at $t = 50$ min. Solid curves show the response for controller $C_{\mu new}$ and dashed curves are for controller $C_{\mu B}$. We note that controller $C_{\mu new}$ gives a rather sluggish return to the setpoint. This dominant (low-frequency) part of the response is significantly improved with the controller $C_{\mu B}$. The controller, $C_{\mu new}$ for approach A, could have been improved by using a performance weight, w_P, with slope two at intermediate frequencies. Also, note that the disturbance in z_F is simpler to reject because it is almost exclusively in the "good" direction.

Fig. 2.10 shows the setpoint response with and without model error (Eq. 2.27) for controller $C_{\mu B}$. We note that in terms of setpoints the response is *not* better than with

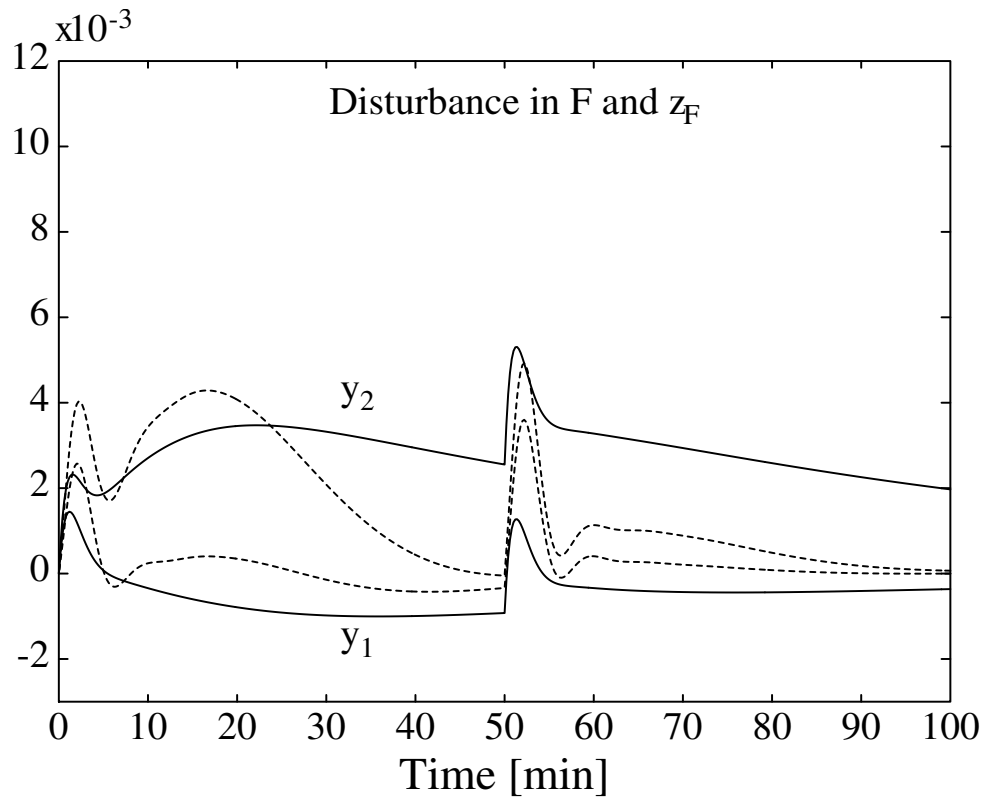

Figure 2.9: Simulation of a disturbance in F (+30%) at time $t = 0$ and in z_F (+40%) at $t = 50$ min using controller $C_{\mu new}$ (solid curves) and $C_{\mu B}$ (dashed curves). The input error in Eq. 2.27 is used in the simulations.

controller $C\mu new$ (Fig. 2.7).

2.6 Some comments on μ-synthesis

The μ-synthesis procedure employed today makes use of the upper bound of μ, trying to "solve"

$$\min_{C,D} ||DN_{RP}(C)D^{-1}||_\infty \tag{2.34}$$

The algorithm, often called "D-K iteration", is as follows:

1 Scale the original problem with a stable and minimum-phase transfer matrix D with appropriate structure.

2 Find a controller C by minimizing the H_∞-norm of $DN_{RP}(C)D^{-1}$.

3 Compute $\mu(N_{RP}(C))$ and obtain at each frequency the optimal "D-scales" from $\min_D \bar{\sigma}(DN_{RP}D^{-1})$.

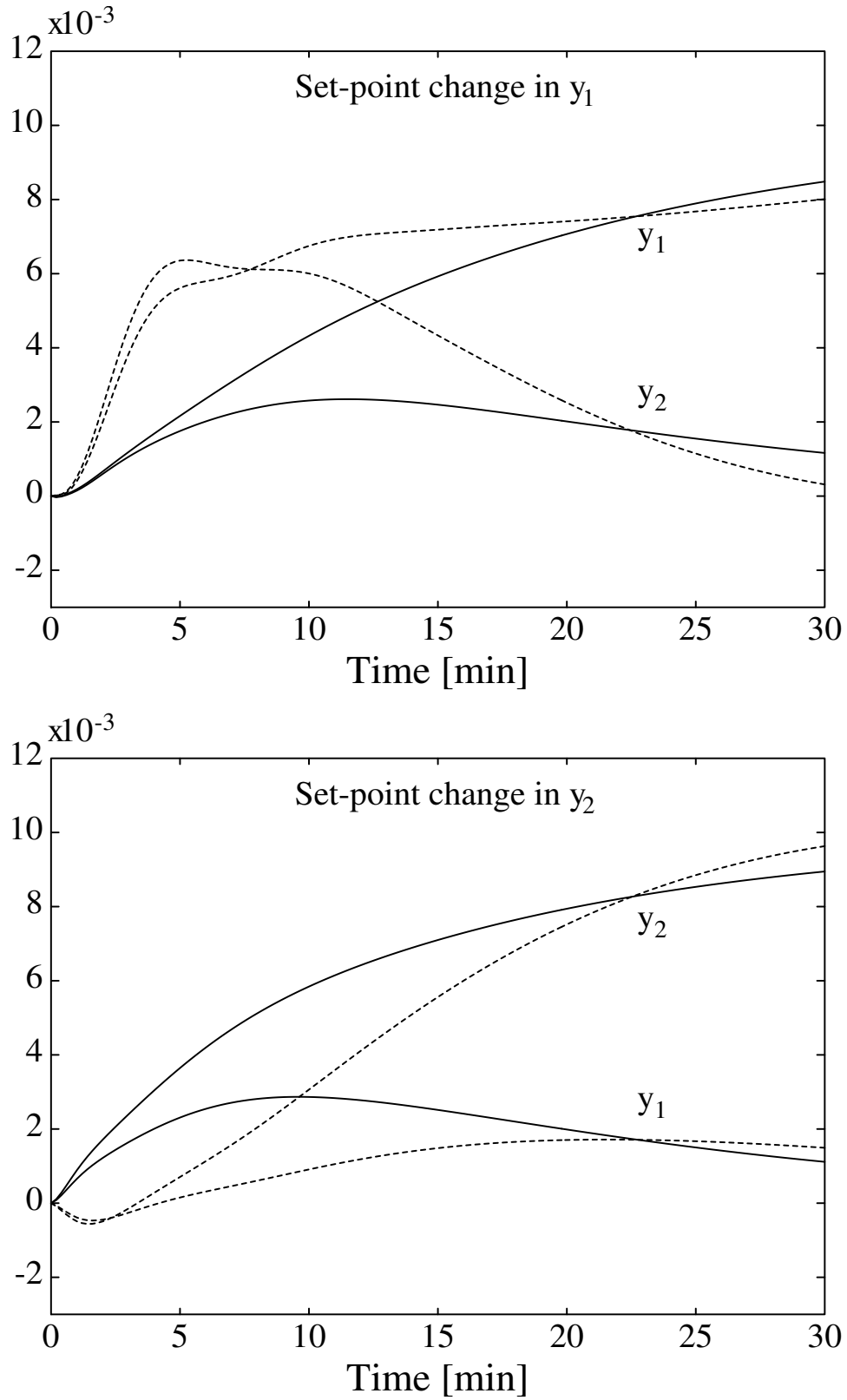

Figure 2.10: Simulation of setpoint changes using controller $C_{\mu B}$. Responses are shown both for nominal case (solid curves) and with input uncertainty given in Eq. 2.27 (dashed curves).

4 Fit the magnitude of each element of $D(\omega)$ to a stable and minimum- phase transfer function.

5 Test a stop criterion. Stop or go to 1.

The major problem with μ-synthesis is that the D-K iteration is not guaranteed to find the global optimum of Eq. 2.34. Both step 2 and step 3 in this algorithm are convex optimization problems, but this does not imply joint convexity for the whole algorithm (Doyle and Chu, 1985). A second problem is the difficulty to define a stop criterion for the optimization.

Good initial D-scales in step 1 of the algorithm, reduces the number of iterations, and may even, because of local minimas, affect the final minimum μ-value. For our example problem with the original problem definition, we observed that a natural physical scaling of the problem (using "logarithmic compositions" as discussed by Skogestad and Morari, 1988), that corresponds to multiplying all elements in $G(s)$ by a factor 100, gave very good initial D-scales. With this simple scaling the μ-value after the first iteration was 1.2, as compared to 14.9 without scaling. An other way to obtain good scalings is to start the algorithm at step 3 using a "good" controller obtained by any design method.

The D-K iteration depends heavily on optimal solutions in step 2 and 3, and also on good fits in step 4. The H_∞-design (step 2) generally works fine using the μ-toolbox. The μ software does sometimes not compute a sufficiently tight upper bound of μ. Thereby the D-scales are not optimal, and the D-K iteration suffers. We have experienced cases where, for some frequencies, the computed μ-value has been larger than the maximum singular value. When this occurs the D-K iteration often starts diverging.

The last critical factor is the fitting of the D-scales. It is important to get a good fit, preferably by a transfer function of low order. The software for D-scale fitting in the μ-toolbox requires that the user specifies the order of the transfer function and decides if the fit is good enough. The optimal order of the transfer function D varies as the D-K iteration progress. It is sometimes better to *increase* the order, and sometimes the order should be *decreased*. If it is difficult to obtain a good fit it often helps to use a different frequency range for the fit. It may also help to use a finer frequency grid.

The final problem is to determine when to stop the iteration. Two intuitive candidates for criterion for terminating the iteration are:
1) An iteration criterion

$$\mu_{\mathrm{k}-1} - \mu_{\mathrm{k}} < \epsilon_1 \tag{2.35}$$

and,
2) A "flatness" criterion

$$\max_{\omega}(\mu_{\mathrm{peak}} - \mu(\omega)) < \epsilon_2 \tag{2.36}$$

1) In Eq. 2.35 the subscript denotes the $\mathrm{k}-1^{\mathrm{th}}$ and the k^{th} iteration respectively. This is a standard criterion, the iteration terminates if the objective function (μ) does not improve. There are two problems with this criterion. First, we may have found a local

minimum, which means it is possible to improve μ by using a different D. Second, this criterion would terminate the iteration if μ increases. That may sound reasonable, but we have experienced situations where μ increases for a number of iterations and then start to decrease again. 2) Eq. 2.36 relies on the optimal controller giving a flat μ versus frequency plot. However, this is not always possible to obtain. For instance, the optimal solution to the problem in Skogestad *et al.* (1988) does not give a flat μ-plot, instead μ always goes to 0.5 at high frequencies (since S goes to I, and w_P goes to 0.5 I). As the number of iterations are increased one is able to extend the frequency where μ starts dropping down to 0.5, but the curve never becomes flat at all frequencies.

The results presented in this paper are obtained by terminating the D-K iteration when the H_∞-norm equals μ and μ is totally flat for frequencies less than 10 rad/min.

2.7 Conclusions

In this paper we have addressed performance weight selection when using the H_∞-norm. We have stressed the difference between an approach where we try to shape directly a few important transfer functions such as S and T, which gives us the opportunity to, for example, specify directly minimum and maximum bandwidth requirements (Approach A), and an approach where we consider the magnitude of signals (Approach B). The difference between the two performance approaches is probably most clear when one consider disturbance rejection; in this case the required bandwidth to achieve acceptable disturbance rejection is not clear (at least not for multivariable systems), and Approach B is preferable. An important advantage with Approach A, is that one may to some extent combine performance and robustness issues. For example, there may be bandwidth limitations related to robustness or the sampling time. With Approach B, robustness is generally handled by modelling the uncertainty explicitly and evaluating Robust Performance using the structured singular value. In practice, most engineers will probably use a combination of Approach A and B when selecting weights, but when doing this it is important to realize the different ways of thinking that are involved.

Acknowledgements. Support from NTNF is gratefully acknowledged.

Nomenclature

A - steady-state offset specification (Eq. 2.13)
$C(s)$ - controller
D - D-scaling matrix (Eq. 2.8)
$G(s)$ - linear model of process
k - controller gain
$M = \max_\omega \bar{\sigma}(S)(j\omega)$ - maximum peak of sensitivity function (Eq. 2.13)
NP - Nominal Performance
ODF - One Degree of Freedom

RP - Robust Performance
RGA - Relative Gain Array
RS - Robust Stability
$S(s) = (I + G(s)C(s))^{-1}$ - sensitivity function
$T(s) = G(s)C(s)(I + G(s)C(s))^{-1}$ - complementary sensitivity function
TDF - Two Degree of Freedom
w_P - performance weight (Eq. 2.13)

Greek symbols

$\|N\|_\infty = \sup_\omega \bar{\sigma}(N(j\omega))$ - H_∞-norm of N
Δ - complex perturbation matrix
δ - complex perturbation scalar
μ - structured singular value
$\mu_{RP} = \sup_\omega \mu(N_{RP}(j\omega))$
$\bar{\sigma}$ - maximum singular value
τ - time constant
τ_{cl} - (maximum) closed-loop time constant
τ_D - controller derivative time constant [min]
τ_I - controller integral time constant [min]
ω - frequency [rad/min]
Also see Fig. 2.3

References

[1] Balas, G.J, Doyle, J.C., Glover, K., Packard, A.K. and Smith, R. (1990). "Manual to μ-Analysis and Synthesis Toolbox, Beta Test Version", MUSYN Inc., Minneapolis, MN.

[2] Chiang, R.Y. and Safonov, M.G. (1988). "Robust-control toolbox for MATLAB. User's guide", The MathWorks Inc., South Natick, MA.

[3] Chiang, R.Y., Safonov, M.G. and Tekawy, J.A. (1990). "H^∞ flight control design with large parametric robustness", *Proc. ACC*, San Diego, CA, 2496-2501.

[4] Doyle, J.C. (1982). "Analysis of Feedback Systems with Structured Uncertainties", *IEE Proc.*, **129**, Part D, 242-250.

[5] Doyle, J.C. (1985). "Structured uncertainty in control system design", *Proc. IEEE Conf. Decision Contr.*, Ft. Lauderdale, FL.

[6] Doyle, J.C. (1987). "A review of μ for case studies in robust control", *Preprints 10th IFAC World Congress on Automatic Control*, Munich, Germany, Vol.8, 395-402.

[7] Doyle, J.C. and Chu, C. (1985). "Matrix interpolation and H_∞ performance bounds", *Proc. American Control Conference*, Boston, MA, 129-134.

[8] Doyle, J.C., Lenz, K. and Packard, A.K. (1987). "Design examples using μ-synthesis: Space shuttle lateral axis FCS during reentry", NATO ASI Series, vol. F34, "Modelling, Robustness and Sensitivity Reduction in Control Systems", R.F. Curtin, Editor, Springer-Verlag, Berlin-Heidelberg.

[9] Doyle, J.C., Glover, K., Khargonekar, P. and Francis, B. (1989). "State-space solutions to standard H_2 and H_∞ control problems", *IEEE Trans. Autom. Control*, **34**, 8, 831-847.

[10] Freudenberg, J.S. (1989). "Analysis and design for ill-conditioned plants, Part 2. Directionally uniform weightings and an example", *Int. J. Control*, **49**, 3, 873-903.

[11] Grace, A. (1990). "Optimization toolbox for MATLAB. User's guide", The MathWorks Inc., South Natick, MA.

[12] Kwakernaak, H. and Siwan, R. (1972). Linear Optimal Control Systems, New York: Wiley.

[13] Lundström, P., Skogestad, S., Hovd, M. and Wang Z.-Q. (1991). "Non-uniqueness of robust H_∞ decentralized control", *Proc. American Control Conference*, Boston, 1830-1835.

[14] McFarlane, D.C. and Glover, K. (1990). "Lecture Notes in Control and Information Science", **138**, Springer-Verlag, Berlin, Germany.

[15] Mejdell, T. (1990). "Estimators for product composition in distillation columns", Ph.D. Thesis, Univ. of Trondheim, NTH, Norway.

[16] Skogestad, S. and Lundström, P. (1990). "Mu-optimal LV-control of distillation columns", *Computers chem Engng.*, **14**, 4/5, 401-413.

[17] Skogestad, S. and Morari, M., (1987). "Effect of disturbance directions on closed-loop performance", *Ind. Eng. Chem. Res.*, **26**, 10, 2029-2035.

[18] Skogestad, S. and Morari, M. (1988). "Understanding the Dynamic Behavior of Distillation Columns", *Ind. Eng. Chem. Res.*, **27**, 10, 1848-1862.

[19] Skogestad, S., Morari, M. and Doyle, J.C (1988). "Robust Control of Ill-conditioned Plants: High-purity Distillation", *IEEE Trans. Autom. Control*, **33**, 12, 1092-1105 (Also see correction to μ-optimal controller in **34**, 6, 672).

[20] Yaniv, O. and Barlev, N. (1990). "Robust non iterative synthesis of ill-conditioned plants", *Proc. of 1990 American Control Conference*, San Diego, 3065-3066.

[21] Yue, A. and Postlethwaite, I. (1988). "H^∞-optimal design for helicopter design", *Proc. of 1988 American Control Conference*, Atlanta, 1679-1684.

[22] Zhou, K., Doyle, J.C., Glover, K. and Bodenheimer, B. (1990). "Mixed H_2 and H_∞ control", Proc. American Control Conference, San Diego, CA, 2502-2507.

Appendix 1

State space description of $C_{\mu new}(s) = C(sI - A)^{-1}B + D$. The controller has 22 states, 2 inputs and 2 outputs. The A matrix is given in tridiagonal form with the complex conjugate roots in real two by two form, *i.e.* A is a bandmatrix with all non-zero elements on the main diagonal and the two adjacent diagonals. The D matrix is a zero 2 by 2 matrix.

A:

row number	diagonal below main	main diagonal	diagonal above main
1		$-1.0000e-07$	0
2	0	$-1.0000e-07$	0
3	0	$-5.3681e-04$	0
4	0	$-6.8364e-04$	0
5	0	$-3.4883e-03$	0
6	0	$-5.5976e-02$	0
7	0	$-5.7017e-02$	0
8	0	$-2.0050e-01$	0
9	0	$-2.6267e-01$	$-1.1744e-01$
10	$1.1744e-01$	$-2.6267e-01$	0
11	0	$-4.8527e-01$	0
12	0	$-3.1117e+00$	$-6.9774e-01$
13	$6.9774e-01$	$-3.1117e+00$	0
14	0	$-1.9255e+01$	0
15	0	$-4.1007e+01$	0
16	0	$-1.1341e+02$	0
17	0	$-1.2966e+02$	$-8.7070e+01$
18	$8.7070e+01$	$-1.2966e+02$	0
19	0	$-1.3042e+02$	$-8.6556e+01$
20	$8.6556e+01$	$-1.3042e+02$	0
21	0	$-1.8112e+02$	0
22	0	$-6.3929e+05$	

B and C^T:

B column one	B column two	C row one	C row two
$8.5088e-01$	$1.0625e+00$	$9.6138e-01$	$-9.6366e-01$
$1.6792e+00$	$-1.3426e+00$	$1.5210e+00$	$1.5194e+00$
$2.6054e-02$	$-2.0838e-02$	$-2.3158e-02$	$-2.3122e-02$
$1.1099e-01$	$1.3877e-01$	$1.1712e-01$	$-1.1731e-01$
$-7.4077e-02$	$-9.2619e-02$	$7.4475e-02$	$-7.4592e-02$
$1.1255e+00$	$1.4072e+00$	$1.2294e+00$	$-1.2313e+00$
$6.1913e-01$	$-4.9518e-01$	$5.1127e-01$	$5.1046e-01$
$-1.4905e+00$	$-1.8635e+00$	$-1.6054e+00$	$1.6079e+00$
$-6.5002e+00$	$5.1989e+00$	$-5.6709e+00$	$-5.6620e+00$
$7.4959e+00$	$-5.9952e+00$	$-2.4034e+00$	$-2.3997e+00$
$-1.0500e+00$	$-1.3128e+00$	$-7.4675e-01$	$7.4792e-01$
$8.4252e-01$	$1.0534e+00$	$-6.4611e-01$	$6.4712e-01$
$-3.0556e+00$	$-3.8204e+00$	$-1.9699e-01$	$1.9730e-01$
$-8.0530e+01$	$6.4408e+01$	$5.4282e+01$	$5.4197e+01$
$4.1453e+01$	$-3.3154e+01$	$-3.3348e+01$	$-3.3296e+01$
$7.7061e+02$	$9.6349e+02$	$-1.7348e+02$	$1.7375e+02$
$-2.4073e+01$	$1.9254e+01$	$-1.8973e+02$	$-1.8944e+02$
$3.3649e+02$	$-2.6913e+02$	$2.4277e+01$	$2.4239e+01$
$-5.1808e+02$	$-6.4776e+02$	$-5.7626e+01$	$5.7717e+01$
$-3.8541e+02$	$-4.8188e+02$	$3.3056e+02$	$-3.3108e+02$
$1.3625e+03$	$1.7036e+03$	$2.8059e+02$	$-2.8103e+02$
$-1.2773e+04$	$-1.5970e+04$	$-1.4449e+04$	$1.4471e+04$

Appendix 2

This Appendix is not a part of the published paper, but has been added specifically for this thesis.

The purpose of this Appendix is to present a controller with less states and a slightly lower μ_{RP}-value than the controller in Appendix 1. We also want to demonstrate that presenting the "optimal" D-scales is a much more compact way of defining a controller than presenting the state space matrices as in Appendix 1.

In the paper we reported problems with obtaining good transfer function approximations, $D(s)$, of the frequency response D-scales, $D(j\omega)$, from the μ software. This software has now been improved, Balas *et al.* (1991). After some iterations with the new software we obtained a controller with $\mu_{RP} = 0.9735$, as compared to the old result 0.978, and with 18 states, which is 4 states less than the old controller. This new controller can be obtained by H_∞-synthesis for a D-scaled problem with the following "optimal" D-scales and the desired H_∞-norm ("gamma value") set equal to 0.9735.

$$D(s) = \text{diag}\{d(s), d(s), I_{2\times 2}\} \tag{2.37}$$

$$d(s) = 2.0 * 10^{-5} \frac{(s+1000)(s+0.25)(s+0.054)}{(s+0.67+j0.56)(s+0.67-j0.56)(s+0.013)} \tag{2.38}$$

Note that these D-scales are for *unstructured* uncertainty. In the paper we mentioned that both structured and unstructured uncertainty yield the same μ_{RP} value for the studied example, but we did not present any explanation to this phenomenon. Later, Hovd *et al.* (1993) have proved that the uncertainty structure does not affect μ for this problem.

References

Balas, G.J, Doyle, J.C., Glover, K., Packard, A.K. and Smith, R. (1991).
"The μ-Analysis and Synthesis Toolbox", The MathWorks Inc., Natick, MA.

Hovd, M., Braatz R.D. and Skogestad S. (1993).
"On the structure of the robust optimal controller for a class of problems", *Preprints IFAC World Congress on Automatic Control*, Sydney, Australia.

Chapter 3

Models of Gain and Delay Uncertainty for the Structured Singular Value Framework

Petter Lundström, Zi-Qin Wang and Sigurd Skogestad

Chemical Engineering,
University of Trondheim, NTH,
N-7034 Trondheim, Norway

Extended and revised version of
Modelling of Gain and Delay Uncertainty in the Structured Singular Value Framework
presented at *12th World Congress IFAC*, Sydney, Australia, 18-23 July 1993

Abstract

Gain and delay uncertainty is commonly used to quantify plant-model mismatch in the process control community. This parametric uncertainty description cannot be directly used for robustness analysis and controller synthesis in the structured singular value (μ) framework. This paper provides tight approximations of gain and delay uncertainty on linear fractional form, suitable for the μ-framework. The derived uncertainty models are divided into four classes with different restrictions imposed on perturbations and weight functions. Complex perturbations and rational weights yield the most useful uncertainty models from a practical engineering point of view. However, irrational weights allow tighter uncertainty models. Real perturbations also allow tighter uncertainty models, but makes it much harder to compute μ. A distillation example is used to illustrate differences between the derived uncertainty models.

3.1 Introduction

The structured singular value, μ (Doyle, 1982), has proven to be a very powerful tool for robustness analysis of linear feedback systems (*e.g.* Skogestad *et al.*, 1988). μ provides, by definition, a *necessary* and *sufficient* condition for robustness of a set of "possible" plants. The μ-robustness condition may be formulated as a Robust Stability (RS) test or as a Robust Performance (RP) test, using the $\mathcal{H}_\infty$-norm to specify the required performance. The test is a "worst-case" test and the underlying assumption for necessity and sufficiency of the robustness condition is that the uncertainty description is "tight", *i.e.* the set of "possible" plants used in the test should include *only* plants of interest, for necessity, and *all* plants of interest, for sufficiency.

In the process control community it is very common to quantify plant-model mismatch in terms of gain and delay uncertainty. This uncertainty description generates a set $\Pi(s)$ of "possible" plants $\hat{g}$

$$\Pi(s) = \left\{ \hat{g}(s) \,\middle|\, \hat{g}(s) = ke^{-\theta s} \;;\; k \in [k_{min},\ k_{max}] \;,\; \theta \in [\theta_{min},\ \theta_{max}] \right\}. \qquad (3.1)$$

The uncertainty set Π cannot be directly used in the μ framework, but has to be transformed (approximated) into the linear fractional form shown in Fig. 3.1. A robustness test based on an approximation of Π may yield a conservative result, or a too optimistic result, depending on how well Π is approximated. It is therefore important to obtain a tight approximation of Π. One may of course argue that an exact representation of Π is not very important for controller analysis and design, since the gain-delay uncertainty itself is only an approximation of the actual plant-model mismatch. However, from an engineering point of view, a collection of tight "off the shelf" models for commonly used uncertainty descriptions is very useful and will substantially reduce the effort associated with analysis and synthesis of robust controllers. From a theoretical point of view, it is interesting and useful to find the limits for how well the gain and delay uncertainty set may be approximated into a linear fractional form.

The purpose of this paper is then to

1. Derive and present some tight linear fractional models of the gain and delay uncertainty set Π (Eq. 3.1).

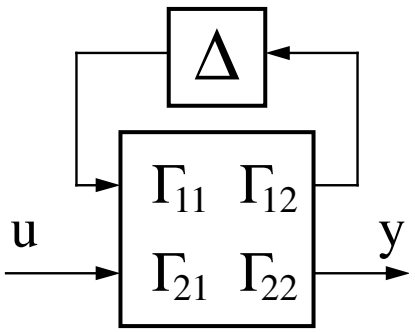

Figure 3.1: Linear fractional uncertainty

2. Demonstrate the difference between modelling with complex and real perturbations, Δ, as well as with rational and irrational weights, Γ.

In the μ framework each uncertainty is modelled as a "norm bounded linear fractional perturbation" as illustrated in Fig. 3.1, where Δ is an unknown perturbation with bounded magnitude. The perturbation Δ and the interconnection matrix Γ forms a Linear Fractional Transformation (LFT) which defines a set of possible mappings from input u to output y.

$$y = F_u(\Gamma, \Delta)u = [\Gamma_{22} + \Gamma_{21}\Delta(I - \Gamma_{11}\Delta)^{-1}\Gamma_{12}]u \tag{3.2}$$

A plant model may include several uncertainties at different locations, which may be combined into one big LFT and a *block diagonal* perturbation matrix, Δ, *i.e.* a Δ with a specific *structure*. The structured singular value, μ, was introduced as a refinement of the $\mathcal{H}_\infty$-norm stability condition, which measures stability with respect to an *unstructured* perturbation matrix Δ, *i.e.* without utilizing locational information about the uncertainties. The main reason for introducing $\mathcal{H}_\infty$ methods for controller design and analysis was to obtain a framework where *non-parametric* uncertainties could be dealt with, *i.e* uncertainties that cannot be assigned to a specific uncertain parameter, but may be viewed as uncertain frequency domain data. This type of uncertainty is modelled using complex perturbations. However, while the $\mathcal{H}_\infty$ condition can only deal with non-parametric uncertainties (complex perturbations), μ may deal with both parametric and non-parametric uncertainties (mixed real/complex perturbations).

Using mixed real/complex uncertainty perturbations we may derive tighter (less conservative) uncertainty descriptions than with pure complex perturbations. However, the *mathematical* properties of μ are better for pure complex perturbations, so the tightness gained by modelling with mixed perturbations may be lost when computing the upper and lower bounds on a "mixed" μ.

The term "structured uncertainty" is here used to denote that the perturbation matrix Δ has a structure. In the literature "structured uncertainty" is sometimes used to denote *parametric* uncertainty and "unstructured uncertainty" is sometimes used to denote *non-parametric* uncertainty.

The uncertainty models $F_u(\Gamma, \Delta)$ presented in this paper are divided into four classes based on different restrictions imposed on Γ and Δ as illustrated in Table.3.1, where C = complex, M = mixed, R = rational and I = irrational..

Table 3.1: Classes of uncertainty models.

	$\Gamma(s)$	$\Gamma(j\omega)$
Δ complex	CR	CI
Δ mixed	MR	MI

In class CR all perturbations are complex and all weights are rational transfer functions of the Laplace operator s. This class of uncertainty models may be used for both analysis and synthesis and is therefore the most useful from a practical point of view. However, when it comes to deriving tight uncertainty models, CR is the most restrictive class, since real perturbations are not allowed and all weights have to be rational. In class CI irrational transfer functions may be used, which allows tighter uncertainty models to be derived, but these models can not be used for synthesis. Class MR also yields tighter models than CR, however, the tightest models are obtained in class MI where both complex and real perturbations may be used, in combination with both irrational and rational weights.

Gain and delay uncertainty modelling in the μ framework has previously been studied by Laughlin *et al.* (1986,1987), Lundström *et al.* (1991) and Wang *et al.* (1994). Laughlin *et al.* studied gain-delay and time constant uncertainty for a first order system with dead time. They restricted their study to complex perturbations and rational weights (class CR) and fixed the nominal model to be equal to the parametric average model. Lundström *et al.* (1991) defined an uncertainty set in class CI where the nominal model was chosen in order to minimize the uncertain disk shaped region generated on the complex plane, and presented a numerical solution to this problem. In the present paper we present an analytical solution to the same problem. Wang *et al.* (1994) studied several gain and delay uncertainty models in class CR, evaluating what kind of model properties that are advantageous for μ synthesis. They demonstrated that it is not trivial to choose the "best" approximation of some given uncertainty. They also showed that μ-optimal controllers seem to be very sensitive to unconsidered (uncovered) possible plants. This means that too "optimistic" uncertainty models should be avoided.

The paper is organized as follows. In section 3.2 the structured singular value framework is briefly reviewed. In section 3.3 the gain-delay uncertainty models are derived. In section 3.4 an example process from the literature (Skogestad *et al.*, 1988) is used to evaluate the derived uncertainty models. Finally, the obtained results are discussed and the conclusions are presented.

3.2 The μ-framework

This section gives a very brief overview of the structured singular value framework, focusing on issues with special importance for this paper. A detailed introduction to the mathematical aspects of μ for complex perturbations is found in Packard and Doyle (1993). Computation of bounds on μ for mixed real/complex perturbations is treated in Fan *et al.* (1991) and Young *et al.* (1991). Introductions to μ focusing on control aspects are available in Skogestad *et al.* (1988), Stein and Doyle (1991) and Balas *et al.* (1991), for example.

The general problem formulation in the μ framework is illustrated in Fig. 3.2. The left block diagram consists of an augmented plant P (including nominal plant model

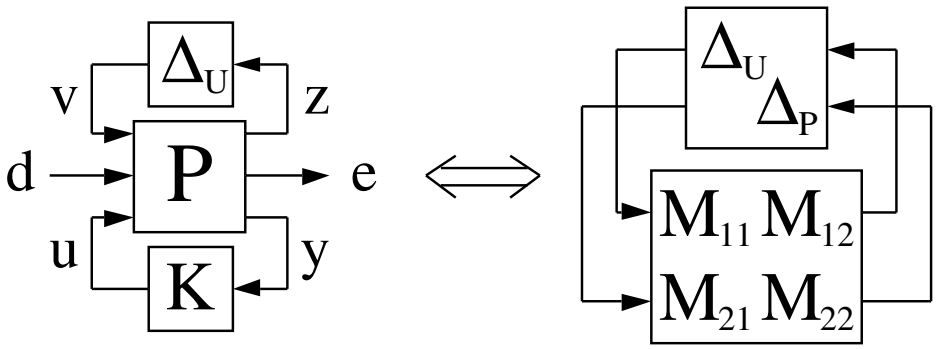

Figure 3.2: General problem description

and weight functions), a controller K, and a (block-diagonal) perturbation matrix $\Delta_U = \text{diag}\{\Delta_1, \cdots, \Delta_n\}$ representing uncertainty. $\mathbf{d}$ is a vector of external input signals (*e.g.* disturbances and set-points). $\mathbf{e}$ is a vector of output signals which should be kept small (*e.g.* manipulated inputs and deviation from set-points). The weights in P are used to specify performance requirements and to normalize each Δ_i to be less than one in magnitude at each frequency.

The right block diagram in Fig. 3.2 is used for robustness analysis. M is a function of P and K, and Δ_P is a fictitious "performance perturbation" connecting $\mathbf{e}$ to $\mathbf{d}$. Provided that the closed loop system is nominally stable the conditions for RS and RP are:

$$RS \quad \Leftrightarrow \quad \mu_{RS} = \sup_{\omega} \mu_{\Delta_U}(M_{11}(j\omega)) < 1 \tag{3.3}$$

$$RP \quad \Leftrightarrow \quad \mu_{RP} = \sup_{\omega} \mu_{\Delta}(M(j\omega)) < 1 \tag{3.4}$$

where $\Delta = \text{diag}\{\Delta_U, \Delta_P\}$.

The following remarks are important for this paper:

1. The μ framework can only deal with linear fractional uncertainties (LFT, Eq. 3.2).

2. The *necessity* of the μ robustness conditions requires that the uncertainty description includes *only* "allowed" uncertainties.

3. The *sufficiency* of the μ robustness conditions requires that the uncertainty description includes *all* "allowed" uncertainties.

4. μ can generally not be computed exactly, but tight computable upper and lower bounds on μ exist for pure complex perturbations.

5. Bounds on μ for mixed real/complex perturbations is much more difficult to compute than for pure complex perturbations.

6. μ analysis is performed on a frequency by frequency basis, while μ synthesis is performed in a state-space setting (Balas *et al.* 1991). For analysis it is therefore sufficient to obtain the frequency response of the interconnection matrix M, which means that even irrational uncertainty models may be used. For μ synthesis, M has to be a finite dimensional state-space model. Because of this, tighter bounds may be derived for analysis than for synthesis.

7. At present there is no μ synthesis method for systems where the perturbation matrix Δ includes real entries.

8. $\mu_{RP} = 0.8$ means that the uncertainty perturbations in Δ_U could be increased by a factor $1/0.8 = 1.25$ (*i.e.* a larger uncertainty set) and still the performance specifications would be satisfied by a margin of 1.25. The performance margin for the *specified uncertainty set*, i.e. $||\Delta_U||_\infty \leq 1$ may be computed using a "skewed μ" (Packard 1988), here denoted J and defined by

$$J(\omega) = \left\{ J(\omega) \left| \mu \left(\begin{bmatrix} M_{11}(\omega) & M_{12}(\omega) \\ J(\omega)^{-1} M_{21}(\omega) & J(\omega)^{-1} M_{22}(\omega) \end{bmatrix} \right) = 1 \right. \right\} \tag{3.5}$$

$J = 0.8$ means that the performance is satisfied by a margin of 1.25 for $||\Delta_U||_\infty \leq 1$.

3.3 Uncertainty Models

In this section we derive linear fractional uncertainty models which approximates the gain and delay uncertainty set Π defined in Eq.3.1. The models derived here are divided into the four classes defined in Table 3.1. We start with models based on purely complex perturbations and continue with mixed real-complex perturbations. The following notation is used:

$$\bar{k} = \frac{k_{max} + k_{min}}{2} \tag{3.6}$$

$$\bar{\theta} = \frac{\theta_{max} + \theta_{min}}{2} \tag{3.7}$$

$$k_\delta = \frac{k_{max} - k_{min}}{2} \tag{3.8}$$

$$\theta_\delta = \frac{\theta_{max} - \theta_{min}}{2} \tag{3.9}$$

$$k_r = \frac{k_{max} - k_{min}}{k_{max} + k_{min}} \tag{3.10}$$

$$\theta^\star = \max\{|\theta_{min}|,\ |\theta_{max}|\} \tag{3.11}$$

$\bar{k}$ and $\bar{\theta}$ are the average gain and delay, respectively, k_δ and θ_δ are the maximum *absolute* gain and delay errors, k_r is the *relative* gain error and $\theta^\star$ is the maximum

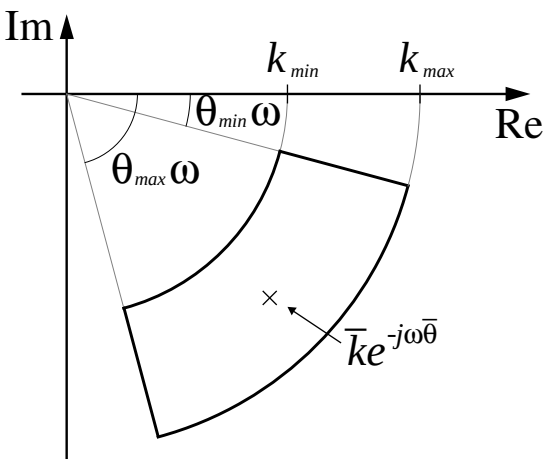

Figure 3.3: Gain and delay uncertainty template on the complex plane (set Π).

delay, if $|\theta_{max}| > |\theta_{min}|$, or the maximum *prediction*, if $|\theta_{max}| < |\theta_{min}|$. $\theta^\star$ is defined in order to obtain simple formulas which cover cases both *with* and *without* prediction error. If there is no prediction error, $\theta^\star$ may be replaced by θ_{max} in the following formulas.

3.3.1 The gain and delay uncertainty set

The set Π (Eq.3.1) maps onto a "template" on the complex plane at each frequency, as illustrated in Fig. 3.3. At zero frequency, $\omega = 0$, the entire set Π covers only a segment of the real axis, namely from k_{min} to k_{max}. At each frequency in the range $0 < \omega < 2\pi/|\theta_{max} - \theta_{min}|$, Π covers a segment of an annular region with center at $0 + j0$, inner radius k_{min} and outer radius k_{max}. At sufficiently high frequencies, $\omega \geq 2\pi/|\theta_{max} - \theta_{min}|$, Π will cover the entire annular region defined above.

The set Π may in principle be *exactly* described by

$$\Pi = \{(\bar{k} + k_\delta \Delta_k) e^{-(\bar{\theta} + \theta_\delta \Delta_\theta)s} \ ; \ -1 \leq \Delta_k \leq 1 \ , \ -1\Delta_\theta \leq 1\} \tag{3.12}$$

where Δ_k and Δ_θ are *real* scalars. However, this representation cannot be written as an LFT (Eq.3.2) due to the delay uncertainty where Δ_θ enters in the exponent. The expression in Eq.3.12 is therefore not suitable for the μ-framework.

3.3.2 Complex uncertainty, irrational weight

The simplest way to represent Π within the μ-framework is by a nominal plant model subject to a single complex additive or multiplicative perturbation, which generates a "disk"-shaped region on the complex plane at each frequency. In this section three different choices of nominal models are considered and for each of them analytical expressions for the smallest perturbation needed to *cover* every plant in Π are presented.

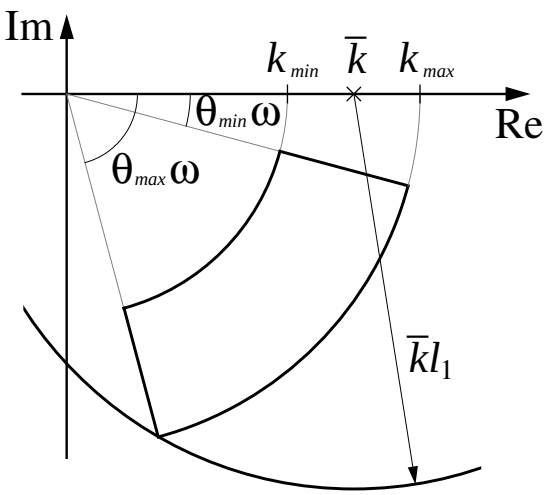

Figure 3.4: Disk with delay free nominal model (set Π_{CI1}).

i.e. these models yield sufficient conditions for robustness with respect to the original set Π. For all three models, Δ is complex and $|\Delta(j\omega)| \leq 1 \forall \omega$.

Set Π_{CI1} : Delay free nominal model.
Multiplicative uncertainty with nominal model $\bar{k}$.

$$\Pi_{\text{CI1}} = \{\hat{g}(j\omega) | \hat{g}(j\omega) = \bar{k}[1 + l_1(\omega)\Delta(j\omega)]\} \tag{3.13}$$

$$l_1(\omega) = \begin{cases} |(1+k_r)e^{-j\theta^\star\omega} - 1| = \sqrt{k_r^2 + 2(1+k_r)(1-\cos(\theta^\star\omega))} & \text{for } \omega < \pi/\theta^\star \\ 2 + k_r & \text{for } \omega \geq \pi/\theta^\star \end{cases} \tag{3.14}$$

Set Π_{CI2} : Average gain and delay in nominal model.
Multiplicative uncertainty with nominal model $\bar{k}e^{-j\omega\bar{\theta}}$.

$$\Pi_{\text{CI2}} = \{\hat{g}(j\omega) | \hat{g}(j\omega) = \bar{k}e^{-j\omega\bar{\theta}}[1 + l_2(\omega)\Delta(j\omega)]\} \tag{3.15}$$

$$l_2(\omega) = \begin{cases} |(1+k_r)e^{-j\omega\theta_\delta} - 1| = \sqrt{k_r^2 + 2(1+k_r)(1-\cos(\theta_\delta\omega))} & \text{for } \omega < \pi/\theta_\delta \\ 2 + k_r & \text{for } \omega \geq \pi/\theta_\delta \end{cases} \tag{3.16}$$

Set Π_{CI3} : Smallest disk that covers Π.
This set may be represented as additive uncertainty with an irrational nominal model. A pure multiplicative description cannot be used because the nominal model is 0 at high frequencies. We use a mixed multiplicative/additive representation.

$$\Pi_{\text{CI3}} = \{\hat{g}(j\omega) | \hat{g}(j\omega) = \bar{k}e^{-j\omega\bar{\theta}}[m_3(\omega) + l_3(\omega)\Delta(j\omega)]\} \tag{3.17}$$

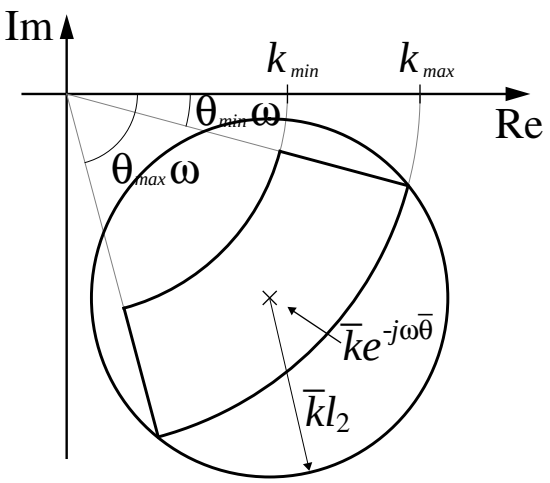

Figure 3.5: Disk with average gain and delay in nominal model (set Π_{CI2}).

$m_3(\omega)$ and $l_3(\omega)$ are obtained by minimizing

$$\min_{m_3(\omega)} l_3(\omega) \ , \ \text{s.t. } \Pi \subset \Pi_{\text{CI3}} \ , \ \forall\omega \tag{3.18}$$

This constrained optimization may be solved analytically and yields

ω	$m_3(\omega)$	$l_3(\omega)$
ω_A	$\frac{1}{\cos(\theta_\delta\omega)}$	$\sqrt{k_r^2+\tan^2(\theta_\delta\omega)}$
ω_B	$(1+k_r)\cos(\theta_\delta\omega)$	$(1+k_r)\sin(\theta_\delta\omega)$
ω_C	0	$1+k_r$

where $0 \le \omega_A < \frac{1}{2\theta_\delta}\arccos\left(\frac{1-k_r}{1+kr}\right) \le \omega_B < \frac{\pi}{2\theta_\delta} \le \omega_C$.

Comparison of the sets

Π_{CI1} and Π_{CI2} are special cases of the uncertainty model studied by Laughlin *et al.* (1987). The two sets are identical if $\theta_{max} = -\theta_{min}$.

Π_{CI1} generates the largest disk on the complex plane at each frequency, of the three sets above, and Π_{CI3} generates the smallest, *i.e.* $l_1(\omega) \ge l_2(\omega) \ge l_3(\omega)\ \forall\omega$, as shown in Fig. 3.7. Π_{CI1} and Π_{CI2} have equally large radii at high frequencies, $2+k_r$, while the radius of Π_{CI3} is only $1+k_r$. Intuitively, one may believe that Π_{CI3} is the least conservative approximation of Π, since it is the smallest at each frequency. However, this is not necessarily the case, it is not the *size* of the set, but the *worst case plant* within the set that matters, and there are plants (possibly "worst-case") within the smallest set Π_{CI3} which do not belong to the larger sets Π_{CI1} and Π_{CI2}, as illustrated in Fig. 3.8.

There is no unique parametrization of the Γ interconnection matrix for the sets above, but the following parametrizations are valid.

$$\Gamma_{\text{CI1}}(j\omega) = \begin{bmatrix} 0 & l_1(\omega) \\ \bar{k} & \bar{k} \end{bmatrix} \tag{3.19}$$

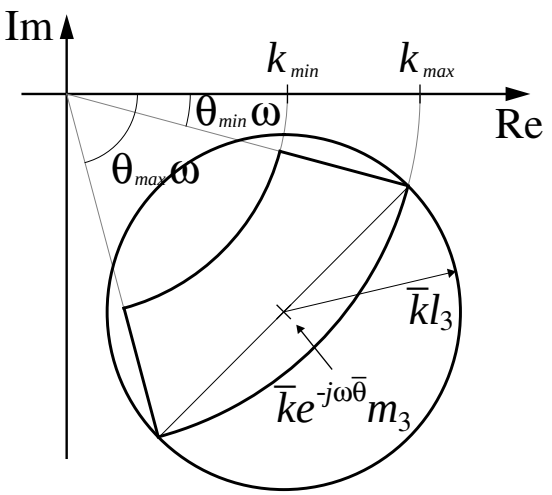

Figure 3.6: Smallest disk that covers Π (set Π_{CI3}).

$$\Gamma_{\text{CI2}}(j\omega) = \begin{bmatrix} 0 & l_2(\omega) \\ \bar{k}e^{-j\omega\bar{\theta}} & \bar{k}e^{-j\omega\bar{\theta}} \end{bmatrix} \tag{3.20}$$

$$\Gamma_{\text{CI3}}(j\omega) = \begin{bmatrix} 0 & l_3(\omega) \\ \bar{k}e^{-j\omega\bar{\theta}} & \bar{k}e^{-j\omega\bar{\theta}}m_3(\omega) \end{bmatrix} \tag{3.21}$$

$\Gamma_{\text{CI1}}(j\omega)$ has only one irrational element, $l_1(\omega)$, while $\Gamma_{\text{CI2}}(j\omega)$ has two, $l_2(\omega)$ and $e^{-j\omega\bar{\theta}}$, and $\Gamma_{\text{CI3}}(j\omega)$ has three, $l_3(\omega)$, $e^{-j\omega\bar{\theta}}$ and $m_3(\omega)$.

3.3.3 Complex uncertainty, rational weight

A proper rational transfer function $P(s)$ (Fig. 3.2) is required for μ-synthesis (DK-iteration) using the state-space $\mathcal{H}_\infty$ synthesis method (Doyle *et al.*, 1989). This means that neither of the uncertainty sets in the previous section can be used for synthesis, since all of them include irrational elements. To obtain an uncertainty model for synthesis we derive a proper rational transfer function $w_1(s)$ which is an upper bound of $l_1(\omega)$ in Π_{CI1}, $|w_1(j\omega)| \geq l_1(\omega)\ \forall\omega$. Substituting $l_1(\omega)$ by $w_1(j\omega)$ in Eq.3.13 yields the set Π_{CR} which is suitable for μ synthesis and covers every plant in Π.

Set Π_{CR} : Delay free nominal model with rational weight.

$$\Pi_{\text{CR}} = \{\hat{g}(s)|\hat{g}(s) = \bar{k}[1 + w_1(s)\Delta(j\omega)]\} \tag{3.22}$$

$$w_1(s) = \frac{(1+\frac{k_r}{2})\theta^\star s + k_r}{\frac{\theta^\star}{2}s + 1} \frac{\left(\frac{\theta^\star s}{c}\right)^2 + 2\zeta_z\left(\frac{\theta^\star s}{c}\right) + 1}{\left(\frac{\theta^\star s}{c}\right)^2 + 2\zeta_p\left(\frac{\theta^\star s}{c}\right) + 1} \tag{3.23}$$

The first part of $w_1(s)$ is derived from a first order Padé approximation[1], the second part is a second order correction factor used to obtain $\Pi \subset \Pi_{\text{CR}}$, *i.e.* $|w_1(j\omega)| \geq l_1(\omega)$. The

[1]

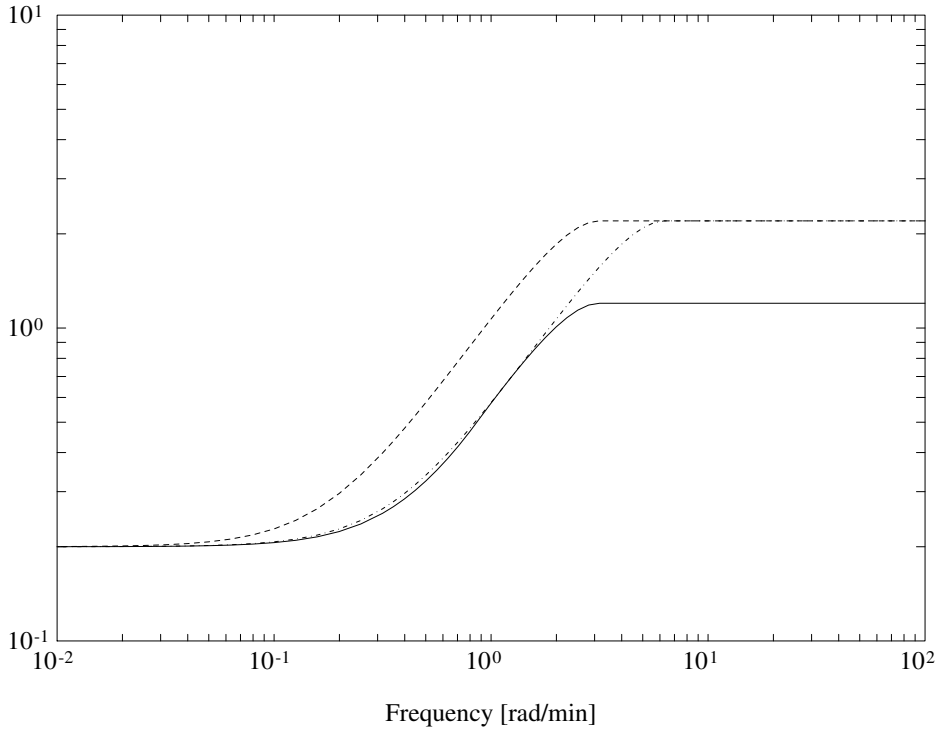

Figure 3.7: Comparison of $l_1(\omega)$ (dashed), $l_2(\omega)$ (dash-dot) and $l_3(\omega)$ (solid) for $k \in [0.8,\ 1.2]$ and $\theta \in [0,\ 1]$.

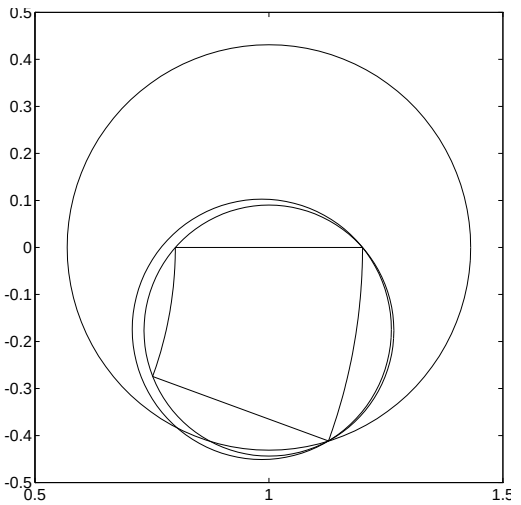

Figure 3.8: Comparison of Π (template), Π_{CI1} (largest disk), Π_{CI2} (second smallest disk) and Π_{CI3} (smallest disk) on the complex plane at $\omega = 0.35$ [rad/min] for $k \in [0.8,\ 1.2]$ and $\theta \in [0,\ 1]$.

Table 3.2: Maximum relative error, $\max_\omega \left\{ \frac{|w_1(j\omega)|-l_1(\omega)}{l_1(\omega)} \right\}$, for optimal and fixed parameters c, ζ_z and ζ_p for different k_r's.

	Optimal parameters (Eq.3.25)				Fixed (Eq.3.26)
k_r	c	ζ_z	ζ_p	error	error
0	2.3625	0.8376	0.6849	0.0202	0.0204
0.1	2.3740	0.8121	0.6644	0.0181	0.0211
0.2	2.3864	0.7889	0.6464	0.0163	0.0229
0.3	2.4022	0.7698	0.6324	0.0149	0.0256
0.4	2.4179	0.7528	0.6203	0.0137	0.0288
0.5	2.4327	0.7376	0.6098	0.0126	0.0324
0.6	2.4470	0.7233	0.6002	0.0115	0.0362
0.7	2.4600	0.7112	0.5924	0.0106	0.0401
0.8	2.4685	0.7075	0.5915	0.0104	0.0441
0.9	2.4758	0.7060	0.5925	0.0103	0.0480
1.0	2.4830	0.7046	0.5936	0.0103	0.0519

optimal values of c, ζ_z and ζ_p are dependent of k_r, but independent of $\theta^\star$. Numerical minimization of the worst case relative mismatch between $|w_1(j\omega)|$ and $l_1(\omega)$ over frequency for different values of k_r

$$\min_{c,\zeta_z,\zeta_p} \max_{\omega} \left\{ \frac{|w_1(j\omega)| - l_1(\omega)}{l_1(\omega)} \right\} \quad \text{s.t. } |w_1(j\omega)| \geq l_1(\omega) \ , \ \forall\omega \tag{3.25}$$

yields the results shown in Table 3.2 (100% relative gain uncertainty is of course unrealistic, but is included to make the table complete). As seen from Table 3.2 the optimal c, ζ_z and ζ_p do not vary much for different values of k_r. To simplify $w_1(s)$, we may therefore neglect the dependency of k_r and use fixed parameter values

$$c = 2.363, \ \zeta_z = 0.838 \text{ and } \zeta_p = 0.685 \tag{3.26}$$

The last column of Table 3.2 shows that fixed parameter values do not introduce much extra conservativeness. This is also demonstrated in Fig. 3.9, which shows that $|w_1(j\omega)|$ (dashed) is a very tight upper bound on $l_1(\omega)$ (solid) even when fixed parameter values (Eq.3.26) are used in the correction weight. Fig. 3.9 also demonstrates that the

$$\left| k_{max} e^{-\theta^\star s} - \bar{k} \right| \approx \bar{k} \left| (1+k_r) \frac{1 - \frac{\theta^\star s}{2}}{1 + \frac{\theta^\star s}{2}} - 1 \right| = \bar{k} \left| \frac{-\left(1 + \frac{k_r}{2}\right) \theta^\star s + k_r}{\frac{\theta^\star s}{2} + 1} \right| \tag{3.24}$$

Only the magnitude of the weight matters.

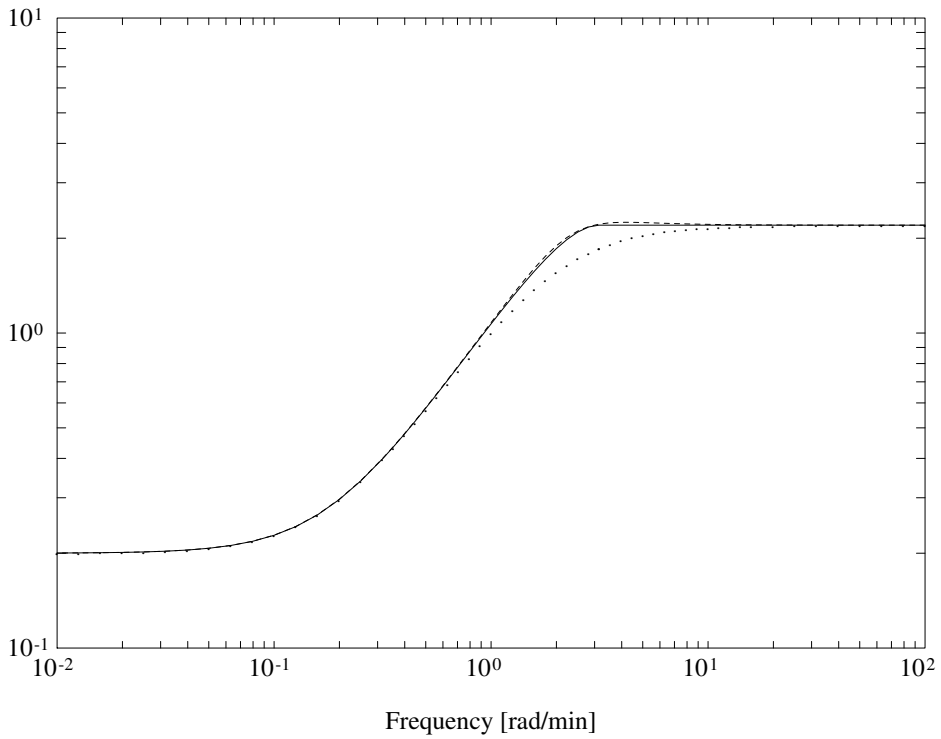

Figure 3.9: Comparison of the irrational uncertainty weight, $l_1(\omega)$ (solid), the approximation $|w_1(j\omega)|$ with fixed parameters (Eq.3.26) (dashed) and $|w_1(j\omega)|$ without correction factor (dotted). The plotted curves are for $k_r = 0.2$ and $\theta^\star = 1$ min.

correction factor in $w_1(s)$ is required in order to avoid a too optimistic weight (dotted).

To sum up, Π_{CR} is only slightly more conservative than Π_{CI1}, but may be used for both analysis and synthesis (DK-iteration).

3.3.4 Real uncertainty, irrational weight

In the previous sections all perturbations have been restricted to be complex. With real perturbations it is possible to derive tighter descriptions of Π by avoiding covering a template with a disk. In this section we allow real perturbations in Δ as well as irrational weights in Γ, *i.e.* the class of uncertainty models studied here is the least restrictive w.r.t. Δ and Γ.

To derive the uncertainty model presented in this section we start by approximating the uncertain delay (not including the nominal part) of Eq.3.12 using a first order Padé approximation.

$$e^{-j\theta_\delta \omega \Delta_\theta} \approx \frac{1 - \frac{j\theta_\delta}{2}\omega\Delta_\theta}{1 + \frac{j\theta_\delta}{2}\omega\Delta_\theta} \tag{3.27}$$

The Padé approximation may be represented by the block diagram shown in Fig. 3.10. The magnitude of the approximation is always correct, namely 1, while the phase of the

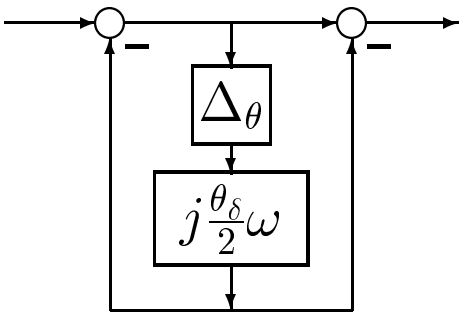

Figure 3.10: Block diagram representation of the Padé approximated delay uncertainty.

approximation lags behind the correct value. However, inspection of Fig. 3.10 shows that it is extremely simple to correct this if an irrational weight Γ may be used. We simply replace $\frac{\theta_\delta}{2}\omega$ in the block diagram by a function which is *defined* to give the correct phase. To find this function we use

$$e^{-j\theta_\delta\omega\Delta_\theta} = \frac{e^{-j\frac{\theta_\delta\omega}{2}\Delta_\theta}}{e^{+j\frac{\theta_\delta\omega}{2}\Delta_\theta}} = \frac{\cos(\frac{\theta_\delta\omega}{2}\Delta_\theta) - j\sin(\frac{\theta_\delta\omega}{2}\Delta_\theta)}{\cos(\frac{\theta_\delta\omega}{2}\Delta_\theta) + j\sin(\frac{\theta_\delta\omega}{2}\Delta_\theta)} = \frac{1 - j\tan(\frac{\theta_\delta\omega}{2}\Delta_\theta)}{1 + j\tan(\frac{\theta_\delta\omega}{2}\Delta_\theta)} \tag{3.28}$$

and obtain for $\omega < \frac{\pi}{\theta_\delta}$

$$\left\{e^{-j\theta_\delta\omega\Delta_1} \;;\; -1 \le \Delta_1 \le 1\right\} \Longleftrightarrow \left\{\frac{1 - j\tan(\frac{\theta_\delta\omega}{2})\Delta_2}{1 + j\tan(\frac{\theta_\delta\omega}{2})\Delta_2} \;;\; -1 \le \Delta_2 \le 1\right\} \tag{3.29}$$

So the desired function is $\tan(\frac{\theta_\delta\omega}{2})$. Note that $\Delta_1 \neq \Delta_2$ in Eq. 3.29, however the two *sets* are equivalent.

Set Π_{MI1} : Real uncertainty, average gain and delay in nominal model.

This uncertainty set may be used for frequencies $\omega < \frac{\pi}{\theta_\delta}$.

$$\Pi_{\text{MI1}} = \left\{\hat{g}(j\omega) \,\middle|\, \hat{g}(j\omega) = \bar{k}(1 + \Delta_k k_r)e^{-\bar{\theta}j\omega}\frac{1 - j\tan(\frac{\theta_\delta\omega}{2})\Delta_\theta}{1 + j\tan(\frac{\theta_\delta\omega}{2})\Delta_\theta} \;\;;\;\; -1 \le \Delta_k \le 1\,,\; -1 \le \Delta_\theta \le 1\right\} \tag{3.30}$$

where both Δ_k and Δ_θ are *real valued* perturbations.

Π_{MI1} may also be represented as shown in Fig. 3.11, using the following matrices.

$$\Gamma_k = \begin{bmatrix} 0 & k_r \\ \bar{k} & \bar{k} \end{bmatrix} \tag{3.31}$$

$$\Gamma_\theta = \begin{bmatrix} 1 & 0 \\ 0 & e^{-j\bar{\theta}\omega} \end{bmatrix} \quad \begin{bmatrix} -1 & 1 \\ -2 & 1 \end{bmatrix} \quad \begin{bmatrix} j\tan\frac{\theta_\delta\omega}{2} & 0 \\ 0 & 1 \end{bmatrix}$$

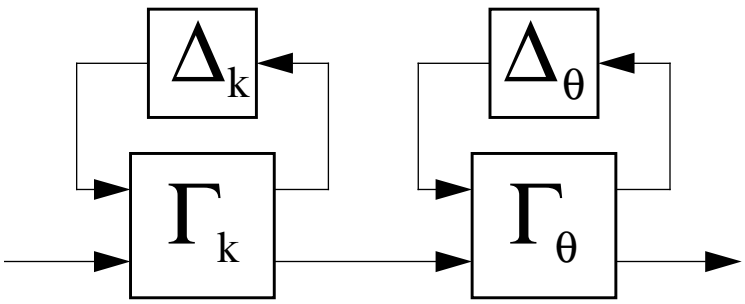

Figure 3.11: Uncertainty model with real Δ's

$$-1 \leq \Delta_k \leq 1 \text{ and } -1 \leq \Delta_\theta \leq 1 \tag{3.32}$$

The map of Π onto the complex plane is covered *exactly* by Π_{MI1} for frequencies $0 \leq \omega < \pi/\theta_\delta$, *i.e.* until Π covers 360 deg around the origin on the complex plane, and becomes an annular region. Often it is sufficient to analyze a system up to this frequency only, however, we may combine Π_{MI1} and Π_{CI3} to obtain an approximation of Π which is *non-optimistic* and *non-conservative* for *all* frequencies. The combined uncertainty set also belongs to class MI and we denote it Π_{MI2}. With non-optimistic and non-conservative we mean that the approximation shall include all plants in Π (non-optimistic) and may also include other plants if it can be guaranteed that these plants are not worst case plants (non-conservative).

Set Π_{MI2} : Non-optimistic non-conservative gain and delay uncertainty model.

$$\Pi_{\text{MI2}} = \begin{cases} \Pi_{\text{MI1}} & \text{for } \omega < \pi/2\theta_\delta \\ \Pi_{\text{CI3}}\ (m_3 = 0\ ,\ l_3 = 1 + k_r) & \text{for } \omega \geq \pi/2\theta_\delta \end{cases} \tag{3.33}$$

At low frequencies, Π_{MI2} covers Π exactly, using model Π_{MI1}. At high frequencies, $w \geq \pi/2\theta_\delta$, model Π_{CI3} is used, which *exactly* covers the annular region Π *and* the disk inside this region. However, including this interior disk does not introduce conservativeness since the worst case uncertainty is known to be at the boundary of the disk. Therefore, we know that the worst case plant within Π is also the worst case plant within Π_{MI2}. Note that Π_{CI3} is used in the frequency range $\pi/2\theta_\delta < \omega < \pi/\theta_\delta$ where both Π_{CI3} and Π_{MR} are valid. We do this because the complex set has better computational properties.

3.3.5 Real uncertainty, rational weight

At present there is no μ synthesis method for systems where the perturbation matrix Δ includes real entries. However, it seems likely that a possible future synthesis method will require a proper rational interconnection matrix $P(s)$, just like the present DK-iteration synthesis method for complex Δ's.

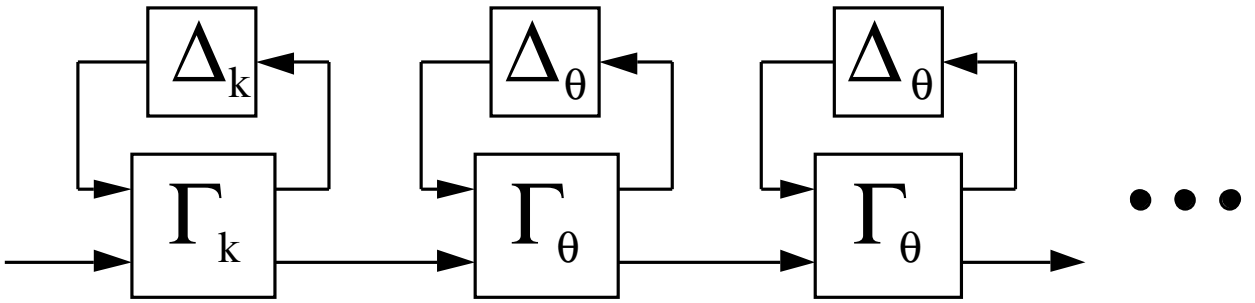

Figure 3.12: Uncertainty model with real Δ's

In this section we derive a model where the interconnection matrix Γ is restricted to be a proper rational transfer function. The gain uncertainty model in the previous section yields a proper rational interconnection matrix and does not have to be modified to fit the restriction imposed on Γ in this section. The delay model on the other hand has to be modified.

The following approximation of the time delay, including both the nominal and uncertain parts, yields a proper rational LFT.

$$e^{-(\bar{\theta}+\theta_\delta\Delta_\theta)s} \approx \left(\frac{1-\frac{\bar{\theta}}{2n}s-\frac{\theta_\delta\Delta_\theta}{2n}s}{1+\frac{\bar{\theta}}{2n}s+\frac{\theta_\delta\Delta_\theta}{2n}s}\right)^n = \left(\frac{1-\frac{\bar{\theta}}{2n}s}{1+\frac{\bar{\theta}}{2n}s}+\frac{-\frac{\theta_\delta}{n}s}{1+\frac{\bar{\theta}}{2n}s}\Delta_\theta\left[1-\frac{-\frac{\theta_\delta}{2n}s}{1+\frac{\bar{\theta}}{2n}s}\Delta_\theta\right]^{-1}\frac{1}{1+\frac{\bar{\theta}}{2n}s}\right)^n \tag{3.34}$$

In this form, the delay model requires n repeated real scalar Δ_θ's and $4n$ states, *i.e.* the representation is not minimal. We may, however, reduce the number of states to the minimal number n by utilizing the fact that the interconnection matrix Γ_θ may be written in a form where the state matrix A is the same for all four $\Gamma_{\theta,ij}$-elements and $B_{11}=B_{21},\ B_{12}=B_{22},\ C_{11}=C_{12}$ and $C_{21}=C_{22}$.

Set Π_{MR} : Real uncertainty, rational nth order delay approximation.

This uncertainty set may be represented as shown in Fig. 3.12 with n $F_u(\Gamma_\theta,\Delta_\theta)$'s in series, meaning that Δ_θ is an n *repeated* perturbation.

$$\Gamma_k = \begin{bmatrix} 0 & k_r \\ \bar{k} & \bar{k} \end{bmatrix} \tag{3.35}$$

$$\Gamma_\theta = \begin{bmatrix} \Gamma_{11} & \Gamma_{12} \\ \Gamma_{21} & \Gamma_{22} \end{bmatrix} = \left[\begin{array}{c|cc} A & B_{11} & B_{12} \\ \hline C_{11} & D_{11} & D_{21} \\ C_{21} & D_{21} & D_{22} \end{array}\right] = \left[\begin{array}{c|cc} -\frac{2n}{\bar{\theta}} & \frac{2n\theta_\delta}{\bar{\theta}^2} & \frac{2n}{\bar{\theta}} \\ \hline 1 & -\frac{\theta_\delta}{\bar{\theta}} & 0 \\ 2 & -\frac{2\theta_\delta}{\bar{\theta}} & -1 \end{array}\right] \tag{3.36}$$

$$-1 \le \Delta_k \le 1 \text{ and } -1 \le \Delta_\theta \le 1 \tag{3.37}$$

This set does not quite cover Π, but is a tight approximation. By increasing n, the number of Γ_θ's, an arbitrary close approximation may be obtained. However, in most practical applications a second order approximation would probably suffice. In many cases $\Pi_{\rm MR}$ is a *subset* of Π, *i.e.* $\Pi_{\rm MR}$ is an *inner* approximation and yields a *necessary* robustness conditions with respect to the original set Π. These special cases are:

1. The delay uncertainty includes both prediction and delay, *i.e.* $\theta_{min} < 0$ and $\theta_{max} > 0$, or
2. Either $\theta_{min} = 0$ or $\theta_{max} = 0$.

The parameterization of Γ_θ causes problems if:

1. $\theta_{max} = -\theta_{min} \Rightarrow \bar{\theta} = 0$, and some elements of Γ_θ will be infinite;
2. $\theta_{min} = 0 \Rightarrow (1 - \Gamma_{\theta,11}\Delta)^{-1}$ improper for $\Delta = -1$;
3. $\theta_{max} = 0 \Rightarrow (1 - \Gamma_{\theta,11}\Delta)^{-1}$ improper for $\Delta = 1$.

These problems are avoided by adding or subtracting a small quantity to θ_{min} or θ_{max}.

3.4 Distillation Example

The purpose of this section is to demonstrate the tightness of the uncertainty sets presented in the previous section. The example processes is a high-purity distillation column presented in Skogestad *et al.* (1988), however, here we let the uncertainty be *defined* in terms of gain-delay uncertainty, while Skogestad *et al.* defined the uncertainty in terms of a proper rational bound on a complex multiplicative perturbation.

3.4.1 Problem definition

The uncertain plant model is

$$\hat{G}(s) = \frac{1}{75s+1}\begin{bmatrix} 0.878 & -0.864 \\ 1.082 & -1.096 \end{bmatrix}\begin{bmatrix} k_1 e^{-\theta_1 s} & 0 \\ 0 & k_2 e^{-\theta_2 s} \end{bmatrix} \tag{3.38}$$

where

$$k_i \in [0.8,\ 1.2] \ \ ; \ \ \theta_i \in [0,\ 1] \ \ ; \ \ i = 1, 2 \tag{3.39}$$

i.e. 20% relative gain uncertainty and up to 1 min delay in each input channel.

The required performance is specified in terms of a frequency dependent bound, $W_p(s)$, on the sensitivity function $\hat{S} = (I + \hat{G}K)^{-1}$ for the worst case plant $\hat{G}$.

$$RP \Leftrightarrow \sup_{k_1,k_2,\theta_1,\theta_2} ||W_p(I + \hat{G}K)^{-1}||_\infty < 1 \tag{3.40}$$

$$W_p(s) = \frac{1}{2}\frac{(20s+2)}{(20s+10^{-3})} I_{2\times 2}. \tag{3.41}$$

3.4.2 Analysis

In this section we compare sets $\Pi_{\rm CR}, \Pi_{\rm CI1}, \Pi_{\rm CI2}, \Pi_{\rm CI3}, \Pi_{\rm MR}$ and $\Pi_{\rm MI2}$. The controller, used in this comparison, was synthesised by DK-iteration (Balas *et al.*, 1991) with uncertainty set $\Pi_{\rm CR}$ representing the gain-delay uncertainty in each input channel. Parameter values used in the uncertainty weight are the optimal values for $k_r = 0.2$, *i.e.* $c = 2.386$, $\zeta_z = 0.789$ and $\zeta_p = 0.646$, and the 'optimal' D-scales are

$$D(s) = \mathrm{diag}\{d(s), d(s), I_{2\times 2}\} \tag{3.42}$$

$$d(s) = 2.8 * 10^{-4} \frac{(s+69.6)(s+0.172)(s+0.071)}{(s+0.445+j0.61)(s+0.445-j0.61)(s+0.015)} \tag{3.43}$$

The controller yields $\mu_{RP} = 1.028$, so RP is almost satisfied.

The complex perturbation sets $\Pi_{\rm CR}, \Pi_{\rm CI1}, \Pi_{\rm CI2}$ and $\Pi_{\rm CI3}$ are all *outer* approximations of the gain-delay set Π. Because of this we know that upper bounds of J (Eq.3.5) for these approximations will yield upper bounds of $J(\Pi)$ (denotes J for uncertainty set Π). Similarly, since $\Pi_{\rm MR}$ is an *inner* approximation (for the uncertainty in this example), a lower bound of $J(\Pi_{\rm MR})$ yields a lower bound of $J(\Pi)$. Finally, both the upper and lower bounds of $J(\Pi_{\rm MI2})$ are also bounds of $J(\Pi)$, since $\Pi_{\rm MI2}$ is a non-optimistic and non-conservative approximation of Π.

Fig. 3.13 shows J for the distillation example where the uncertainty is modelled by sets $\Pi_{\rm CR}$ (solid), $\Pi_{\rm CI1}$ (dash-dot), $\Pi_{\rm CI2}$ (dotted), $\Pi_{\rm CI3}$ (dash), $\Pi_{\rm MR}$ (using $n = 2$) (dash-dot) and $\Pi_{\rm MI2}$ (solid). An interesting observation is that at most frequencies the tightest smallest upper and lower bounds are quite close to each other, *i.e.* $J(\Pi)$ is determined by rather tight bounds. At some frequencies between 0.01 and 0.1 [rad/min] $J(\Pi_{\rm CI3}) > J(\Pi_{\rm CR})$, which shows that at these frequencies the smaller set $\Pi_{\rm CI3}$ includes plants which are worse than any plant within the larger set $\Pi_{\rm CR}$. However, at most frequencies the smallest set $J(\Pi_{\rm CI3})$ yields the tightest upper bound on $J(\Pi)$. $J(\Pi_{\rm CR})$ and $J(\Pi_{\rm CI1})$ are almost identical for all frequencies except $1 < \omega < 20$, which is natural since $w_1(s)$ in $\Pi_{\rm CR}$ yields a very tight upper bound on $l_1(\omega)$ in $\Pi_{\rm CI1}$. Of the two lower bounds we see that $J(\Pi_{\rm MI2})$ is the tighter at most frequencies, in particular for $1 < \omega < \pi$. However, the upper bound obtained with uncertainty set $\Pi_{\rm MI2}$ is not very tight, which demonstrates the difficulties in computing upper bounds for real valued perturbations. At high frequencies we see that uncertainty set $\Pi_{\rm CI2}$ does not perform very well, but yields a J which oscillates between very high values and the values obtained for $\Pi_{\rm CI3}$.

3.5 Discussion

The only uncertainty model suitable for synthesis, presented in this paper, is $\Pi_{\rm CR}$ which has the advantage of a very simple nominal model with no delay. The main reason for not including any delay in the nominal model is to keep the order of $P(s)$ as low as possible, since a controller obtained by DK-iteration has the same number of states as

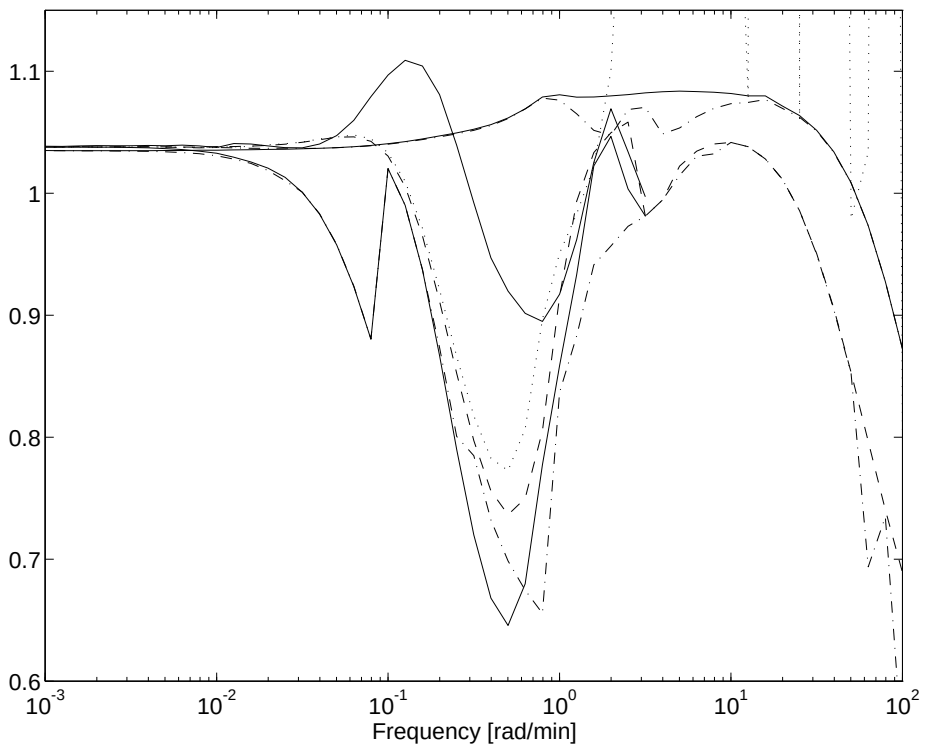

Figure 3.13: The "skewed μ" J as a function of frequency for different uncertainty sets.

the augmented plant $P(s)$ (Fig. 3.2) including the D-scales. Of the same reason, the correction factor in $w_1(s)$ (Eq.3.23) may be omitted when it is not necessary to cover every plant in Π. Another reason for not including any delay in the nominal model, when a rational model (Γ) is used, is to avoid approximation of this delay.

Set Π_{CI2}, where the average delay is included in the nominal model, could of course also be approximated by a rational model suitable fo synthesis. This is done by Laughlin *et al.* (1987), however, the result is often more conservative, as shown by Wang *et al.* (1994) and also illustrated in Fig. 3.13.

The analysis in section 3.4.2 is based on J (Eq.3.5) instead of μ, since a comparison based on μ may be misleading when different representations of a given uncertainty set are studied. Consider a gain-delay uncertain plant with $k_r = 0.2$ and $\theta_\delta = 1$ and represent this uncertainty by sets Π_{CI3} and Π_{MR}. At a frequency $\omega > \frac{\pi}{2\theta_\delta}$, Π_{CI3} covers all plants within a disk with center on the origin and radius $1 + k_r$, Π_{MR} covers all plants within an annular region with outer radius $1 + k_r$. It can be shown that the worst case plant is at a maximum distance from the origin, so Π_{CI3} and Π_{MR} covers the same worst case plant. Assume that a controller K_{CI3} yields $\mu = 1.1$ for uncertainty set Π_{CI3}, *i.e.* a performance margin of 1/1.1 for all plants within a radius $\Delta_U(1 + k_r) = \frac{1}{1.1}(1 + 0.2) \approx 1.09$. Consider another controller K_{MR} which yields the same μ but for Π_{MR}, *i.e.* the same performance margin but for a *larger* radius $1 + \Delta_U k_r = 1 + \frac{1}{1.1}0.2 \approx 1.18$. This shows that μ for the two cases cannot be directly

compared , since μ in case 1 gives the performance margin with respect to a smaller uncertainty set than in case 2.

3.6 Conclusions

The smallest single complex perturbation that covers a gain-delay uncertainty may be derived analytically (Set Π_{CI3}, Eq. 3.17). This uncertainty set may be used for analysis but not for synthesis (DK-iteration), since it requires an irrational weight.

The smallest set is not always the least conservative. It is not the *size* of the set, but the worst case plant within the set that determines the conservativeness.

A delay free nominal model subject to a low order multiplicative perturbation (Set Π_{CR}, Eq. 3.22) is recommended for μ-synthesis.

It is possible to derive, on a frequency by frequency basis, a model which yields a necessary and sufficient condition for robustness with respect to a single-input-single-output gain-delay uncertainty. In this model (Set Π_{MI2}, Eq. 3.33), the delay uncertainty is modelled by an irrational weight and a real perturbation at low frequencies and a complex perturbation at high frequencies.

An arbitrary tight approximation of the gain-delay uncertainty may be derived using real structured uncertainty (Set Π_{MR}, Eq. 3.35-3.37). This uncertainty set may in principle be used both for analysis and synthesis, but no synthesis method for real perturbations is available at present.

Acknowledgements The authors want to thank Richard D. Braatz for helpful discussions, and Matthew P. Newlin and Peter M. Young for providing the program *rmu* for calculating μ with mixed real/complex perturbations.

Nomenclature

$G(s)$ - MIMO linear model of process
$g(s)$ - SISO linear model of process
$J(\omega)$ - skewed μ (Eq.3.5)
$K(s)$ - controller
k - gain
k_r - relative gain error
$l(\omega)$ - uncertainty weight
$m_3(\omega)$ - complex scalar (Eq.3.17)
$W(s)$ - weight matrix
$w(s)$ - weight scalar
$\|M\|_\infty = \sup_\omega \bar{\sigma}(M(j\omega))$ - H_∞-norm of M
Δ - perturbation matrix
θ - time delay (min)
θ_δ - time delay error (min)

μ - structured singular value
$\bar{\sigma}$ - maximum singular value
ω - frequency (rad min^{-1})

References

[1] Balas, G.J, Doyle, J.C., Glover, K., Packard, A.K. and Smith, R. (1991). "The μ-Analysis and Synthesis Toolbox", The MathWorks Inc., Natick, MA.

[2] Doyle, J.C. (1982). "Analysis of Feedback Systems with Structured Uncertainties", *IEE Proc.*, **129**, Part D, 242-250.

[3] Doyle, J.C., Glover, K., Khargonekar, P. and Francis, B. (1989). "State-space solutions to standard H_2 and H_∞ control problems", *IEEE Trans. Autom. Control*, **34**, 8, 831-847.

[4] Fan, M.K.H., Tits, A.L. and Doyle, J.C. (1991). "Robustness in the presence of mixed parametric uncertainty and unmodelled dynamics", *IEEE Trans. Autom. Control*, **36**, 25-38.

[5] Laughlin, D.L, Jordan, K.G. and Morari, M. (1986). "Internal Model Control and Process Uncertainty: Mapping Uncertainty Regions for SISO Controller Design", *Int. J. Control*, **44**, 1675-1698.

[6] Laughlin, D.L., Rivera, D.E. and Morari M. (1987). "Smith predictor design for robust performance", *Int. J. Control*, **46**(2), 477-504.

[7] Lundström, P., Skogestad, S. and Wang Z.-Q. (1991). "Uncertainty weight selection for H-infinity and mu-control methods", *Proc. IEEE Conf. Decision Contr.*, Brighton, England, 1537-1542.

[8] Packard, A.K. (1988). "What's new with μ: Structured Uncertainty in Multivariable Control", Ph.D. Thesis, Univ. of California, Berkeley, CA.

[9] Packard, A. and Doyle, J. (1993). "The complex structured singular value", *Automatica*, **29**, 1, 71-109.

[10] Skogestad, S., Morari, M. and Doyle, J.C (1988). "Robust Control of Ill-conditioned Plants: High-purity Distillation", *IEEE Trans. Autom. Control*, **33**, 12, 1092-1105. (Also see correction to μ-optimal controller in **34**, 6, 672).

[11] Stein, G., Doyle, J.C. (1991). "Beyond singular values and loop shapes", *J. of Guidance Control and Dynamics*, **14**, 1, 5-16.

[12] Wang, Z.-Q., Lundström, P. and Skogestad, S. (1994). "Representation of uncertain time delays in the H_∞ framework", *Int. J. Control*, **59**, 3, 627-638.

[13] Young, P.M., Newlin M.P. and Doyle, J.C. (1991). "μ analysis with real parametric uncertainty", *Proc. IEEE Conf. Decision Contr.*, Brighton, England, 1251-1256.

Chapter 4

Two Degree of Freedom Controller Design for an Ill-conditioned Plant Using μ-synthesis

Petter Lundström, Sigurd Skogestad
Chemical Engineering
University of Trondheim, NTH
N-7034 Trondheim, Norway

and

John Doyle
Electrical Engineering 116-81
California Institute of Technology
Pasadena, California 91125, USA

Presented at *ECC-93*

Abstract

The structured singular value framework is applied to a distillation benchmark problem formulated for the 1991 CDC. A two degree of freedom controller, which satisfies all control objectives of the CDC problem, is designed using μ-synthesis. The design methodology is presented and special attention is paid to approximation of given control objectives into frequency dependent weights.

4.1 Introduction

The purpose of this paper is to demonstrate, by an example, how the structured singular value (SSV, μ) framework, Doyle [4], may be used to design a robust controller for a given control problem, defined by an uncertain model and control objectives that cannot be directly incorporated into the μ-framework. In particular, we consider how to approximate the given problem into a μ-problem by deriving suitable frequency dependent weights, which define model uncertainty and control objectives in the μ-framework.

The control problem studied in this paper was introduced by Limebeer [8] as a benchmark problem at the 1991 CDC, where it formed the basis for a design case study aimed to investigate advantages and disadvantages of various controller design methods for ill-conditioned systems.

The problem originates from Skogestad *et al.* [17] where a simple model of a high purity distillation column was used to demonstrate that ill-conditioned plants are potentially extremely sensitive to model uncertainty. In [17] uncertainty and performance specifications were given as frequency dependent weights, *i.e.* the problem was *defined* to suit the μ-framework and therefore a μ-optimal controller yields the optimal solution to that problem.

However, in the CDC benchmark problem [8] uncertainty is defined in terms of parametric gain and delay uncertainty and the control objectives are a mixture of time domain and frequency domain specifications. These specifications cannot be directly transformed into frequency dependent weights, but has to be approximated to fit into the μ-framework.

The distillation problem in [17] and variants of this problem, like the CDC problem [8], has been studied by several authors, *e.g* Freudenberg [6], Yaniv and Barlev [21], Lundström *et al.* [10], Hoyle *et al.* [7], Postlethwaite *et al.* [14], Yaniv and Horowitz [22] and Zhou and Kimura [24]. In three recent studies; Limebeer *et al.* [9], van Diggelen and Glover [3] and Whidborne *et al.* [20], two degree of freedom controllers are designed for the CDC problem. The three latter papers are all based on the loop shaping design procedure by McFarlane and Glover [13], where uncertainties are modelled as $\mathcal{H}_\infty$-bounded perturbations in the normalized coprime factors of the plant. To obtain the desired performance, [9] use a reference model design approach, [3] use the Hadamard weighted $\mathcal{H}_\infty$-Frobenius formulation from [2], while [20] use the method of inequalities (Zakian and Al-Naib [23]) where the performance requirements are explicitly expressed as a set of algebraic inequalities.

The two degree of freedom design in this paper differs from [9], [3] and [20] in that we use μ-synthesis for our design. With this method uncertainty is modelled as linear fractional uncertainty and performance is specified as in a standard $\mathcal{H}_\infty$-control problem. Like [9], we specify some of the control objectives as a model-matching problem.

The paper is organized as follows: A brief introduction to the μ-framework is presented in section 4.2. The definition of the benchmark problem is given in section 4.3.

In section 4.4 we outline the design method used in this paper. In section 4.5 we gradually transform (approximate) the given problem into a μ-problem and demonstrate the effect of different weight adjustments. The final controller designed in this section demonstrates that the control objectives defined by Limebeer [8] are obtainable. Finally the results are discussed and summerized.

All results and simulations presented in this paper has been computed using the MATLAB "μ-Analysis and Synthesis Toolbox" [1].

4.2 CDC problem definition

The plant model and design specifications for the CDC benchmark problem [8] are presented in this section.

4.2.1 Plant model

The plant is an ill-conditioned distillation column, modelled by

$$\hat{G}(s) = \frac{1}{75s+1}\begin{bmatrix} 0.878 & -0.864 \\ 1.082 & -1.096 \end{bmatrix}\begin{bmatrix} k_1 e^{-\theta_1 s} & 0 \\ 0 & k_2 e^{-\theta_2 s} \end{bmatrix} \tag{4.1}$$

$$k_i \in [0.8 \quad 1.2] \;\; ; \;\; \theta_i \in [0.0 \quad 1.0] \tag{4.2}$$

In physical terms this means 20% relative gain uncertainty and up to 1 min delay in each input channel. The set of possible plants defined by Eq.4.1-4.2 is in the following denoted Π.

4.2.2 Design specifications

Specifications **S1** to **S4** should be fulfilled for *every* plant $\hat{G} \in \Pi$:

S1 Closed loop stability.

S2 For a unit step demand in channel 1 at $t = 0$ the plant outputs y_1 (tracking) and y_2 (interaction) should satisfy:

- $y_1(t) \geq 0.9$ for all $t \geq 30$ min.
- $y_1(t) \leq 1.1$ for all t
- $0.99 \leq y_1(\infty) \leq 1.01$
- $y_2(t) \leq 0.5$ for all t
- $-0.01 \leq y_2(\infty) \leq 0.01$

Corresponding requirements hold for a unit step demand in channel 2.

S3 $\bar{\sigma}(K_y \hat{S}) < 316, \;\; \forall \omega$.

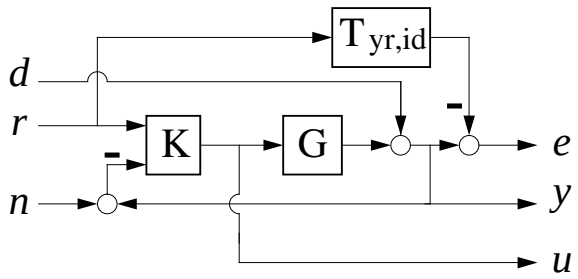

Figure 4.1: Block diagram without weight functions.

S4 Alt.1: $\bar{\sigma}(\hat{G}K_y) < 1$ for $\omega \geq 150$
Alt.2: $\bar{\sigma}(K_y\hat{S}) < 1$ for $\omega \geq 150$

Here K_y denotes the feedback part of the controller and $\hat{S} = (I + \hat{G}K_y)^{-1}$ the sensitivity function for the worst case $\hat{G}$.

Specifications **S3** and **S4** are not explicitly stated in [8], but formulated as "the closed loop transfer function between output disturbance and plant input $[K_y\hat{S}]$ be gain limited to about 50 dB [$\approx$ 316 (**S3**)] and the unity gain cross over frequency of the largest singular value should be below 150 rad/min [(**S4**)]." Different researchers have given the latter specification different interpretations, *e.g.* [3] use Alt.1. while [20] use Alt.2. For the purpose of this paper, this diversity is advantageous, since it gives us the opportunity to start with the easier alternative (Alt.1) and then show how to refine the μ-problem to achieve the tougher requirement (Alt.2).

Note that **S4** Alt.1 in practice is implied by **S1** which in turn is implied by **S2**, so the actual performance requirements are **S2** and **S3** (and **S4** Alt.2).

Most of the specifications in this paper may be viewed as bounds on transfer functions from some inputs to some outputs. The notation for these transfer functions is defined by Fig. 4.1 and the matrices in Eq. 4.4 - 4.5. The controller K in Fig. 4.1 may be a One Degree of Freedom controller (ODF) or a Two Degree of Freedom controller (TDF). A TDF controller may be partitioned into two parts

$$K = [K_r \; K_y] = \left[\begin{array}{c|cc} A_K & B_{Kr} & B_{Ky} \\ \hline C_K & D_{Kr} & D_{Ky} \end{array}\right] \tag{4.3}$$

where K_y is the feedback part of the controller.

For an ODF controller $K_r = K_y$, which yields the following transfer functions:

$$\begin{bmatrix} e \\ y \\ u \end{bmatrix} = \begin{bmatrix} S & T - T_{yr,id} & T \\ S & T & T \\ K_yS & K_yS & K_yS \end{bmatrix} \begin{bmatrix} d \\ r \\ n \end{bmatrix} \tag{4.4}$$

Note that if $T_{yr,id} = I$, then the transfer function from r to e is the sensitivity function, $T - T_{yr,id} = S$.

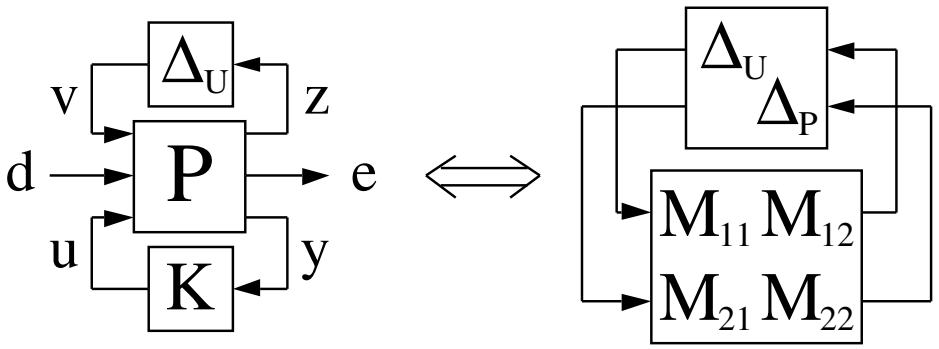

Figure 4.2: General problem description

For a TDF controller $K_r \neq K_y$, which yields the following transfer functions:

$$\begin{bmatrix} e \\ y \\ u \end{bmatrix} = \begin{bmatrix} S & SGK_r - T_{yr,id} & T \\ S & SGK_r & T \\ K_yS & (I + K_yG)^{-1}K_r & K_yS \end{bmatrix} \begin{bmatrix} d \\ r \\ n \end{bmatrix} \tag{4.5}$$

In this case, the transfer function from r to e is not equal to the sensitivity function if $T_{yr,id} = I$.

4.3 The μ-framework

This section gives a very brief introduction to μ-analysis and synthesis and define some of the nomenclature used in the rest of the paper. For more details, the interested reader may consult for example [17], [18] and [1].

The $\mathcal{H}_\infty$-norm of a transfer function $M(s)$ is the peak value of the maximum singular value over all frequencies.

$$||M(s)||_\infty \equiv \sup_\omega \bar{\sigma}(M(j\omega)) \tag{4.6}$$

The left block diagram in Fig.4.2 shows the general problem formulation in the μ-framework. It consists of an augmented plant P (including a nominal model and weighting functions), a controller K and a (block-diagonal) perturbation matrix $\Delta_U = \text{diag}\{\Delta_1, \cdots, \Delta_n\}$ representing uncertainty.

Uncertainties are modelled by the perturbations (Δ_i's) and uncertainty weights included in P. These weights are chosen such that $\|\Delta_U\|_\infty \leq 1$ generates the family of possible plants to be considered. In principle Δ_U may contain both real and complex perturbations, but in this paper only complex perturbations are used.

Performance is specified by weights in P normalizing **d** and **e** such that a closed-loop $\mathcal{H}_\infty$-norm form **d** to **e** less than 1 (for the worst case Δ_U) means that the control objectives are achieved [1].

[1]Note that **d** and **e** in Fig. 4.2 are not equivalent to d and e in Fig. 4.1, but may *contain* d and e among other signals.

The framework in Fig.4.2 may be used for both one degree of freedom (ODF) and two degree of freedom (TDF) controllers. In the ODF case the controller input $\mathbf{y}$ is the difference between set-points and measured plant outputs, $\mathbf{y} = r - y_m$, while in the TDF case $\mathbf{y} = [r \ , \ -y_m]^T$.

The right block diagram in Fig.4.2 is used for robustness analysis. M is a function of P and K, and Δ_P ($\|\Delta_P\|_\infty \leq 1$) is a fictitious "performance perturbation" connecting $\mathbf{e}$ to $\mathbf{d}$. Provided that the closed loop system is nominally stable the condition for Robust Performance (RP) is:

$$RP \quad \Leftrightarrow \quad \mu_{RP} = \sup_\omega \mu_\Delta(M(j\omega)) < 1 \tag{4.7}$$

where $\Delta = \text{diag}\{\Delta_U, \Delta_P\}$.

μ is computed frequency-by-frequency through upper and lower bounds. Here we only consider the upper bound

$$\mu_\Delta(M(j\omega)) \leq \inf_{D \in \mathbf{D}} \bar{\sigma}(DMD^{-1}) \tag{4.8}$$

where $\mathbf{D} = \{D | D\Delta = \Delta D\}$.

At present there is no direct method to synthesize a μ-optimal controller, however, μ-synthesis (DK-iteration) which combines μ-analysis and $\mathcal{H}_\infty$-synthesis often yields good results. This iterative procedure was first proposed in [5] and [15]. The idea is to attempt to solve

$$\min_K \inf_{D \in \mathbf{D}} \sup_\omega \bar{\sigma}(DMD^{-1}) \tag{4.9}$$

(where M is a function of K) by alternating between minimizing $\sup_\omega \bar{\sigma}(DMD^{-1})$ for either K or D while holding the other fixed. The iteration steps are:

DK1 Scale the interconnection matrix M with a stable and minimum phase rational transfer matrix $D(s)$ with appropriate structure (an identity matrix with right dimensions is a common initial choice).

DK2 Synthesize an $\mathcal{H}_\infty$-controller for the scaled problem, $\min_K \sup_\omega \bar{\sigma}(DMD^{-1})$.

DK3 Stop to iterate if the performance is satisfactory or if the $\mathcal{H}_\infty$-norm does not decrease, else continue.

DK4 Compute the upper bound on μ (Eq.4.8) to obtain new D-scales as a function of frequency $D(j\omega)$.

DK5 Fit the magnitude of each element of $D(j\omega)$ to a stable and minimum phase rational transfer function and go to **DK1**.

Each of the minimizations (steps **DK2** and **DK4**) are convex, but joint convexity is not guaranteed.

The $\mathcal{H}_\infty$-controller synthesised in step **DK2** has the same number of states as the augmented plant P plus two times the number of states of D, so it is desirable to keep the order of P and the D-scales as low as possible.

4.4 Design procedure

The CDC specifications in section 4.2 cannot be directly applied in the μ-framework. The reasons for this are: 1) The gain-delay uncertainty in Eq. 4.1-4.2 has to be approximated into linear fractional uncertainty (Fig.4.2); 2) Specification **S2** need to be approximated since it is defined in the time domain; 3) In the μ-framework it is not possible to directly bound the four SISO transfer functions associated with **S2** and the 2×2 transfer function associated with **S3** (and **S4 Alt.2**). Instead these control objectives must be reflected in the $\mathcal{H}_\infty$-norm of the transfer function from **d** to **e** (Fig.4.2).

The following approach makes it possible to apply μ-synthesis to this kind of a problem:

1 Approximate the given problem into a μ-problem.

2 Synthesize a robust controller for the μ-problem.

3 Verify that the controller satisfies the original specifications (**S1-S4**) for the original set of plants (Π).

Step 1 is our major concern in this paper. Several approaches may be used to obtain the μ-problem, however, the following guidelines are general: A) Choose **d** and **e** such that all essential control objectives are reflected in the $\mathcal{H}_\infty$-norm of the transfer function between these signals. At the same time keep the dimension of **d** and **e** as small as possible. B) Use low order uncertainty and performance weights to keep the order of P and thereby the order of the controller low. The complexity and order of these weights may later be increased, if required. C) Use weight parameters with physical meaning, since these parameters are the tuning knobs during the design. Derivation of such weights for the CDC problem is treated in detail in the next section.

Step 2 is fairly straight-forward with DK-iteration using available software (*e.g.* [1]). Experience with this iterative scheme shows that for the first iterations it is best if the controller synthesized in step **DK2** is slightly sub-optimal ($\mathcal{H}_\infty$-norm 5-10% larger than the optimal) and the D-scale fit in step **DK5** are of low order. In subsequent iterations more optimal controllers and higher order D-scales may be used if required. However, it is recommended that also the final controller is slightly sub-optimal since this yields a blend of $\mathcal{H}_\infty$ and $\mathcal{H}_2$ optimality with generally better high frequency roll-off than the optimal $\mathcal{H}_\infty$-controller.

Step 3 is in this paper performed using time simulations with the four extreme combinations of gain uncertainty (Eq.4.2) and a 1 minute delay (approximated as a second order Padé).

4.5 Controller design

In this section we design controllers for the benchmark problem, using the design procedure outlined above. Actually, we start with a controller designed for the "original"

problem defined in Skogestad *et al.* [17] and check the performance of this controller with respect to the CDC specifications defined in section 4.2. We then gradually refine the μ-formulation by adding more input and output signals to $\mathbf{d}$ and $\mathbf{e}$ and adjusting the uncertainty and performance weights.

This gradual approach clearly demonstrates the effect of the weight refinements, and thereby it has a tutorial value. Moreover, it is also a good approach for "real" problems, since one should not put more effort into the μ-formulation than required, *i.e.* try to use as simple a problem formulation as possible.

4.5.1 ODF-controller for "original" specifications

The "original" problem presented in Skogestad et al. (1988) is defined by Fig. 4.3 and the following transfer function matrices.

$$G(s) = \frac{1}{75s+1}\begin{bmatrix} 0.878 & -0.864 \\ 1.082 & -1.096 \end{bmatrix} \tag{4.10}$$

$$W_\Delta(s) = \frac{(s+0.2)}{(0.5s+1)} I_{2\times 2} \tag{4.11}$$

$$W_e(s) = \frac{1}{2}\frac{(20s+2)}{20s} I_{2\times 2} \tag{4.12}$$

$$\Delta_U(s) = \mathrm{diag}\{\Delta_1, \Delta_2\} \ ; \ ||\Delta_U(s)||_\infty \leq 1 \tag{4.13}$$

Note that the uncertainty weight above does not quite cover the gain and delay uncertainty defined in section 4.2 (for details see Lundström *et al.* [11]).

Lundström *et al.* [10] synthesized a controller with 22 states and $\mu_{RP} = 0.978$ for the problem above. In the following we use a slightly improved controller with 18 states and $\mu_{RP} = 0.9735$. This controller may be synthesized using $\mathcal{H}_\infty$-synthesis and the following D-scales.

$$D(s) = \mathrm{diag}\{d(s), d(s), I_{2\times 2}\} \tag{4.14}$$

$$d(s) = 2.0 * 10^{-5}\frac{(s+1000)(s+0.25)(s+0.054)}{(s+0.67+j0.56)(s+0.67-j0.56)(s+0.013)} \tag{4.15}$$

We denote this controller "ODF-original". The performance of this controller applied to the CDC problem is demonstrated in Fig. 4.4 where time responses are shown

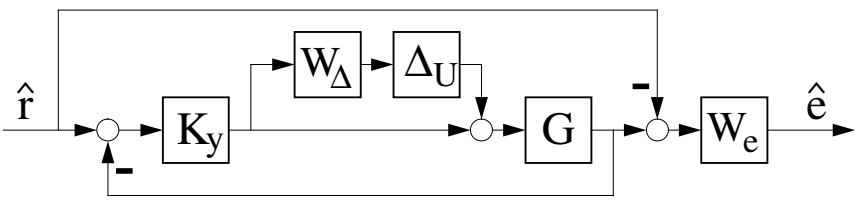

Figure 4.3: Original ODF-problem formulation.

for the four extreme uncertainty combinations defined in Eq. 4.1, *i.e.* the four gain combinations and maximum delay. The simulation results are also summerized in Table 4.1 where bold entries mark violations on **S2**. We see that the closed loop system is stable, so **S1** is satisfied. The setpoint tracking requirements in **S2** are almost satisfied, but the interaction is much too strong.

The performance with respect to **S3** is demonstrated in Fig. 4.5. It is clear that $\bar{\sigma}(K_y S)$ (the gain from setpoints r, n oise n and disturbances d to manipulated inputs u) is much too high at high frequencies and also around the closed loop bandwidth ($\omega \approx 0.1$ rad/min).

The performance specification in the original problem is a bound on the sensitivity function S. Fig. 4.6 shows the maximum and minimum singular values of the sensitivity function for the four extreme combinations of uncertainty. From this plot we see that the original performance requirement $\bar{\sigma}(S) < |1/W_e|$ is NOT satisfied for $\omega \approx 2$ rad/min despite the fact that $\mu_{RP} < 1.0$. The explanation is of course that the uncertainty weight W_Δ does not quite cover the four extreme combinations.

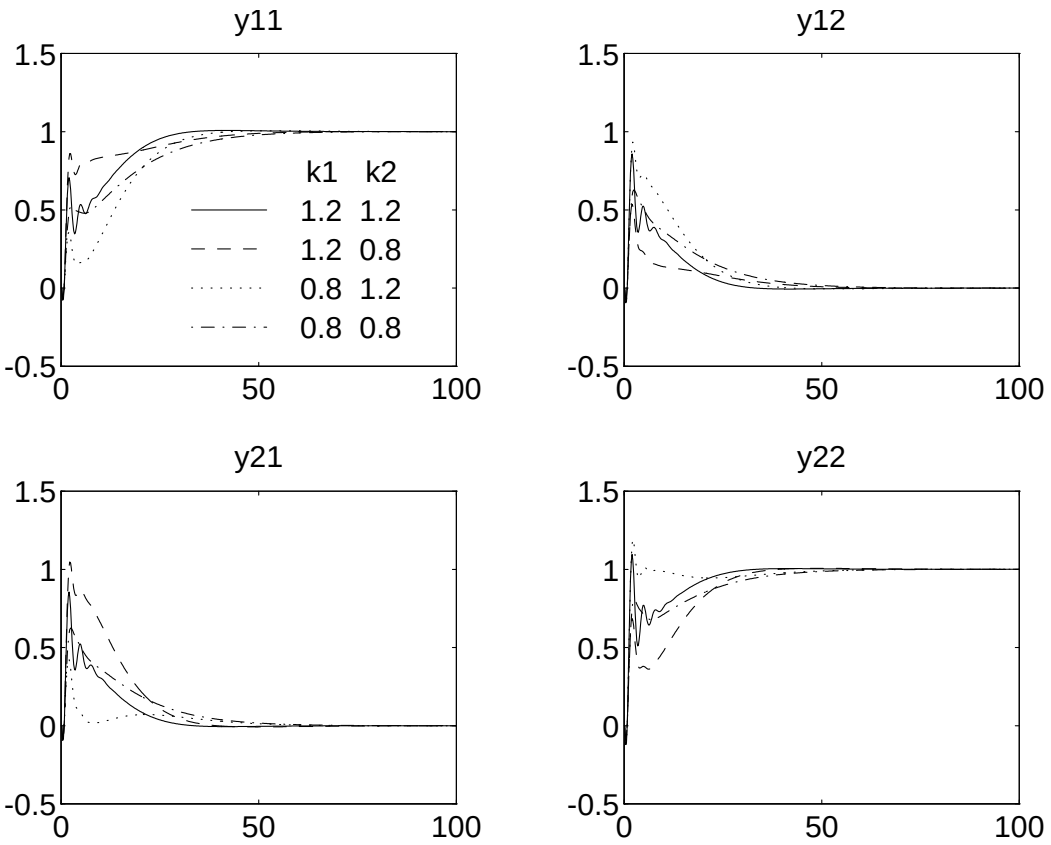

Figure 4.4: Output responses for ODF-original controller with plant-model mismatch. y_{ij} shows response in output i for step change of set-point j at $t = 0$. All responses with 1 min. delay (2nd order Padé).

Table 4.1: Control performance for ODF-original with gain uncertainty and a second order Padé approximation of a 1 min. delay. (See also Fig.4.4)

step	gain unc.		set-point tracking			interaction	
ch.	k_1	k_2	$t = 30$	max	$t = 100$	max	$t = 100$
1	1.2	1.2	0.989	1.008	1.000	**0.856**	0.000
1	1.2	0.8	0.934	1.001	1.001	**1.047**	0.000
1	0.8	1.2	0.941	1.006	1.000	0.427	-0.001
1	0.8	0.8	**0.889**	1.000	1.000	**0.625**	0.000
2	1.2	1.2	0.993	1.095	1.000	**0.859**	0.001
2	1.2	0.8	0.964	1.007	1.000	**0.536**	-0.001
2	0.8	1.2	0.956	**1.198**	1.001	**0.934**	0.000
2	0.8	0.8	0.929	1.000	1.000	**0.627**	0.000

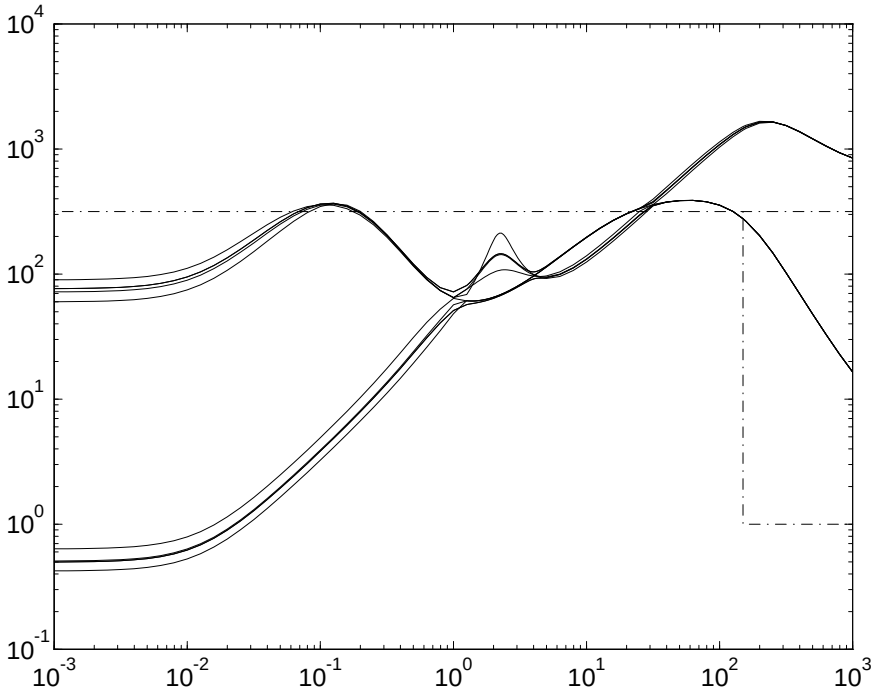

Figure 4.5: Maximum and minimum singular values of $K_y S$ for ODF-original. Dashed: Specification **S3** and **S4** Alt.2, respectively.

To sum up: The ODF-controller above does almost satisfy the tracking requirements, but suffers from strong interactions and excessive use of manipulated inputs, in particular at extremely high frequencies ($\omega > 10$ rad/min).

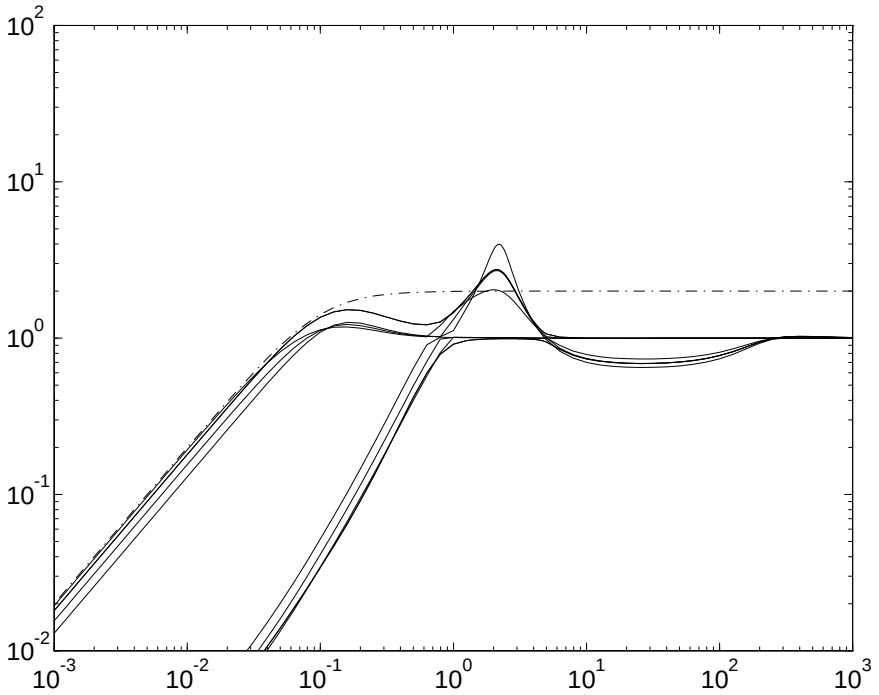

Figure 4.6: Maximum and minimum singular values of S for ODF-original. Dashed: Original upper bound on S ($1/W_e$, Eq.4.12).

4.5.2 TDF-controller for "original" specifications

In this section we check performance of a TDF controller from [10] with respect to the CDC specifications. This controller yields $\mu_{RP} = 0.926$ for the "original " problem and we denote it "TDF-original". Note that, in the design of this controller, W_e is not a weight on the sensitivity function S, since the controller K_r in Fig. 4.3 is replaced by a TDF controller with two inputs r and y (recall Eq.4.4-4.5).

Simulations and tabulated data for TDF-original are shown in Fig. 4.7 and Table 4.2. The setpoint tracking is still not quite satisfied, but the interactions have almost disappeared compared to the ODF-original response. However, there are unpleasant high frequency oscillations in all responses. This oscillation also shows up as a "ringing peak" in the transfer function from r to e ($SGK_r - I$) as illustrated in Fig. 4.8. This peak could have been eliminated if a better uncertainty weight had been used, *i.e.* an uncertainty weight that covers a 1 min delay and 20% gain uncertainty.

TDF-original also suffers from a very high sensitivity function. This deficiency does not show up in the simulations but is illustrated in Fig. 4.9. The high sensitivity function signals that disturbances in the frequency range about 2 rad/min may be amplified up to 100 times! The reason is that W_e is not a weight on S in the TDF problem, but on $SGK_r - I$.

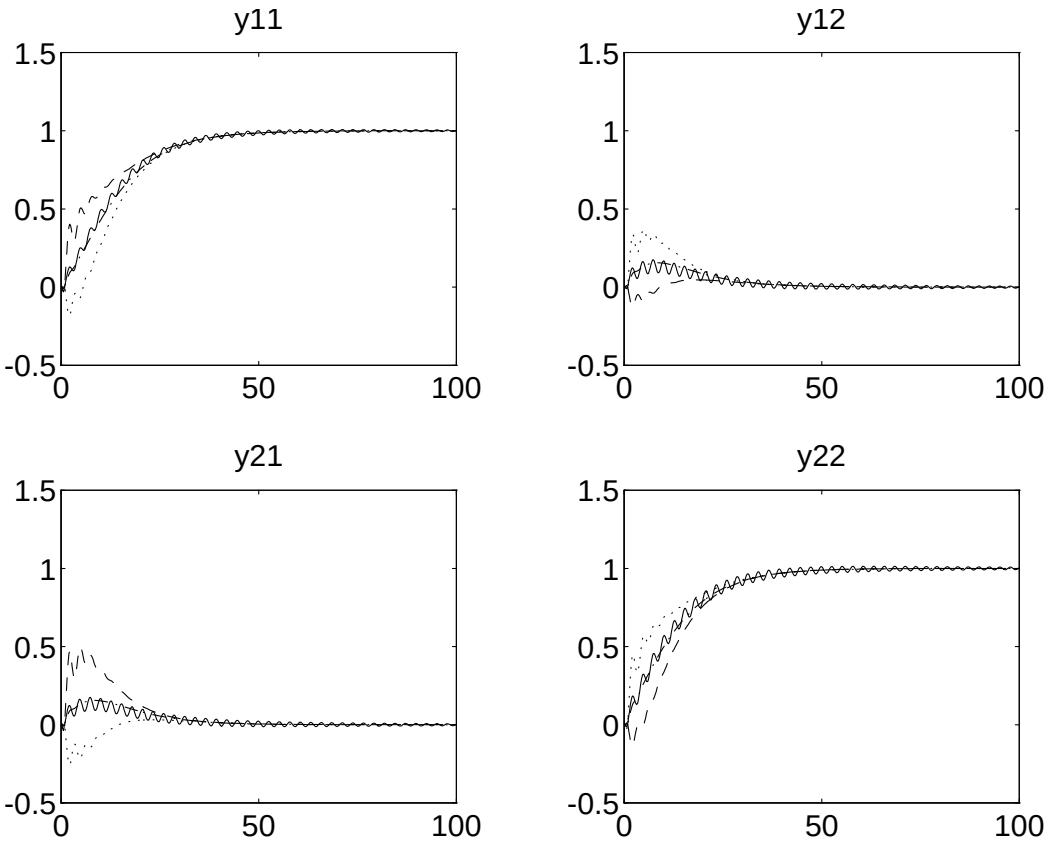

Figure 4.7: Output responses for TDF-original controller with plant-model mismatch. y_{ij} shows response in output i for step change of set-point j at $t = 0$. All responses with 1 min. delay (2nd order Padé).

Table 4.2: Control performance for TDF-original with gain uncertainty and a second order Padé approximation of a 1 min. delay. (See also Fig.4.7)

step	gain unc.		set-point tracking			interaction	
ch.	k_1	k_2	$t = 30$	max	$t = 100$	max	$t = 100$
1	1.2	1.2	**0.889**	1.008	1.003	0.175	0.004
1	1.2	0.8	0.913	1.000	1.000	0.497	0.000
1	0.8	1.2	0.902	1.000	1.000	0.257	0.000
1	0.8	0.8	0.905	1.000	1.000	0.156	0.000
2	1.2	1.2	**0.891**	1.014	1.005	0.175	0.004
2	1.2	0.8	0.917	1.000	1.000	0.126	0.000
2	0.8	1.2	0.928	1.000	1.000	0.368	0.000
2	0.8	0.8	0.921	1.000	1.000	0.156	0.000

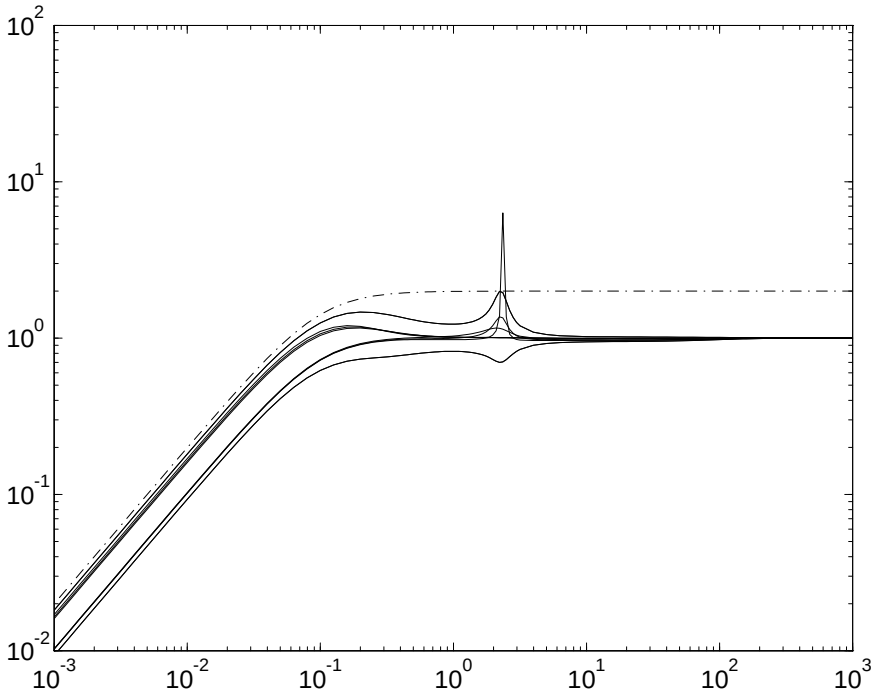

Figure 4.8: Maximum and minimum singular values of $SGK_r - I$ for TDF-original. Dashed: Original upper bound on S ($1/W_e$, Eq.4.12).

4.5.3 Weight selection for CDC specifications

In this section we approximate the CDC specifications into frequency dependent weight.

Uncertainty weights

The gain-delay uncertainty in Eq.4.2 is not quite covered by the uncertainty weight defined in Eq.4.11. A better weight is presented in [12]:

$$W_\Delta(s) = \frac{(1+\frac{k_r}{2})\theta_{max}s + k_r}{\frac{\theta_{max}}{2}s+1} I_{2\times 2} = \frac{1.1s+0.2}{0.5s+1} I_{2\times 2} \tag{4.16}$$

where $k_r = 0.2$ is the relative gain uncertainty and $\theta_{max} = 1$ is the maximum delay. This weight has the same low order as Eq. 4.11 but does *almost* cover the gain and delay uncertainty. A slight modification of Eq.4.16 yields a weight that *completely* covers the uncertainty ([12]), but is of higher order:

$$W_\Delta(s) = \frac{1.1s+0.2}{0.5s+1} * \frac{\left(\frac{s}{2.363}\right)^2 + 2*0.838\frac{s}{2.363}+1}{\left(\frac{s}{2.363}\right)^2 + 2*0.685\frac{s}{2.363}+1} I_{2\times 2} \tag{4.17}$$

Often is fruitful to start with the simpler weight (Eq. 4.16) and if the performance verification (step 3 of the design procedure) shows that this uncertainty model does

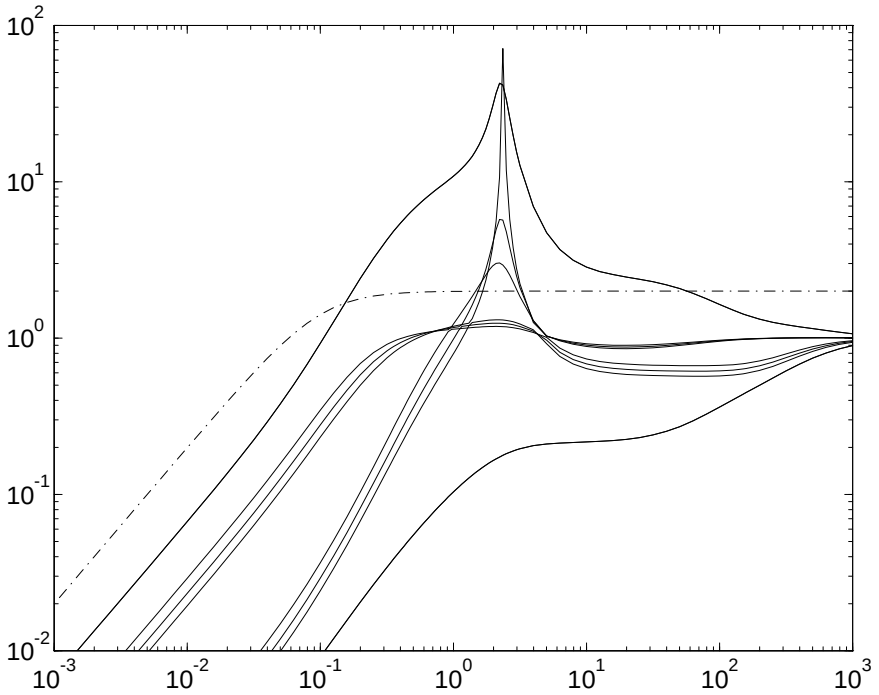

Figure 4.9: Maximum and minimum singular values of S for TDF-original. Dashed: Original upper bound on S ($1/W_e$, Eq.4.12).

not yield a robust controller for the set of plants Π, then the more rigorous uncertainty model (Eq. 4.17) should be used.

ODF performance weights

A simple way to approximate the performance specifications **S2** and **S3** into a μ-problem is shown in Fig.4.10, where K_y is an ODF-controller.

The time domain requirements of specification **S2** is approximated by a frequency domain bound (W_{S2}) on the sensitivity function S, just like in the original formulation

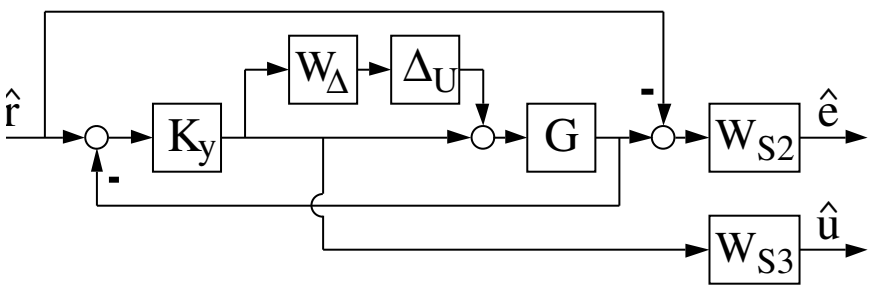

Figure 4.10: Block diagram for one degree of freedom controller.

[17].

$$W_{S2}(s) = \frac{1}{M_S}\frac{\tau_{cl}s + M_S}{\tau_{cl}s + A}I_{2\times 2}. \tag{4.18}$$

For $||W_{S2}S_p||_\infty < 1$ this weight yields: 1) Steady-state error less than A; 2) Closed-loop bandwidth higher than $\omega_B = 1/\tau_{cl}$; and 3) Amplification of high-frequency output disturbances less than a factor M_S.

Specification **S3** yields a simple frequency independent weight

$$W_{S3} = \frac{1}{M_{KS}}I_{2\times 2} \tag{4.19}$$

For $||W_{S3}K_yS_p||_\infty < 1$ this weight guarantees $\bar{\sigma}(K_yS_p)$ less than M_{KS} for all frequencies.

Note that the formulation in Fig.4.10 lumps the four SISO requirements of **S2** and the 2×2 requirement of **S3** into a bound on the entire 4×2 transfer function from $\hat{r}$ to $[\hat{e}\ ,\ \hat{u}]^T$. From the relation

$$\max\{\bar{\sigma}(A), \bar{\sigma}(B)\} \leq \bar{\sigma}([A\ B]^T) \leq \sqrt{2}\max\{\bar{\sigma}(A), \bar{\sigma}(B)\} \tag{4.20}$$

it is clear that the physical interpretation of the weights results in slightly too 'hard' performance requirements.

The results in section 4.5.1 indicates that an ODF-controller probably not will yield the required performance, so in the following we focus on TDF-design.

TDF performance weights

The block diagram in Fig.4.11 defines the μ-approximation of the CDC problem that we will use for the TDF design.

Specification **S2** is here approximated by a 'model-matching problem'. Compared to a weight on the sensitivity function, this allows a more direct way to deal with both the set-point tracking and interaction specifications of **S2**. The reference model $T_{yr,id}$ defines the *ideal* transfer function from set-points to plant outputs, and the signal weights W_r and W_e are used to penalize the difference between desired and actual response.

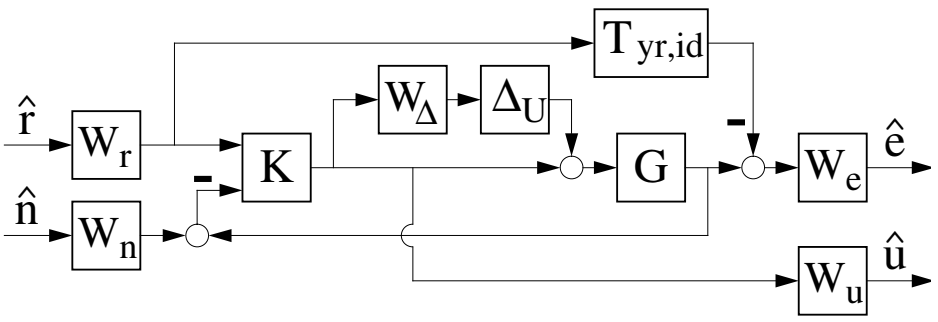

Figure 4.11: Block diagram for two degree of freedom controller.

The set-point tracking should ideally be decoupled and the response and overshoot requirements are the same for both channels. To keep the order of $T_{yr,id}$ small, while at the same time have the freedom to allow for some overshoot in the ideal response, we use a second order reference model in each channel

$$T_{yr,id} = \frac{1}{\tau_{id}^2 s^2 + 2\zeta_{id}\tau_{id} s + 1} I_{2\times 2} \tag{4.21}$$

The weights W_n and W_u in Fig.4.11 are used to obtain specification **S3** by bounding $||K_y S_p||_\infty$. Note that even without **S3** it is necessary to include the noise $\hat{n}$ or another signal (non-zero for $\omega \to \infty$) between G and K to obtain a proper controller, since G is strictly proper ($\lim_{\omega\to\infty} \bar{\sigma}(G(j\omega)) = 0$).

Figure 4.11 gives

$$\begin{bmatrix} \hat{e} \\ \hat{u} \end{bmatrix} = \begin{bmatrix} W_e N_{11} W_r & -W_e N_{12} W_n \\ W_u N_{21} W_r & -W_u N_{22} W_n \end{bmatrix} \begin{bmatrix} \hat{r} \\ \hat{n} \end{bmatrix} \tag{4.22}$$

where $N_{11} = S_p G_p K_r - T_{yr,id} = T_{yr,p} - T_{yr,id}$; $N_{12} = G_p K_y S_p = T_p$; $N_{21} = (I + K_y G_p)^{-1} K_r$ and $N_{22} = K_y S_p$ (index p denotes a perturbed system, *i.e* $G_p = G(I + \Delta_U W_\Delta)$. For simplicity, we use diagonal weights with the same weight in both channels ($W_i = w_i * I_{2\times 2},\ i = e, u, r, n$), *i.e.* $W_e W_r$ forms a bound on N_{11} and $W_u W_n$ forms a bound on N_{22}.

Now, W_{S2} and W_{S3} (Eq. 4.18 and 4.19) are used as a starting point to find appropriate signal weights W_r, W_n, W_e and W_u. The combined weight $W_u W_n$ should be similar to W_{S3} and $W_e W_r$ may be chosen similar to W_{S2} to obtain a reasonable bound on the mismatch between actual and ideal response. However, the off-diagonal elements in Eq.4.22, $W_e N_{12} W_n$ and $W_u N_{21} W_r$ also have to be considered when selecting the signal weights, since it is the $\mathcal{H}_\infty$-norm of the entire transfer function that is minimized by the controller. This demonstrates that the weights have to be selected with some care in order to avoid impossible performance specifications.

We may always choose one of the signal weights arbitrary and then shape the other signals relatively to the arbitrary weight. Let $W_r = I$ at all frequencies. This yields N_{11} bounded by $W_e = W_{S2}$ and N_{21} bounded by W_u. At low frequencies [2] $N_{21} \approx N_{22}$, so let $W_u = W_{S3}$. Next consider how to choose W_n such that $W_u N_{22} W_n$ reflects **S3** and $W_e N_{12} W_n$ does not limit the performance of the overall system. At low frequencies $N_{12} \approx I$, so W_n has to be smaller than W_e^{-1} in this frequency range. At higher frequencies W_n is chosen such that $W_u W_n$ becomes an active bound on N_{22}. One way to obtain this is to use

$$W_r(s) = I_{2\times 2} \tag{4.23}$$

$$W_e(s) = \frac{1}{M_S} \frac{\tau_{cl} s + M_S}{\tau_{cl} s + A} I_{2\times 2} \tag{4.24}$$

[2] At low frequencies $(I + GK_y)^{-1} G K_r \approx I \Rightarrow K_y \approx K_r \Rightarrow N_{21} = (I + K_y G)^{-1} K_r \approx K_y (I + GK_y)^{-1} = N_{22}$

$$W_u(s) = \frac{1}{M_{KS}} I_{2\times 2} \tag{4.25}$$

$$W_n(s) = \frac{\tau_{cl}s + A}{\tau_{cl}s + M_T} I_{2\times 2} \tag{4.26}$$

M_T in Eq.4.26 is a bound on the low frequency peak value of N_{12} (the complementary sensitivity function). This parameter is used to adjust the frequency where $W_u W_n$ becomes an active bound on N_{22}.

The performance weights derived above have several parameters, however, it is relatively easy to find reasonable numerical values for these parameters since they all have some physical meaning. In fact, most of the numerical values used in the design below, are almost directly obtained from the specifications in section 4.2.

4.5.4 TDF-controller for CDC specifications; Alt.1

In this section we synthesize a TDF controller for the CDC specifications with **S4** Alt.1. We use an unstructured perturbation matrix Δ_U which gives $D(s) = \text{diag}\{d(s), d(s), I_{4\times 4}\}$. Δ_U in Eq.4.13 is structured, however, it can be shown that the TDF problem (with the diagonal weights defined in the previous section) belongs to a class of problems where an unstructured Δ_U may be used without introducing conservativeness (Hovd *et al.*, 1993).

Initially $d(s)$ were set to 0.01, obtained from a natural physical scaling ('logarithmic compositions' [16]). This simple scaling substantially reduces the number of iterations required to obtain 'good' D-scales.

The initial weight parameters were chosen to: 1) Yield an ideal response which satisfies **S2** with some margin without too large overshoot ($\tau_{id} = 8, \zeta_{id} = 0.71$); 2) Require a close fit to the ideal response at low frequencies ($A = 10^{-4}$) and a looser fit at high frequencies ($\tau_{cl} = 10, M_S = 3$); 3) Yield a loose requirement on $K_y S_p$ to be increased if required ($M_T = 3, M_{KS} = 630$ (56dB)).

Only two DK-iterations was needed to get $\mu_{RP} < 1$, however, the performance with respect to **S2** and **S3** was not quite achieved. M_S, M_T and τ_{cl} was adjusted to 3.5, 2.0 and 9.5, respectively. After two more DK-iterations a controller which satisfies **S1-S4** was obtained. The controller has 24 states, yields a closed loop $\mathcal{H}_\infty$-norm of 1.015 and may be synthesized using the final weights and D-scales given in Table 4.3.

The performance of the TDF controller is demonstrated in Fig.4.12 where time responses for the four extreme combinations of uncertainty are shown. The simulation results are also summerized in Table 4.4 and are seen to satisfy specification **S2**. The maximum peak of $\bar{\sigma}(K_y\hat{S}) = 306$ (Fig. 4.13), which is less than 316 (50 dB), as required in **S3**, and the unit gain cross over frequency, $\bar{\sigma}(\hat{G}K_y) = 1$, is at 1 rad/min, well below 150 rad/min, as required in **S4** Alt.1. Specification **S4** Alt.2 is not satisfied as shown in Fig. 4.13.

The transfer functions N_{12} and N_{21}, which are not part of the CDC problem, have peak values of 3.4 and 420, respectively.

Table 4.3: Final weight parameters and D-scales

Weight parameters						
τ_{id}	ζ_{id}	τ_{cl}	A	M_S	M_T	M_{KS}
8.0	0.71	9.5	10^{-4}	3.5	2.0	630

$$D(s) = \text{diag}\{d(s), d(s), I_{4\times 4}\}$$

$$d(s) = 0.00299 \frac{(s+5.70)}{(s+0.0144)} \frac{(s^2 + 2*0.6645*0.112s + 0.112^2)}{(s^2 + 2*0.622*0.568s + 0.568^2)}$$

Table 4.4: Control performance for TDF-Alt.1 with gain uncertainty and second order Padé approximation of a 1 min. delay. (See also Fig.4.12)

step	gain unc.		set-point tracking			interaction	
ch.	k_1	k_2	$t = 30$	max	$t = 100$	max	$t = 100$
1	1.2	1.2	1.066	1.092	0.998	0.051	0.001
1	1.2	0.8	0.984	1.036	0.999	0.471	-0.001
1	0.8	1.2	0.969	1.030	1.000	0.426	0.001
1	0.8	0.8	0.906	1.000	1.000	0.138	0.000
2	1.2	1.2	1.052	1.074	0.999	0.051	0.001
2	1.2	0.8	0.987	1.030	1.000	0.265	0.001
2	0.8	1.2	1.002	1.038	0.999	0.310	0.000
2	0.8	0.8	0.950	1.002	1.000	0.138	0.000

4.5.5 TDF-controller for CDC specifications; Alt.2

In this section we show that specification **S4** Alt.2 used in [20] can be achieved by the design procedure presented in this paper. The μ-formulation in Fig.4.11 is used also for this TDF-design. However, the signal weights W_u and W_n are not the same as in the previous "Alt.1" design. In addition we use the rigorous uncertainty weight from Eq. 4.17.

Specification **S3** and **S4** Alt.2 yield:

$$\bar{\sigma}(K_y \hat{S}(j\omega)) < \begin{cases} 50 \text{ dB} & \omega < 150 \text{ rad/min} \\ 0 \text{ dB} & \omega \geq 150 \text{ rad/min} \end{cases} \tag{4.27}$$

The high frequency roll-off requirement in Eq. 4.27 is harder than in Alt.1. To deal with this, weights W_u and W_n in Fig.4.11 are modified. We use the same procedure as in the previous design, first approximating Eq.4.27 by a rational transfer function bound (W_{S34}) on $K_y \hat{S}$, and then derive W_u and W_n from W_{S34}.

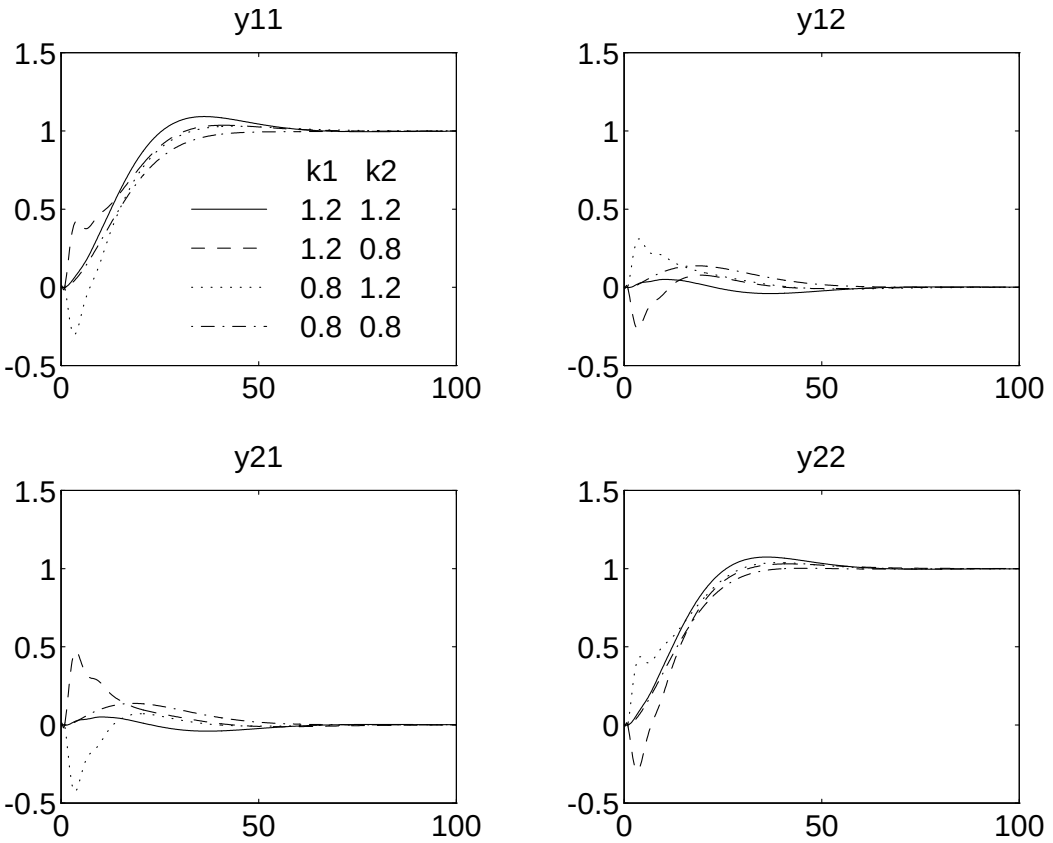

Figure 4.12: Output responses for TDF-Alt.1 controller with plant-model mismatch. y_{ij} shows response in output i for step change of set-point j at $t = 0$. All responses with 1 min. delay (2nd order Padé).

Let

$$W_{S34} = \frac{1}{M_{KS}} \left(\frac{\frac{M_{KS}^{1/n}}{\omega_0} s + 1}{\frac{1}{c\omega_0} s + 1} \right)^n I_{2\times 2} \tag{4.28}$$

For $||W_{S34} K_y S_p||_\infty < 1$ this weight yield:

1 Maximum allowed low frequency peak less than M_{KS}.

2 Maximum unity-gain crossover frequency less than (approximately) ω_0.

The parameter n in Eq.4.28 is an integer. By increasing n, a steeper approximation of Eq.4.27 is obtained at the expense of a higher order weight. The parameter $c \geq 1$ in Eq.4.28 is used to obtain a good approximation around the unity cross over frequency.

From Eq.4.28 the following weights with $n = 3$ and $c = 5$ are obtained:

$$W_u(s) = \frac{1}{M_{KS}} \left(\frac{\frac{M_{KS}^{1/n}}{\omega_0} s + 1}{\frac{1}{c\omega_0} s + 1} \right)^{(n-1)} I_{2\times 2} \tag{4.29}$$

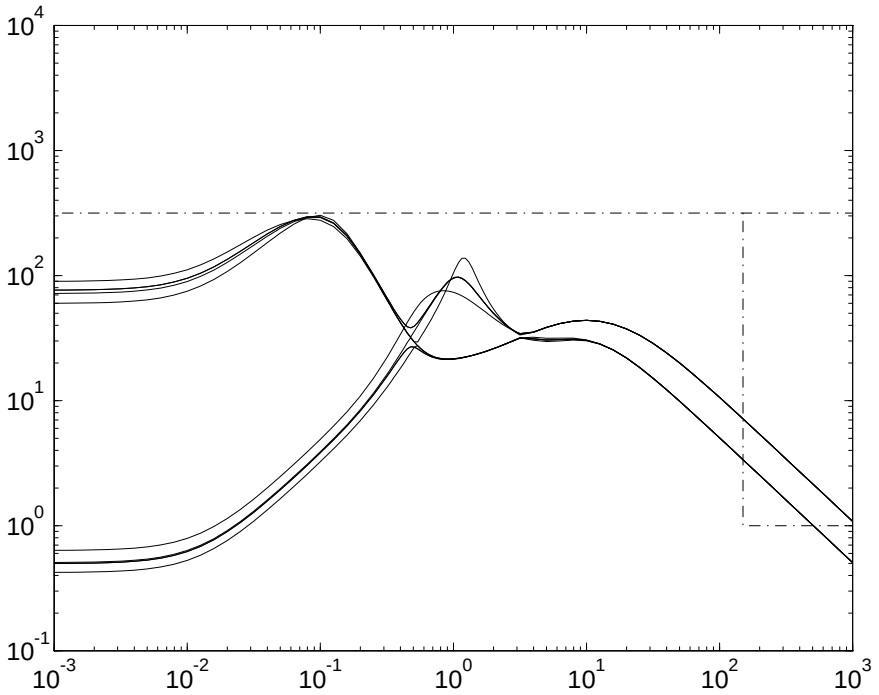

Figure 4.13: Maximum and minimum singular values of K_yS for TDF-Alt.1. Dashed: Specification **S3** and **S4** Alt.2, respectively

Table 4.5: Final weight parameters and D-scales

Weight parameters							
τ_{id}	ζ_{id}	τ_{cl}	A	M_S	M_T	M_{KS}	ω_0
8.0	0.71	9.5	10^{-4}	3.0	2.5	1000	200

$$D(s) = \text{diag}\{d(s), d(s), I_{4\times 4}\}$$

$$d(s) = 7.3 * 10^{-4} \frac{(s+23.1)(s^2 + 2*0.637*0.116s + 0.116^2)}{(s+0.0213)(s+0.372)(s+0.673)}$$

$$W_n(s) = \frac{\tau_{cl}s + A}{\tau_{cl}s + M_T} \left(\frac{\frac{M_{KS}^{1/n}}{\omega_0}s + 1}{\frac{1}{c\omega_0}s + 1} \right) I_{2\times 2} \tag{4.30}$$

After some iterations and parameter adjustments a controller which satisfies **S1**, **S2**, **S3** and **S4** Alt.2 was obtained. The final weight parameters and D-scales are given in Table 4.5. The controller yields a closed loop $\mathcal{H}_\infty$-norm of 1.0 and has 34 states. However, the order may be reduced to 22 without violating the control objectives. The performance of the 22 state controller is shown in Fig.4.14. The simulation results are also summerized in Table 4.6 and are seen to satisfy specification **S2**.

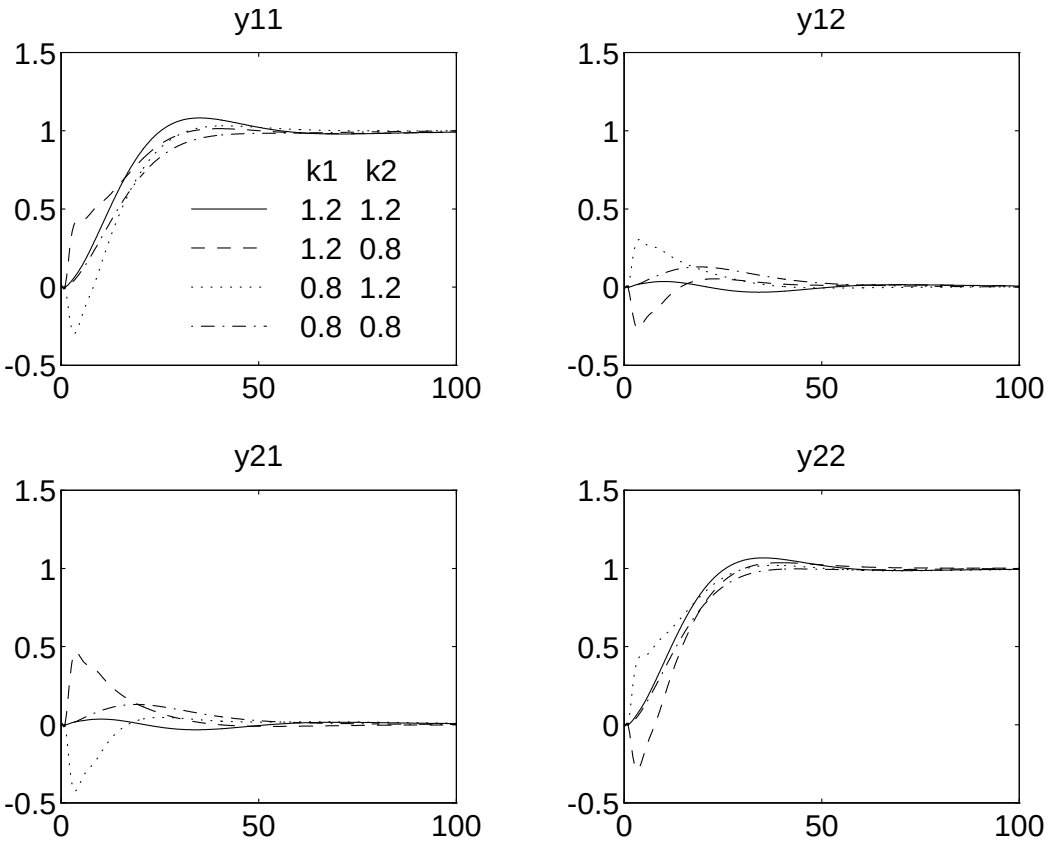

Figure 4.14: Output responses for TDF-Alt.2 controller with plant-model mismatch. y_{ij} shows response in output i for step change of set-point j at $t = 0$. All responses with 1 min. delay (2nd order Padé).

Table 4.6: Control performance for TDF-Alt.2 with gain uncertainty and second order Padé approximation of a 1 min. delay. (See also Fig.4.12)

step	gain unc.		set-point tracking			interaction	
ch.	k_1	k_2	$t = 30$	max	$t = 100$	max	$t = 100$
1	1.2	1.2	1.063	1.082	0.991	0.036	0.008
1	1.2	0.8	0.976	1.013	0.990	0.464	-0.001
1	0.8	1.2	0.977	1.031	0.999	0.424	0.010
1	0.8	0.8	0.908	0.998	0.998	0.130	0.002
2	1.2	1.2	1.050	1.067	0.994	0.036	0.008
2	1.2	0.8	0.995	1.036	1.001	0.264	0.008
2	0.8	1.2	0.994	1.019	0.992	0.305	0.001
2	0.8	0.8	0.951	0.999	0.999	0.130	0.002

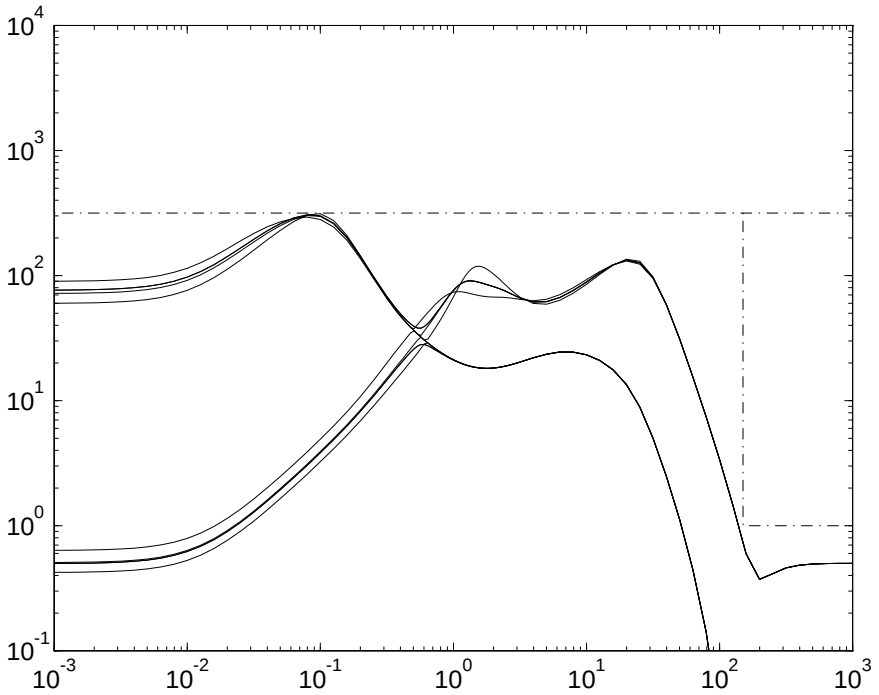

Figure 4.15: Maximum and minimum singular values of $K_y S$ for TDF-Alt.2. Dashed: Specification **S3** and **S4** Alt.2, respectively

Fig. 4.15 shows that the maximum peak of $\bar{\sigma}(K_y\hat{S}) = 313$, which is less than 316 (50 dB), as required in **S3**, and the unit gain cross over frequency, $\bar{\sigma}(K_y\hat{S}) = 1$, is below 150 rad/min, as required in **S4** Alt.2.

To obtain these improvements compared to TDC-Alt.1, the performance with respect to N_{21} has degenerated. N_{12} and N_{21} have peak values of 2.6 and 435, respectively. However, these transfer functions are not strictly part of the specifications.

4.6 Discussion

The inability to independently penalize separate elements of the closed loop transfer function complicates the performance weight selection in the μ-framework. The Hadamard weighted approach [3] does not have this problem and will therefore yield better performance with respect to the specifications in the CDC problem, **S1** - **S4**. However, for a practical engineering problem the transfer functions N_{12} and N_{21} in Fig.4.11 *are* of importance, so it seems reasonable to include them into the control problem.

4.7 Conclusions

μ-synthesis has been successfully applied to a demanding ill-conditioned uncertain problem where uncertainty is defined as parametric gain-delay uncertainty and the design objectives are a mixture of time domain and frequency domain specifications.

Acknowledgements. Support from NTNF is gratefully acknowledged.

References

[1] Balas, G.J, Doyle, J.C., Glover, K., Packard, A.K. and Smith, R. (1991). "The μ-Analysis and Synthesis Toolbox", The MathWorks Inc., Natick, MA.

[2] van Diggelen, F. and Glover, K. (1991). "Element-by-element weighted $\mathcal{H}_\infty$-Frobenius and $\mathcal{H}_2$ norm problems", *Proc. IEEE Conf. Decision Contr.*, Brighton, England, 923-924.

[3] van Diggelen, F. and Glover, K. (1992). "A Hadamard weighted loop shaping design procedure", *Proc. IEEE Conf. Decision Contr.*, Tucson, Arizona, 2193-2198.

[4] Doyle, J.C. (1982). "Analysis of Feedback Systems with Structured Uncertainties", *IEE Proc.*, **129**, Part D, 242-250.

[5] Doyle, J.C. (1983). "Synthesis of robust controllers and filters", *Proc. IEEE Conf. Decision Contr.*, San Antonio, TX.

[6] Freudenberg, J.S. (1989). "Analysis and design for ill-conditioned plants, Part 2. Directionally uniform weightings and an example", *Int. J. Control*, **49**, 3, 873-903.

[7] Hoyle, D.J., Hyde, R.A. and Limebeer, D.J.N, (1991). "An $\mathcal{H}_\infty$ approach to two degree of freedom design", *Proc. IEEE Conf. Decision Contr.*, Brighton, England, 1581-1585.

[8] Limebeer, D.J.N. (1991). "The specification and purpose of a controller design case study", *Proc. IEEE Conf. Decision Contr.*, Brighton, England, 1579-1580.

[9] Limebeer, D.J.N., Kasenally, E.M. and Perkins, J.D. (1993). "On the design of robust two degree of freedom controllers", *Automatica*, **29**, 1, 157-168.

[10] Lundström, P., Skogestad, S. and Wang, Z.-Q. (1991). "Performance weight selection for H-infinity and μ-control methods", *Trans. Inst. MC*, **13**, 5, 241-252.

[11] Lundström, P., Skogestad, S. and Wang Z.-Q. (1991). "Uncertainty weight selection for H-infinity and mu-control methods", *Proc. IEEE Conf. Decision Contr.*, Brighton, England, 1537-1542.

[12] Lundström, P., Wang Z.-Q. and Skogestad, S. (1993). "Modelling of gain and delay uncertainty in the structured singular value framework", *Preprints IFAC World Congress on Automatic Control*, Sydney, Australia.

[13] McFarlane, D.C. and Glover, K. (1992). "A loop shaping design procedure using $\mathcal{H}_\infty$ synthesis", *IEEE Trans. Autom. Control*, **AC-37**, 6, 759-769.

[14] Postlethwaite, I., Lin, J.-L., and Gu, D.-W. (1991). "Robust control of a high purity distillation column using $\mu - K$ iteration", *Proc. IEEE Conf. Decision Contr.*, Brighton, England, 1586-1590.

[15] Safonov, M.G. (1983). "L-infinity optimal sensitivity v.s. stability margin", *Proc. IEEE Conf. Decision Contr.*, San Antonio, TX.

[16] Skogestad, S. and Morari, M. (1988). "Understanding the Dynamic Behavior of Distillation Columns", *Ind. Eng. Chem. Res.*, **27**, 10, 1848-1862.

[17] Skogestad, S., Morari, M. and Doyle, J.C (1988). "Robust Control of Ill-conditioned Plants: High-purity Distillation", *IEEE Trans. Autom. Control*, **33**, 12, 1092-1105. (Also see correction to μ-optimal controller in **34**, 6, 672).

[18] Stein, G., Doyle, J.C. (1991). "Beyond singular values and loop shapes", *J. of Guidance Control and Dynamics*, **14**, 1, 5-16.

[19] Wang, Z.-Q., Lundström, P. and Skogestad, S. (1994). "Representation of uncertain time delays in the H_∞ framework", *Int. J. Control*, **59**, 3, 627-638.

[20] Whidborne, J.F., Postlethwaite, I. and Gu, D.W. (1992). "Robust controller design using $\mathcal{H}_\infty$ loop-shaping and the method of inequalities", Report 92-33, Department of Engineering, University of Leicester.

[21] Yaniv, O. and Barlev, N. (1990). "Robust non iterative synthesis of ill-conditioned plants", *Proc. Am. Control Conf.*, San Diego, CA, 3065-3066.

[22] Yaniv, O. and Horowitz, I. (1991). "Ill-conditioned plants: A Case study", *Proc. IEEE Conf. Decision Contr.*, Brighton, England, 1596-1600.

[23] Zakian, V. and Al-Naib, U. (1973). "Design of dynamical and control systems by the method of inequalities", *IEE Proc.*, **120**, 11, 1421-1427.

[24] Zhou, T. and Kimura, H. (1991). "Controller design of an ill-conditioned plant using robust stability degree assignment", *Proc. IEEE Conf. Decision Contr.*, Brighton, England, 1591-1595.

Chapter 5

Limitations of Dynamic Matrix Control

Petter Lundström, Jay H. Lee, Manfred Morari
Chemical Engineering 210-41
California Institute of Technology
Pasadena, California 91125, USA

and

Sigurd Skogestad
Chemical Engineering
University of Trondheim, NTH
N-7034 Trondheim, Norway

Submitted to *Computers and Chemical Engingeering*
Shorted version presented at
the European Control Conference, Grenoble, France, July 1991

Abstract

Dynamic Matrix Control (DMC) is based on two assumptions which limit the feedback performance of the algorithm. The first assumption is that a stable step response model can be used to represent the plant. The second assumption is that the difference between a measured and a predicted output can be modeled as a step disturbance acting on the output.

These assumptions lead to the following limitations.

1 Good performance may require an excessive number of step response coefficients.

2 Poor performance may be observed for disturbances affecting the plant inputs.

3 Poor robust performance may be observed for multivariable plants with strong interactions.

Limitations 1 and 2 apply when the plant's open-loop time constant is much larger than the desired closed-loop time constant. Limitation 3 is caused by gain uncertainty on the inputs.

In this paper we separate the DMC algorithm into a predictor and an optimizer. This enables us to highlight the DMC limitations and to suggest how they can be avoided. We demonstrate that a new Model Predictive Control (MPC) algorithm, which includes an observer, does not suffer from the listed limitations.

5.1 Introduction

Dynamic Matrix Control (DMC) has been successfully used in industry for more than a decade. Several authors have reported improved control performance by use of DMC as compared to "traditional" control algorithms (Cutler and Ramaker, 1980, Prett and Gillette, 1980, García and Morshedi, 1986). DMC has the ability to deal with constraints, which probably is one of the major reasons for its popularity. It also allows set point changes to be "announced" in advance and it facilitates feedforward control. However, the *feedback* properties of a DMC controller are limited by two restrictive assumptions which are implicit in the algorithm:

A1 A stable step response model can be used to represent the plant.

A2 The difference between a measured and a predicted output can be modeled as a step disturbance acting on the output.

The objective of this paper is to clearly point out these assumptions and to illustrate in which situations they may limit the feedback properties of DMC. We also demonstrate that the limitations can be avoided by use of a new observer based algorithm, by Lee *et al.* (1991), which is a *direct* extension of DMC.

DMC belongs to the family of Model Predictive Control (MPC) algorithms. The main idea behind these algorithms is to use an explicit model of the plant to predict the open-loop future behavior of the controlled outputs over a finite time horizon. The predicted behavior is then used to find a finite sequence of control moves which minimizes a particular objective function without violating prespecified constraints. Usually only the first input move is implemented and the procedure is repeated at the next sampling instant.

This algorithm can be separated into two parts, a predictor and an optimizer. By splitting up the algorithm this way, similarities with state-observer state-feedback controllers become apparent. In fact, Lee *et al.* (1991) show that unconstrained DMC is equivalent to an optimal state observer (Kalman filter) and linear quadratic feedback, using a receding horizon approach and special assumptions about disturbances and measurement noise.

In this paper we use the predictor-optimizer representation of DMC. In this framework the limitations of DMC can be traced to the predictor part of the algorithm. We only consider unconstrained DMC, but the results carry over to the general case with constraints, since the issue of constraints only affects the optimizer.

The limitations we want to illustrate are:

L1 Good performance may require an excessive number of step response coefficients.

L2 Poor performance may be observed for "ramp-like" disturbances acting on the plant outputs. In particular, this occurs for input disturbances for plants with large time constants.

L3 Poor robust performance, due to input gain uncertainty (which always is present in practice), may be observed for multivariable plants with strong interactions.

In addition, there is the obvious limitation that the plant has to be stable.

This paper is organized as follows. In section 2 we present the algorithms we will use. The purpose is to give a coherent overview of the algorithms and to point out the implicit assumptions made in DMC. We also use this section to define the nomenclature. Readers not familiar with MPC are referred to García *et al.* (1989), for instance. In section 3 we use a simple single-input single-output (SISO) plant and a multi-input multi-output (MIMO) distillation column to illustrate the limitations of DMC and demonstrate that the algorithm by Lee *et al.* (1991) can be used to avoid these limitations. Section 4 contains Discussion and Section 5 Conclusions.

5.2 Model Predictive Control

5.2.1 Dynamic Matrix Control

Modeling the plant

In the original DMC formulation (Culter and Ramaker, 1980) a step response model of the plant is used to predict the future behavior of the controlled variables.

Let the step response of a SISO system be represented by the sequence

$$[s_1 \quad s_2 \quad \dots \quad s_{n-1} \quad s_n \quad s_{n+1} \quad \dots] \tag{5.1}$$

where the k^{th} element is the output at time k caused by a unit step input at time 0. For a stable plant this sequence will asymptotically reach a constant value, *i.e.* $s_n \approx s_{n+1}$. For a MIMO system with n_u inputs and n_y outputs we get

$$S_i = \begin{bmatrix} s_{1,1,i} & s_{1,2,i} & \cdots & s_{1,n_u,i} \\ s_{2,1,i} & s_{2,2,i} & \cdots & s_{2,n_u,i} \\ \vdots & \vdots & \ddots & \vdots \\ s_{n_y,1,i} & s_{n_y,2,i} & \cdots & s_{n_y,n_u,i} \end{bmatrix} \quad ; \quad i = 1, \cdots, n \tag{5.2}$$

The step response model can be represented in the following state space form, which is equivalent to that presented by Li *et al.* (1989).

$$Y(k+1) = MY(k) + S\Delta u(k) \tag{5.3}$$

$$y(k) = NY(k) \tag{5.4}$$

where

$$\Delta u(k) = u(k) - u(k-1) \tag{5.5}$$

$$Y(k) = [y(k)^T \; y(k+1)^T \; \dots \; y(k+n-1)^T]^T \tag{5.6}$$

$$M = \left.\begin{bmatrix} 0 & I_{n_y} & 0 & \cdots & 0 & 0 \\ 0 & 0 & I_{n_y} & \ddots & 0 & 0 \\ \vdots & \ddots & \ddots & \ddots & \ddots & \vdots \\ 0 & 0 & 0 & \ddots & I_{n_y} & 0 \\ 0 & 0 & 0 & \ddots & 0 & I_{n_y} \\ 0 & 0 & 0 & \cdots & 0 & I_{n_y} \end{bmatrix}\right\} n * n_y \; ; \quad S = \begin{bmatrix} S_1 \\ S_2 \\ \vdots \\ S_{n-2} \\ S_{n-1} \\ S_n \end{bmatrix} \tag{5.7}$$

and

$$N = [\overbrace{\begin{array}{cccccc} I_{n_y} & 0 & 0 & \cdots & 0 & 0 \end{array}}^{n*n_y}] \tag{5.8}$$

$\Delta u(k)$ is a vector of changes in the manipulated inputs at time k. $y(k)$ is the output vector at time k. The vector $Y(k+1)$ represents the dynamic states of the system. Each state, $y_i(k+l)$, has a special interpretation: it is the i^{th} future output at time $k+l$ assuming constant inputs (*i.e.* $\Delta u(k+j) = 0$ for $j \geq 0$). The new state vector $Y(k+1)$ is the old vector $Y(k)$ shifted up n_y elements plus the contribution made by the latest input change $\Delta u(k)$.

The predictor

The DMC algorithm is illustrated in Fig. 5.1. The objective of the predictor is to generate a vector, $\mathcal{Y}(k+1|k)$, of predicted open-loop outputs over a horizon of p future time steps, the prediction horizon. This prediction vector is then used as an input to the optimizer.

The DMC predictor is described by the following equations.

$$\tilde{Y}(k+1) = M\tilde{Y}(k) + S\Delta u(k) \tag{5.9}$$

$$\tilde{y}(k) = N\tilde{Y}(k) \tag{5.10}$$

$$\mathcal{Y}(k+1|k) = M_p\tilde{Y}(k) + \mathcal{I}[\hat{y}(k) - \tilde{y}(k)] \tag{5.11}$$

where M_p is the first $p * n_y$ rows of M and

$$\mathcal{I} = [\overbrace{\begin{array}{cccc} I_{n_y} & I_{n_y} & \cdots & I_{n_y} \end{array}}^{p*n_y}]^T \tag{5.12}$$

We use $\tilde{}$ to denote that the output is from the model and not from the true plant. $\hat{y}(k)$ is a vector of measured outputs at time k. $\tilde{y}(k)$ and $\hat{y}(k)$ are discontinuous at k_- while $u(k)$ is discontinuous at k_+, *i.e.* $\hat{y}$ is measured slightly before time k and u is adjusted slightly after time k.

The optimizer

We use the QDMC objective function from García and Morshedi (1986):

$$J = \min_{\Delta\mathcal{U}(k|k)} \{\|\Gamma[\mathcal{Y}_m(k+1|k) - \mathcal{R}(k+1|k)\|^2 + \|\Lambda\Delta\mathcal{U}(k|k)\|^2\} \tag{5.13}$$

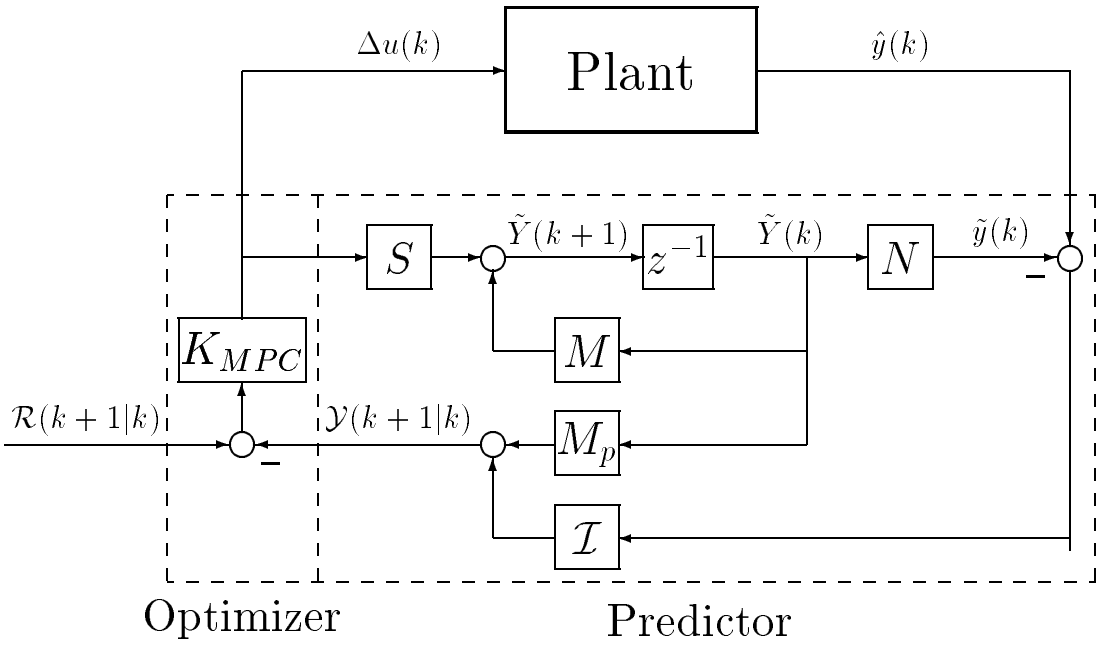

Figure 5.1: DMC controller separated into a predictor and an optimizer.

where

$$\Delta\mathcal{U}(k|k) = [\Delta u(k|k)^T \ \Delta u(k+1|k)^T \ \ldots \ \Delta u(k+m-1|k)^T]^T \tag{5.14}$$

$$\mathcal{Y}_m(k+1|k) = [y_m(k+1|k)^T \ y_m(k+2|k)^T \ \ldots \ y_m(k+p|k)^T]^T \tag{5.15}$$

and

$$\mathcal{R}(k+1|k) = [r(k+1|k)^T \ r(k+2|k)^T \ \ldots \ r(k+p|k)^T]^T \tag{5.16}$$

$\Delta\mathcal{U}(k|k)$ is the optimal control sequence computed at time k for m future input moves, where m is the input horizon. $\mathcal{Y}_m(k+1|k)$ is a vector of outputs predicted at time k, over a horizon of p future time steps, *including* the effect of the m optimal input moves:

$$\mathcal{Y}_m(k+1|k) = \mathcal{Y}(k+1|k) + \mathcal{S}_p^m \Delta\mathcal{U}(k|k) \tag{5.17}$$

where

$$\mathcal{S}_p^m = \begin{bmatrix} S_1 & 0 & \ldots & 0 \\ S_2 & S_1 & \ldots & 0 \\ \vdots & \vdots & \ddots & \vdots \\ S_m & S_{m-1} & \ldots & S_1 \\ \vdots & \vdots & & \vdots \\ S_p & S_{p-1} & \ldots & S_{p-m-1} \end{bmatrix}. \tag{5.18}$$

$\mathcal{R}(k+1|k)$ is a vector describing the desired output trajectory (set points) over p future time steps. Γ and Λ are weighting matrices and are usually chosen to be diagonal.

The least squares solution to this problem is

$$\Delta\mathcal{U}(k|k) = \{(\mathcal{S}_p^m)^T\Gamma^T\Gamma\mathcal{S}_p^m + \Lambda^T\Lambda\}^{-1}(\mathcal{S}_p^m)^T\Gamma^T\Gamma\left[\mathcal{R}(k+1|k) - \mathcal{Y}(k+1|k)\right]. \quad (5.19)$$

Only the first input move is implemented, and the resulting optimizer is a constant gain matrix, K_{MPC}.

$$\Delta u(k) = [I\ 0\ \ldots\ 0]\Delta\mathcal{U}(k|k) = K_{MPC}\left[\mathcal{R}(k+1|k) - \mathcal{Y}(k+1|k)\right] \quad (5.20)$$

$$K_{MPC} = [I\ 0\ \ldots\ 0]\{(\mathcal{S}_p^m)^T\Gamma^T\Gamma\mathcal{S}_p^m + \Lambda^T\Lambda\}^{-1}(\mathcal{S}_p^m)^T\Gamma^T\Gamma \quad (5.21)$$

DMC Assumptions

The DMC controller can only be used with stable plants. There are two reasons for this:
1) The internal model (Eq. 5.9–5.10) can only describe a stable plant;
2) $\hat{y}(k) - \tilde{y}(k)$ can grow unbounded for unstable systems leading to internal instability.

The internal model of the DMC predictor (Eq. 5.9–5.10) does not yield an estimate of the true plant output. It computes the open-loop *model* output, $\tilde{y}(k)$, for previous input moves, but does not account for the effect of disturbances and model-plant mismatch. This means that $\hat{y}(k) - \tilde{y}(k)$ generally is not zero when there is no steady-state offset and $\hat{y}(k) = 0$. Rather, $-\tilde{y}(k)$ equals the accumulated effect of disturbances and model-plant mismatch.

Eq. 5.11 gives the predicted open-loop output vector, $\mathcal{Y}(k+1|k)$. It is the predicted effect of previous input moves, $M_p\tilde{Y}(k)$, plus a simple bias adjustment given by the mismatch between the measured output, $\hat{y}(k)$, and the output form the internal model, $\tilde{y}(k)$.

To achieve good control performance, $\mathcal{Y}(k+1|k)$ should be close to the *true* open-loop output. This requires that n, the number of coefficient matrices in S, is chosen such that $S_n \approx S_{n+1}$, otherwise $M_p\tilde{Y}(k)$ will be in error. It also requires that $\hat{y}(k) - \tilde{y}(k)$ stays approximately constant.

We formulate these requirements as two implicit assumptions made in the DMC algorithm:
A1 A stable step response model with $S_n \approx S_{n+1}$ can be used to represent the plant.
A2 The difference between a measured and a predicted output can be modeled as a step disturbance acting on the output.

5.2.2 DMC with general state space model

The DMC algorithm can also be derived for a general discrete state space model (Prett and García, 1988) instead of the step response model (Eq. 5.3–5.4) used in the previous section. We will denote this algorithm DMCss. The only difference between DMC and DMCss is the representation of the internal model. We include DMCss in this paper because it allows us to study DMC without the effects of truncation errors caused by $S_n \neq S_{n+1}$.

Let the plant model be defined by the following equations.

$$x(k+1) = Ax(k) + Bu(k) \tag{5.22}$$
$$y(k) = Cx(k) \tag{5.23}$$

Using this model the DMC algorithm can be described by the block diagram in Fig. 5.1 by making the following substitutions, $\tilde{Y}(k) = \Delta\tilde{x}(k) = \tilde{x}(k) - \tilde{x}(k-1)$, $M = A, S = B, N = [0 \ \ldots 0]$ and

$$M_p = \begin{bmatrix} CA \\ CA + CA^2 \\ \vdots \\ \sum_{i=1}^{p} CA^i \end{bmatrix} \tag{5.24}$$

5.2.3 Observer Based Model Predictive Control

This algorithm is from Lee *et al.* (1991), we will denote it "OBMPC".

Lee *et al.* use the following extended version of the step response model in Eq. 5.3–5.4. The extension is made in order to include measurement noise and general disturbances acting on the plant outputs. It also allows modeling of integrating systems.

$$Y(k+1) = MY(k) + S\Delta u(k) + T\Delta w(k) \tag{5.25}$$
$$y(k) = NY(k) \tag{5.26}$$
$$\hat{y}(k) = y(k) + v(k) \tag{5.27}$$

$\Delta w(k) = w(k) - w(k-1)$ is a vector of changes in disturbances and $v(k)$ is a vector of measurement noise.

$$M = \left.\begin{bmatrix} 0 & I_{n_y} & 0 & \cdots & 0 & 0 & 0 & 0 \\ 0 & 0 & I_{n_y} & \ddots & 0 & 0 & 0 & 0 \\ \vdots & \ddots & \ddots & \ddots & \ddots & \vdots & \vdots & \vdots \\ 0 & 0 & 0 & \ddots & I_{n_y} & 0 & 0 & 0 \\ 0 & 0 & 0 & \cdots & 0 & I_{n_y} & 0 & 0 \\ 0 & 0 & 0 & \cdots & 0 & I_{n_y} & C_u & C_w \\ 0 & 0 & 0 & \cdots & 0 & 0 & A_u & 0 \\ 0 & 0 & 0 & \cdots & 0 & 0 & 0 & A_w \end{bmatrix}\right\} n * n_y + \dim\{x_u\} + \dim\{x_d\} \tag{5.28}$$

$$S = \begin{bmatrix} S_1 \\ S_2 \\ \vdots \\ S_{n-2} \\ S_{n-1} \\ S_n \\ B_u \\ 0 \end{bmatrix}; \quad T = \begin{bmatrix} 0 \\ 0 \\ \vdots \\ 0 \\ 0 \\ 0 \\ 0 \\ B_w \end{bmatrix} \tag{5.29}$$

$$N = [\ I_{n_y} \quad 0 \quad 0 \quad \cdots \quad 0 \quad 0 \quad 0 \quad 0\ ] \tag{5.30}$$

$$Y(k) = [y(k)^T \quad y(k+1)^T \quad \ldots \quad y(k+n-1)^T \quad x_u(k)^T \quad x_w(k)^T]^T \tag{5.31}$$

A_u, B_u and C_u constitute a state space description of the residual plant dynamics after n sampling intervals. A_w, B_w and C_w describe the dynamics of the disturbances. x_u and x_w are state vectors for residual plant dynamics and disturbance dynamics, respectively.

This representation allows very general modeling of plant and disturbances. However, we will approximate the residual dynamics with $n_y * n_u$ first order systems, each describing the slow response from one input to one output. This approximation gives:

$$A_u = \begin{bmatrix} A_{u1} & & \\ & \ddots & \\ & & A_{un_u} \end{bmatrix} \quad ; \quad A_{uj} = \begin{bmatrix} a_{u1j} & & \\ & \ddots & \\ & & a_{un_yj} \end{bmatrix} \tag{5.32}$$

$$B_u = \begin{bmatrix} B_{u1} & & \\ & \ddots & \\ & & B_{un_u} \end{bmatrix} \quad ; \quad B_{uj} = \begin{bmatrix} b_{u1j} \\ \vdots \\ b_{un_yj} \end{bmatrix} \tag{5.33}$$

$$C_u = \overbrace{[\ I_{n_y} \quad I_{n_y} \quad \cdots \quad I_{n_y}\ ]}^{n_y * n_u} \tag{5.34}$$

We also restrict measurement noise and disturbances to the following special case:
1) The measurement noise at each output is uncorrelated white noise.
2) The disturbances at the outputs are integrated white noise filtered through first order dynamics.
For this special case we get the following diagonal covariance matrices:

$$E\{\Delta w(k)\Delta w(k)^T\} \quad = \quad W = \begin{bmatrix} W_1 & & \\ & \ddots & \\ & & W_{n_y} \end{bmatrix} \tag{5.35}$$

$$E\{v(k)v(k)^T\} \quad = \quad V = \begin{bmatrix} V_1 & & \\ & \ddots & \\ & & V_{n_y} \end{bmatrix} \tag{5.36}$$

and

$$A_w = \mathcal{A} \triangleq \text{diag}\{\alpha_1, \cdots, \alpha_{n_y}\}; \quad B_w = I_{n_y}; \quad C_w = I_{n_y} \tag{5.37}$$

For $\alpha_i = 0$, the disturbance at the i^{th} output is integrated white noise ("type 1" disturbance), while $\alpha_i = 1$ yields *double*-integrated white noise ("type 2" disturbance) at the i^{th} output.

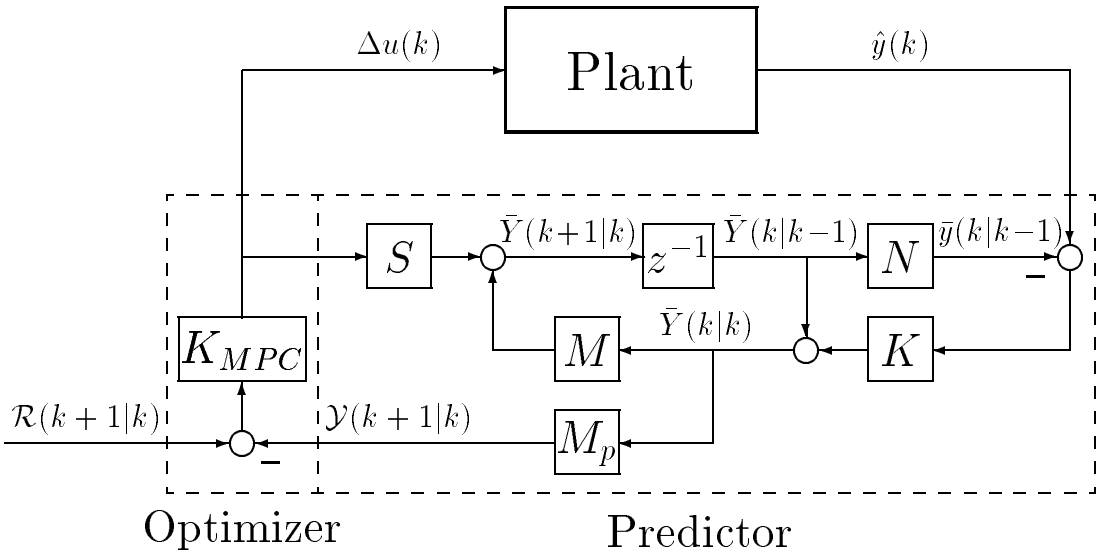

Figure 5.2: Observer based MPC controller separated into a predictor and an optimizer.

The OBMPC predictor

The OBMPC predictor is using an optimal state observer (*i.e.* Kalman filter), as seen in Fig. 5.2. This observer is described by the following equations.

$$\bar{Y}(k|k) = \bar{Y}(k|k-1) + K\{\hat{y}(k) - \bar{y}(k|k-1)\} \tag{5.38}$$

$$\bar{Y}(k+1|k) = M\bar{Y}(k|k) + S\Delta u(k) \tag{5.39}$$

where

$$\bar{Y}(k|k-1) = \left[\bar{y}(k|k-1)^T\ \bar{y}(k+1|k-1)^T\ \ldots\ \bar{y}(k+n-1|k-1)^T\ \bar{x}_u(k|k-1)^T\ \bar{x}_w(k|k-1)^T\right]^T \tag{5.40}$$

$\bar{y}(k+l|k)$ is the estimate of $y(k+l)$ based on measurements up to and including time k. The predicted output vector (the input to the optimizer) is

$$\mathcal{Y}(k+1|k) = M_p\bar{Y}(k|k) \tag{5.41}$$

For the special noise and disturbance case defined in the previous section, the optimal filter gain K in Eq. 5.38 is parametrized as follows (Lee *et al.*, 1991).

$$K = \begin{bmatrix} I_{n_y} \\ I_{n_y} \\ I_{n_y} \\ \vdots \\ I_{n_y} \\ 0 \\ 0 \end{bmatrix} \begin{bmatrix} (f_a)_1 & & \\ & \ddots & \\ & & (f_a)_{n_y} \end{bmatrix} + \begin{bmatrix} 0 \\ I_{n_y} \\ I_{n_y} + \mathcal{A} \\ \vdots \\ \sum_{i=0}^{n-2} \mathcal{A}^i \\ 0 \\ \mathcal{A}^{n-1} \end{bmatrix} \begin{bmatrix} (f_b)_1 & & \\ & \ddots & \\ & & (f_b)_{n_y} \end{bmatrix} \tag{5.42}$$

$$(f_b)_i = \frac{\alpha_i (f_a)_i^2}{1 + \alpha_i - \alpha_i (f_a)_i} \quad ; \quad 1 \leq i \leq n_y \tag{5.43}$$

The adjustable parameters, $(f_a)_i$, are determined by the disturbance-to-noise ratio for the i^{th} output, W_i/V_i.

$$(f_a)_i \to 0 \quad \text{for} \quad W_i/V_i \to 0 \tag{5.44}$$

$$(f_a)_i \to 1 \quad \text{for} \quad W_i/V_i \to \infty \tag{5.45}$$

Hence, we may compute the optimal Kalman filter gain *without* solving a Riccati equation, and $(f_a)_i$ and α_i may be used as on-line tuning parameters.

State-observer State-feedback interpretation

The unconstrained OBMPC described above is a state-observer state-feedback controller using a receding horizon approach. The optimal state-observer is defined by Eq. 5.38–5.39 and the linear quadratic state feedback gain is $K_{MPC}M_p$. The closed-loop dynamics is determined by the following state transmission matrix.

$$\begin{bmatrix} Y(k) \\ Y(k) - \bar{Y}(k|k) \end{bmatrix} = \begin{bmatrix} M - SK_{MPC}M_p & SK_{MPC}M_p \\ 0 & M - KNM \end{bmatrix} \begin{bmatrix} Y(k-1) \\ Y(k-1) - \bar{Y}(k-1|k-1) \end{bmatrix} \tag{5.46}$$

The eigenvalues of $M - SK_{MPC}M_p$ are the regulator poles and the eigenvalues of $M - KNM$ are the observer poles.

If the measurements are noise-free and the disturbances are random steps acting on the plant outputs, then an unconstrained DMC controller where $S_n = S_{n+1}$ is equivalent to the unconstrained OBMPC controller. That is, for this special case

$$M_p \bar{Y}(k|k) = M_p \tilde{Y}(k) + \mathcal{I}[\hat{y}(k) - \tilde{y}(k)] \tag{5.47}$$

and DMC is an optimal state-observer state-feedback controller.

5.3 Limitations of Dynamic Matrix Control

5.3.1 Limitation 1: Good performance may require an excessive number of step response coefficients

In the previous section we stated that the DMC step response model requires $S_n \approx S_{n+1}$. In this section we demonstrate the consequence of sacrificing this requirement.

Assume that a high closed-loop bandwidth is desired for the plant described by the following model.

$$P(s) = \frac{100}{100s + 1} e^{-s} \tag{5.48}$$

In order to achieve the desired bandwidth a short sampling interval is required. (A common rule is to use $\Delta T \leq \frac{2\pi}{10\omega_B}$, where ω_B is the closed-loop bandwidth, *e.g.* Middleton (Eq. 6.1, 1991)). We select $\Delta T = 1$ min. According to common practice (*e.g.*

Table 5.1: Tuning parameters for controllers.

	Type	Γ	Λ	ΔT [min.]	m	p	n	a_{uij}	b_{uij}	α_i	$(f_a)_i$
A	DMC	1	0	1	3	4	30				
B	DMCss	1	0	1	3	4	–				
C	DMCss	$I_{2\times2}$	$0.02I_{2\times2}$	1	5	10	–				
D	OBMPC	1	0	1	3	4	30	1	$s_{n+1} - s_n$	1	0.5
E	OBMPC	$I_{2\times2}$	$0.125I_{2\times2}$	1	5	10	30	0.995	$s_{i,j,n+1} - s_{i,j,n}$	0.995	0.9
F	OBMPC	$I_{2\times2}$	$0_{2\times2}$	1	5	10	30	0.995	$s_{i,j,n+1} - s_{i,j,n}$	0.995	0.22

$$\text{PI} \quad C_{PI}(z) = \frac{K_c\left(\frac{\Delta T}{\tau_I}\right)}{(z-1)} + K_c \; ; \qquad K_c = 0.45, \quad \tau_I = 5.0\text{min}, \quad \Delta T = 1\text{min}$$

Cutler and Ramaker, 1980), the truncation error should not be larger than about 5%, which in our case yields 300 step coefficients. However, there is always a practical limit on the number of coefficients (states) that can be used in the internal model, since a large number of coefficients leads to an excessive use of computer memory and a high computational load.

Consider the case of selecting $n = 30$, which is a typical industrial choice (*e.g.* Cutler and Ramaker, 1980). The effect of this truncation on feedback control is demonstrated in Fig. 5.3 which shows the response to a unit step disturbance acting on the plant output at time $t = 10$. The simulation is performed with a dead beat DMC controller (controller A, Table 5.1). The truncated step response causes an erroneous prediction (a "jump") $n - 1$ sampling intervals after the disturbance occurred. The error here is so large that it leads to instability.

From this example we conclude that heavily truncated models cannot be used, and thereby the computer hardware may restrict the choice of sampling interval and the achievable closed-loop bandwidth. This is especially important for plants with a large open-loop time constant.

5.3.2 Avoiding limitation 1

Limitation 1 may be avoided by using a state space model which has no truncation error. For example, the DMCss algorithm requires only 2 states to represent Eq. 5.48 for $\Delta T = 1$, one state for the first order transfer function and one for the delay. More states are needed if ΔT is less than the delay.

The OBMPC controller can also be used to avoid limitation 1. Instead of truncating the response after n time steps (as would be the case with a DMC step response model) we may use A_u and B_u in Eq. 5.32–5.33 to model the slow dynamics. This way we can reduce the number of states required to represent the plant and thereby allow a short sampling interval. A_u and B_u allows us to use any first order model of the

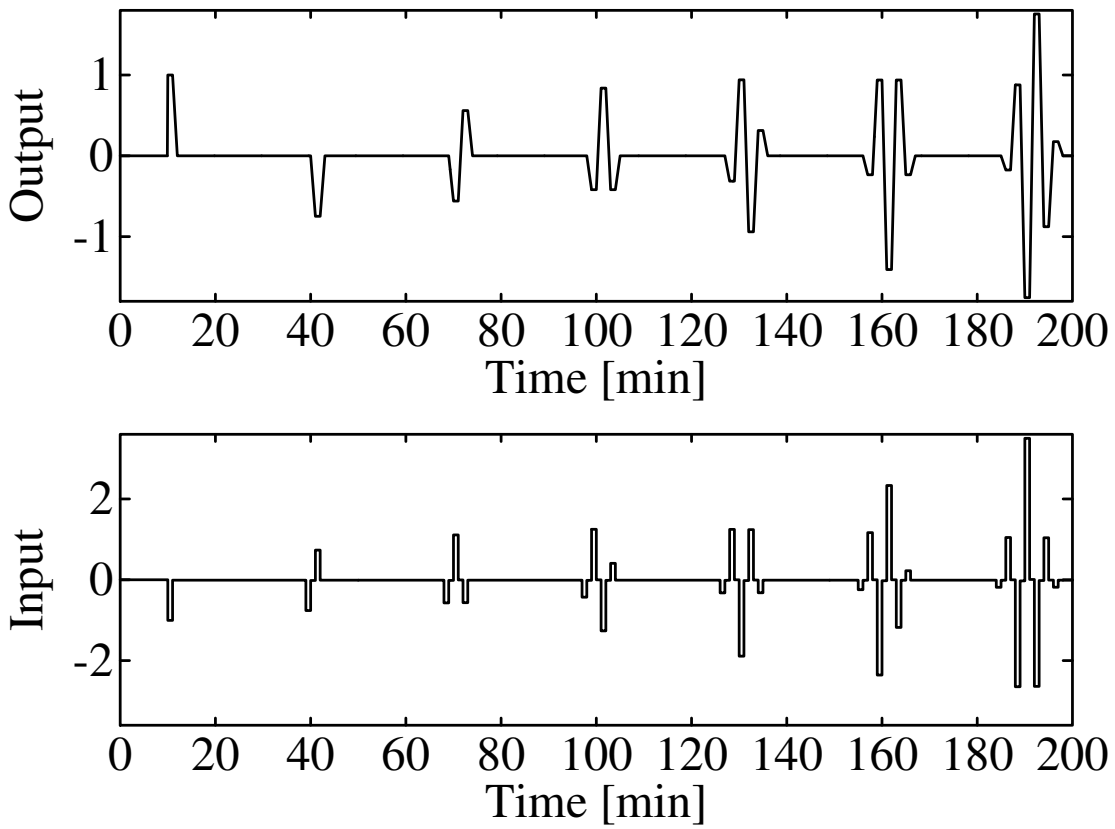

Figure 5.3: Effect of truncation. Response for the SISO plant (Eq. 5.48) with DMC controller A (Table 5.1). A unit step disturbance acts on the plant output at $t = 10$.

slow dynamics. We could obtain an exact model of the plant in Eq. 5.49 by using $A_u = e^{-\Delta T/100}$ and $B_u = s_{n+1} - s_n$. However, in this example we will approximate the slow dynamics with an integrator, and select $A_u = 1$, $B_u = s_{n+1} - s_n$ and $n = 30$.

In Fig. 5.4 we compare the open-loop model response to a unit step in u at time 0 for the exact model (Eq. 5.48) (solid curve) with the truncated DMC model (Eq. 5.3–5.4) (dashed curve) and the OBMPC model (Eq. 5.25–5.26) with the residual dynamic approximation given above (dash-dot curve). The last model gives a large error as time increases, but does not have the abrupt change at $t = n\Delta T$ which is characteristic for the truncated DMC model. In the frequency domain (Fig. 5.5), the truncated DMC model is poor both at high and low frequencies. The integrating OBMPC model on the other hand, yields excellent agreement with the exact model at high frequencies, but displays large deviation at low frequencies.

Simulations with DMC and OBMPC (controllers A and D) are shown in Fig. 5.6. The disturbance is a unit step on the plant output. We conclude that the rough integrating approximation of the residual dynamics is better than the truncated model. Note that controller D is tuned for *ramp* disturbances, $\alpha = 1$ (to take care of the low frequency mismatch) and some measurement noise, $f_a = 0.5$ (to achieve high frequency

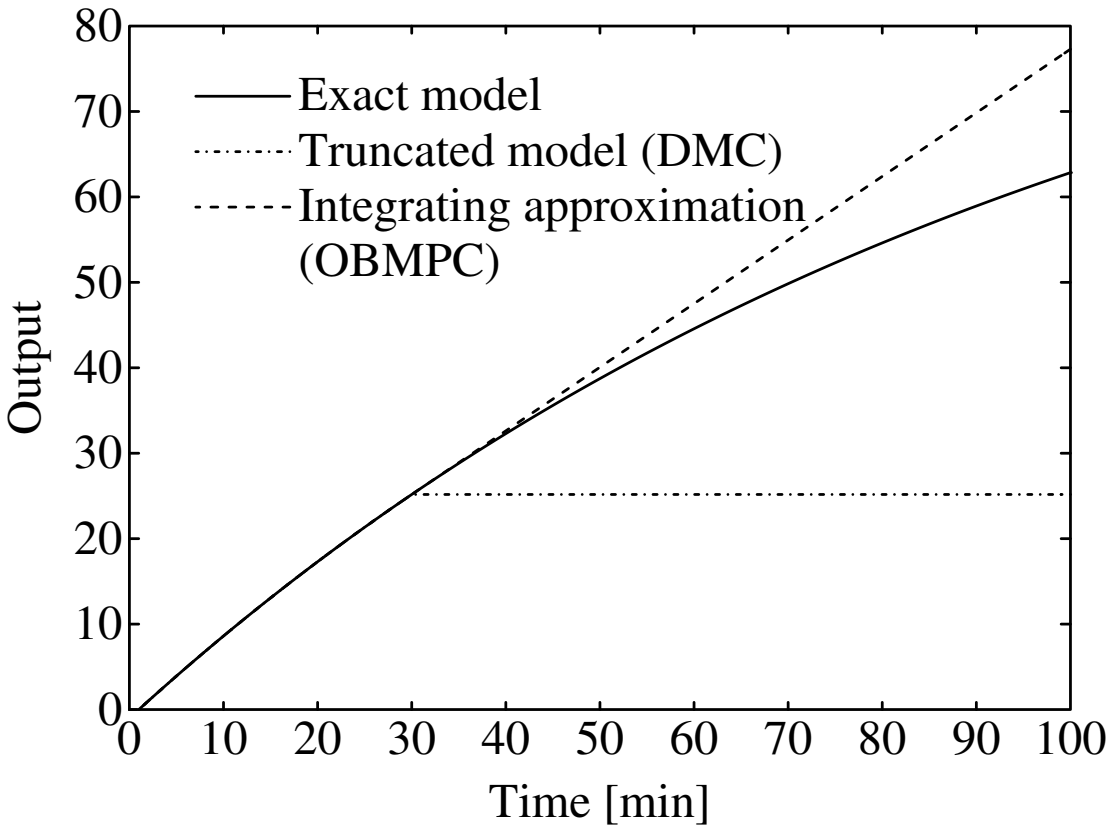

Figure 5.4: Open-loop response to unit step in u at t=0 for different models of $\frac{100}{100s+1}e^{-s}$. The DMC step response model is truncated at $n = 30$, $\Delta T = 1$ (Eq. 5.3–5.4). The OBMPC model uses $A_u = 1$, $B_u = s_{n+1} - s_n$, $n = 30$ and $\Delta T = 1$ (Eq. 5.25–5.26).

robustness).

5.3.3 Limitation 2: Poor response for ramp-like disturbances

The DMC performance may be very poor for disturbances which do not act as steps on the output. Fig. 5.7 shows the responses for the plant in Eq. 5.48 to a unit step acting on the plant output and input, respectively. A DMCss controller is used in both simulations in order to avoid truncation effects. The controller is tuned for dead-beat control (controller B) and the *output* disturbance (solid curve) is rejected in one sampling interval, since the disturbance is in accordance with assumption A2. The response to the *input* disturbance (dashed curve) is extremely sluggish. The reason is that a step disturbance on the input results in a slow, ramp-like disturbance on the output. In this case assumption A2 does not hold and the output prediction used by the algorithm is incorrect which results in poor performance. The response cannot be improved by a different tuning since a dead beat controller gives the highest feedback gain of any choice of Γ, Λ, p and m for a given ΔT.

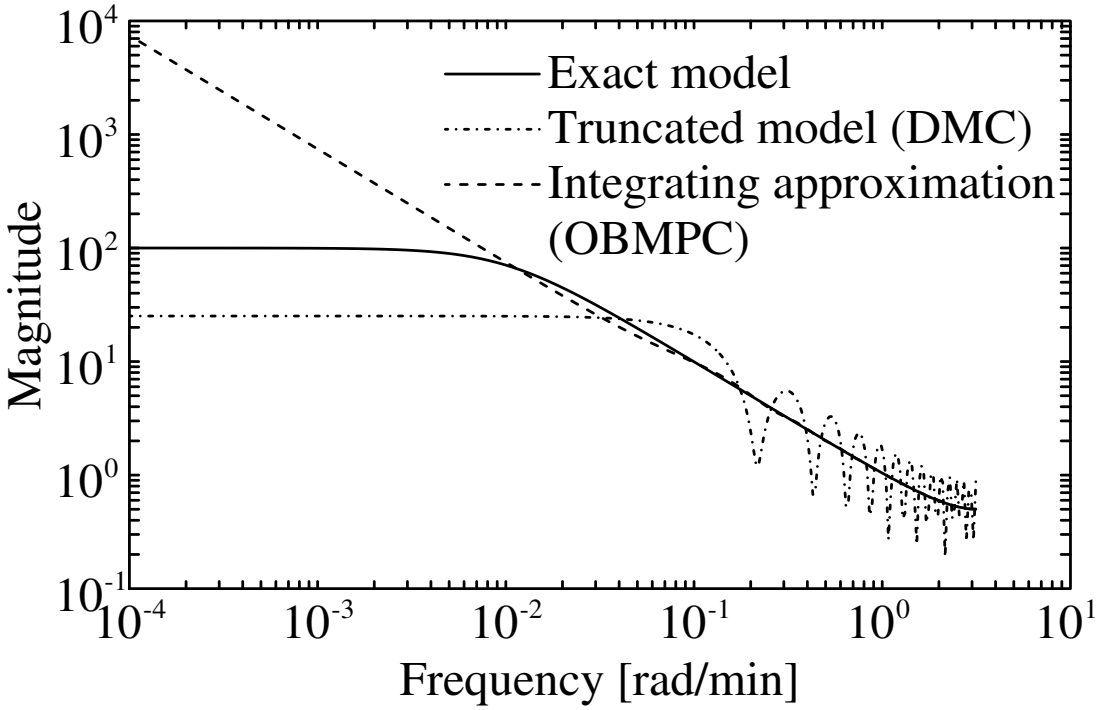

Figure 5.5: Frequency response for different models of $\frac{100}{100s+1}e^{-s}$. The DMC step response model is truncated at $n = 30$, $\Delta T = 1$ (Eq. 5.3–5.4). The OBMPC model uses $A_u = 1$, $B_u = s_{n+1} - s_n$, $n = 30$ and $\Delta T = 1$ (Eq. 5.25–5.26). (Both these models are multiplied with $G(z) = [(z-1)/z]$ to remove the inherent integrator.)

5.3.4 Avoiding limitation 2

An observer based MPC algorithm makes it possible to avoid the output step disturbance assumption (A2) which causes limitation 2. To demonstrate this we compare the dead beat DMCss response (controller B) with the OBMPC response (controller D). We also included a PI controller in this comparison to demonstrate the performance of a very simple controller. The PI controller is tuned according to Ziegler-Nichols rules taking into account an extra delay of half the sampling time (Table 5.1).

Responses to a unit input disturbance are shown in Fig. 5.8. The DMCss response is sluggish, while the other controllers perform well. Actually, the PI controller is almost as good as OBMPC for this simple plant.

The difference between the controllers is also illustrated in Fig. 5.9, showing the sensitivity function vs. frequency. The DMCss controller yields a sensitivity function with slope 1 for frequencies below the bandwidth. This shape of the sensitivity function is optimal for step disturbances and is a consequence of assumption A2. However, for "ramp-like" disturbances we need a stronger disturbance suppression at low frequencies. With a DMC controller this can only be achieved by increasing the bandwidth of the closed-loop system, since the shape of the sensitivity function is fixed (due to A2). The

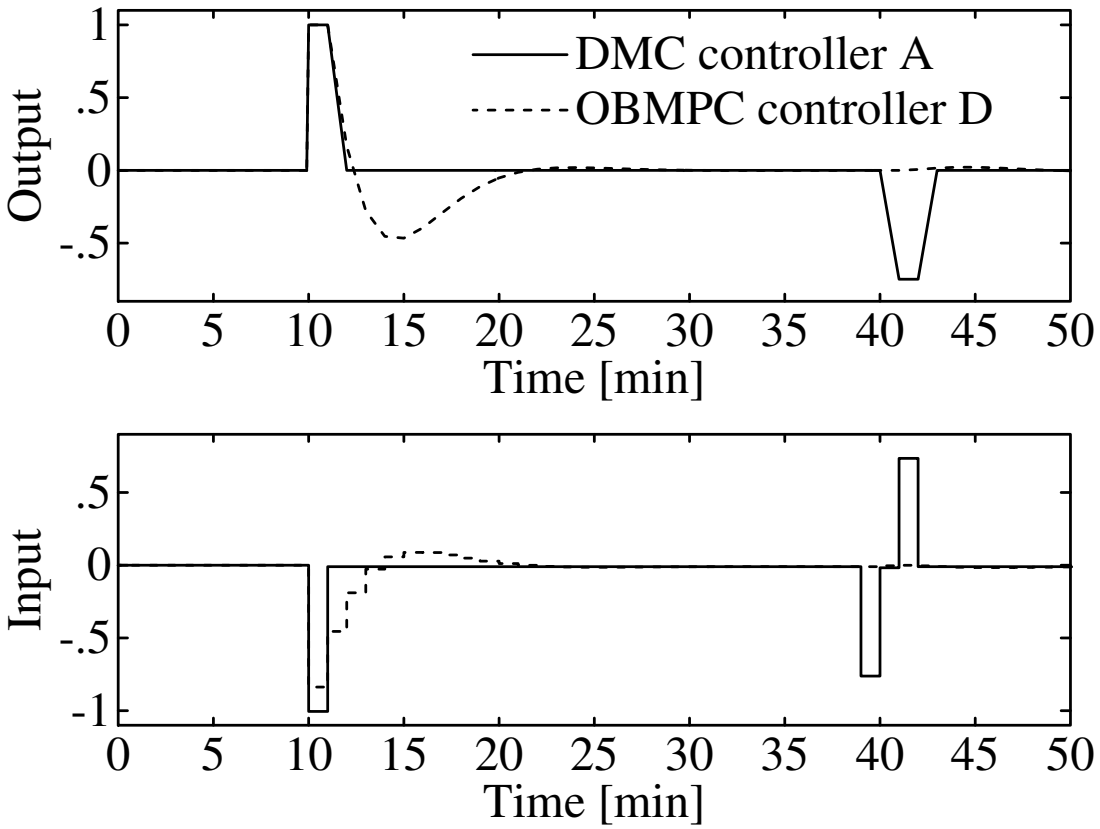

Figure 5.6: Responses for the SISO plant (Eq. 5.48) with different controllers (Table 5.1). A unit step disturbance acts on the plant output at $t = 10$.

maximum bandwidth for a given ΔT is obtained by using $\Lambda = 0$ (dead-beat) and if the resulting suppression of low frequency disturbances is not enough, then a smaller ΔT has to be used. With an OBMPC controller we may use α to adjust the disturbance suppression.

Fig. 5.9 also shows that the sensitivity function for DMCss controller B goes to zero at $\omega = \pi/\Delta T$ rad/min. This is due to the dead-beat tuning and makes the controller very sensitive to high frequency uncertainty, *e.g.* dead time uncertainty.

5.3.5 Limitation 3: Poor response for interactive MIMO plants

In this section we will show that there are cases with model-plant mismatch when a DMC controller does not perform well, even when the disturbance actually *is* a step acting on the output.

There is always a certain mismatch between a real process and a model. The mismatch has various sources: uncertainty in the model parameters and the model structure, inaccuracies of the actuators and measurement devices, *etc.* Multivariable

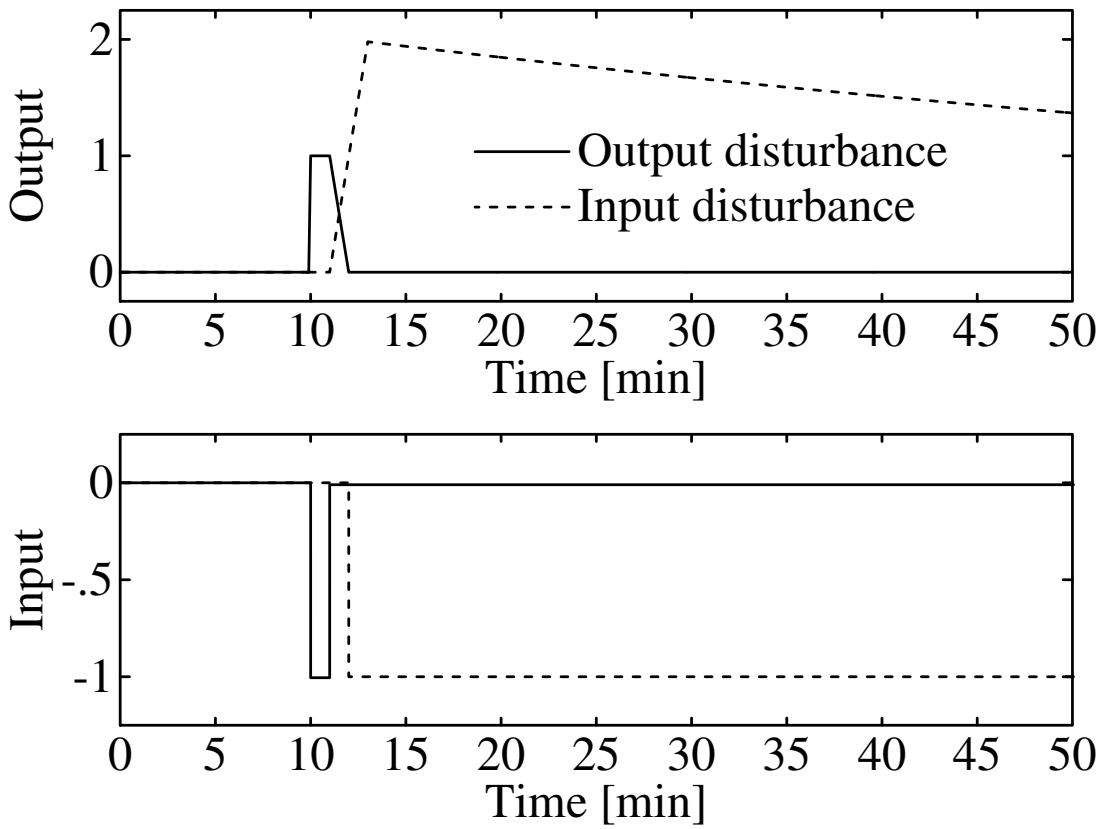

Figure 5.7: Responses for the SISO plant (Eq. 5.48) with DMCss controller B (Table 5.1). Solid curves: Unit step disturbance acting on the plant *output* at $t = 10$. Dashed curves: Unit step disturbance acting on the plant *input* at $t = 10$.

systems introduce a special problem here because the "gain" of a multivariable process varies not only with frequency, but also with "direction". Skogestad *et al.* (1988) show that if a plant is ill-conditioned irrespective of scaling, then the control performance is strongly affected by input uncertainty, in particular, when the controller is trying to invert the plant. The DMC controller is such a controller, especially, if the penalty weight on input moves is low. Since there is always *some* input uncertainty, it should be clear that a DMC controller is potentially bad when used for an ill-conditioned plant.

MIMO example

We use a distillation column as an example process. The model is from Skogestad and Morari (1988) and is denoted "column A" in their paper. The column is described by the following equations:

$$\begin{bmatrix} dy_D \\ dx_B \end{bmatrix} = \begin{bmatrix} \frac{k_{11}}{1+\tau_1 s} e^{-\theta s} & \left(\frac{k_{11}+k_{12}}{1+\tau_2 s} - \frac{k_{11}}{1+\tau_1 s} \right) e^{-\theta s} \\ \frac{k_{21}}{1+\tau_1 s} g_L(s) e^{-\theta s} & \left(\frac{k_{21}+k_{22}}{1+\tau_2 s} - \frac{k_{21}}{1+\tau_1 s} \right) e^{-\theta s} \end{bmatrix} \begin{bmatrix} dL \\ dV_B \end{bmatrix} \tag{5.49}$$

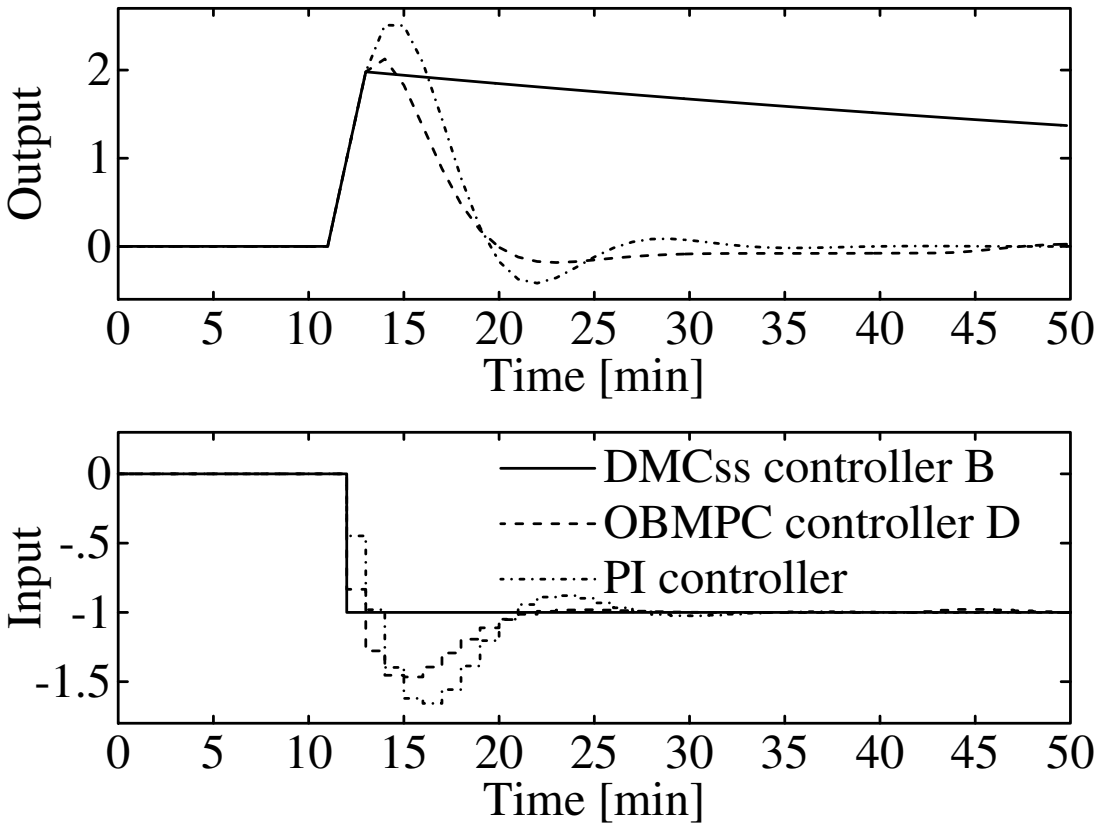

Figure 5.8: Responses for the SISO plant (Eq. 5.48) with different controllers (Table 5.1). A unit step disturbance acts on the plant input at $t = 10$.

where $g_L(s)$ expresses the liquid flow dynamics.

$$g_L(s) = \frac{1}{(1 + (\theta_L/n_T)s)^{n_T}} \tag{5.50}$$

θ_L is the overall liquid lag from the top to the bottom of the column. n_T in Eq. 5.50 should be equal to the number of trays in the column, but we use $n_T = 5$ to avoid a model of unnecessary high order. Reflux, L, and boilup, V_B, are manipulated inputs, top composition, y_D, and bottom composition, x_B, are controlled outputs. We use the following parameter values; $k_{11} = 0.878, k_{12} = -0.864, k_{21} = 1.082, k_{22} = -1.096, \tau_1 =$ 194 min, $\tau_2 = 15$ min, $\theta = 1$ min, $\theta_L = 2.46$ min and n_T=5. Skogestad and Morari do not include any specified delays in their model, instead they use a norm bounded uncertainty description to cover the effect of delays and other unmodeled high frequency dynamics. In Eq. 5.49 we assume the delays to be known and equal to 1 minute for each transfer function. We do this only because known delays fit better into the MPC framework.

Skogestad *et al.* (1990) demonstrate that a frequency dependent relative gain array (RGA) (Bristol, 1966) is a useful tool to check how sensitive a plant is to input

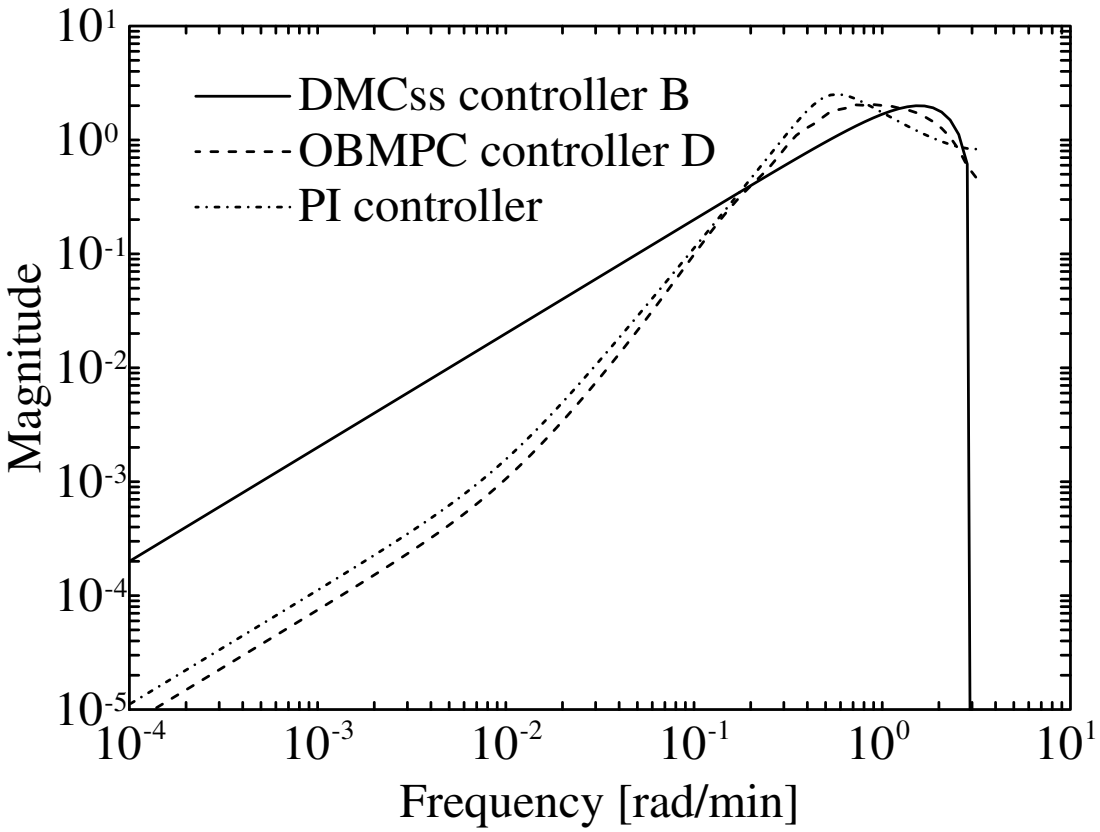

Figure 5.9: Sensitivity function vs. frequency for the SISO plant (Eq. 5.48) with different controllers (Table 5.1).

uncertainty. Fig. 5.10 shows the (1,1) RGA element, $\lambda_{1,1}$, of the distillation column, as a function of frequency. $\lambda_{1,1}$ is high (35.1) at low frequencies but falls to one at higher frequencies. This shows that a DMC controller may have problems with low frequency input uncertainty.

Effect of input uncertainty

We assume that there is 20% uncertainty in the input moves. From a singular value analysis, one can determine that the worst steady state effect is obtained when the uncertainties in ΔL and ΔV_B act in opposite directions (Skogestad *et al.*, 1988). In the simulations we use

$$\Delta L_{\text{actual}} = 1.2\Delta L_{\text{computed}} \quad \text{and} \quad \Delta V_{B\text{actual}} = 0.8\Delta V_{B\text{computed}}. \tag{5.51}$$

Responses for controller C (Table 5.1) to a 0.001 step disturbance acting on y_D are shown in Fig. 5.11. Errors in the input gains lead to very sluggish disturbance rejection although the disturbance is in accordance with the DMC disturbance assumption. The reason for this slow settling is that the effect of the errors in the manipulated inputs is similar to the effect of input step disturbances.

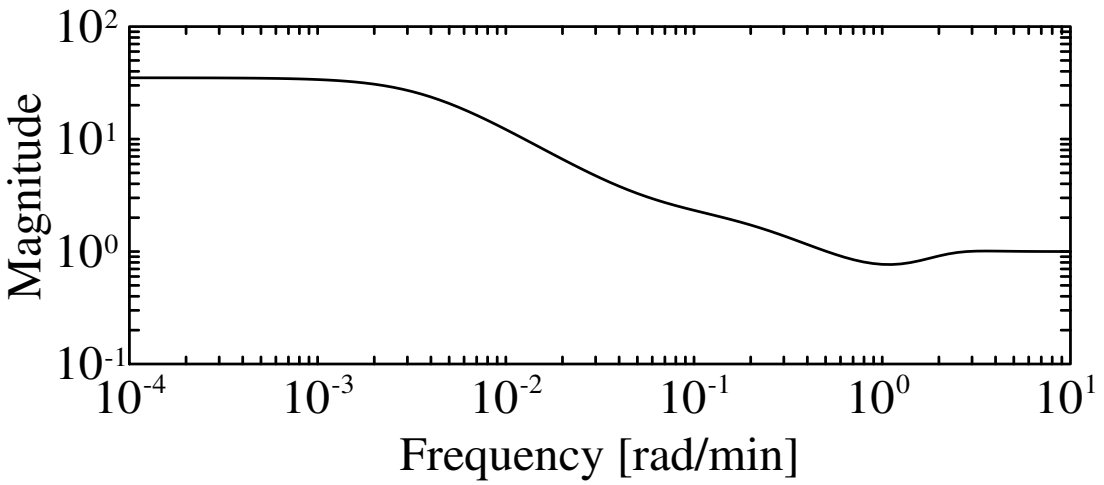

Figure 5.10: Magnitude vs. frequency plot of the (1,1)-RGA element of the distillation column (Eq.5.49). The interactions are large at low frequencies ($\lambda_{1,1} \approx 35.1$), but not at high frequencies ($\lambda_{1,1} \approx 1.0$).

This can also be demonstrated in a plot of the singular values of the sensitivity function (Fig. 5.12). Both the solid curves (no uncertainty) have slope 1 which is a consequence of the disturbance assumption. They also lie close to each other, which shows that the sensitivity function is well-conditioned. Since the plant itself is ill-conditioned we can conclude that the controller is compensating for the directionality of the plant. Such a controller is basically inverting the plant and the system should be sensitive to input uncertainty. Indeed, this is the case as seen both from the simulation in Fig. 5.11 and from the large difference between solid and dotted curves in Fig. 5.12. The dash-dot curve in Fig. 5.12 is included as a reference. It is an upper bound on sensitivity functions which achieve about 20 min closed-loop time constant and a maximum sensitivity peak of 2.

By comparing Fig. 5.10 and Fig. 5.12 we see that there is an excellent agreement between the predicted effect of uncertainty, based on the RGA-plot, and the actual effect seen in the sensitivity plot. (However, this sensitivity plot is only showing how the control performance deteriorate for this specific input error (+20% in L and –20% in V_B), and there may be an even larger effect for other error combinations of the same magnitude, *i.e.* the plot is not showing the "worst case" of a norm bounded uncertainty.)

5.3.6 Avoiding limitation 3

There are two different ways to deal with the problem caused by input uncertainty demonstrated in Fig.5.12:

1 Use a controller that does not correct for the directionality of the plant.

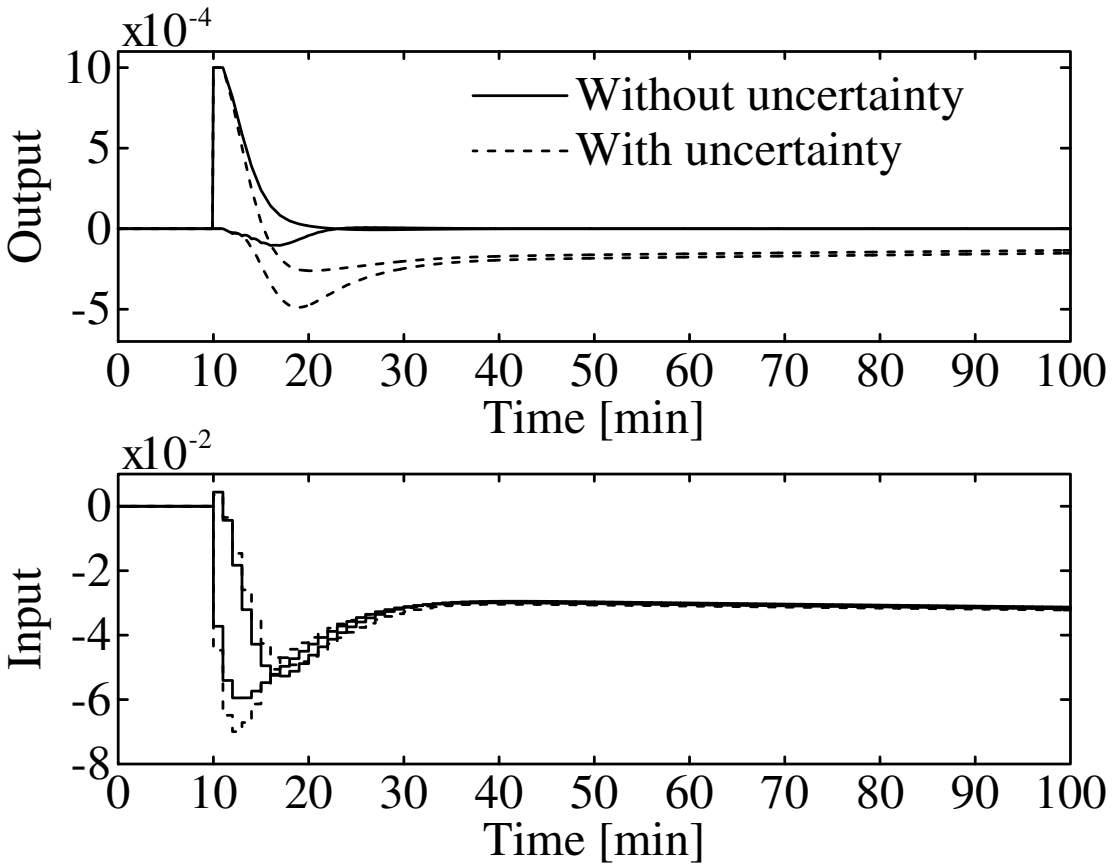

Figure 5.11: Responses for the distillation column (Eq. 5.49) with DMCss controller C (Table 5.1). A 0.001 step disturbance acts on y_D at $t = 10$. Uncertainty as defined in Eq. 5.51.

2 Increase the gain at those frequencies where the suppression of disturbances is poor.

The first method is suggested in Skogestad *et al.* (1988). It gives a controller with somewhat sacrificed nominal performance, but the performance is much less sensitive to uncertainty because the controller does not correct for directionality.

The second approach will work if the uncertainty only causes problem at low frequencies. With this approach the controller is still sensitive to uncertainty, but this is counteracted by increasing the controller gain at low frequencies to make the nominal response much better than what is nominally needed.

We will now demonstrate the two approaches, using OBMPC controllers E and F (Table 5.1). In both cases the residual plant dynamics for each input-output pair is approximated by $b_{ij}/(z - a_{ij})$ where $b_{ij} = s_{i,j,n+1} - s_{i,j,n}$ and $a_{ij} = 0.995$, *i.e.* a first order response with a time constant approximately equal to 200 min and a gain determined at the "truncation" step. The disturbance is assumed to have the same dynamics as the plant, *i.e.* $\alpha_i = 0.995$.

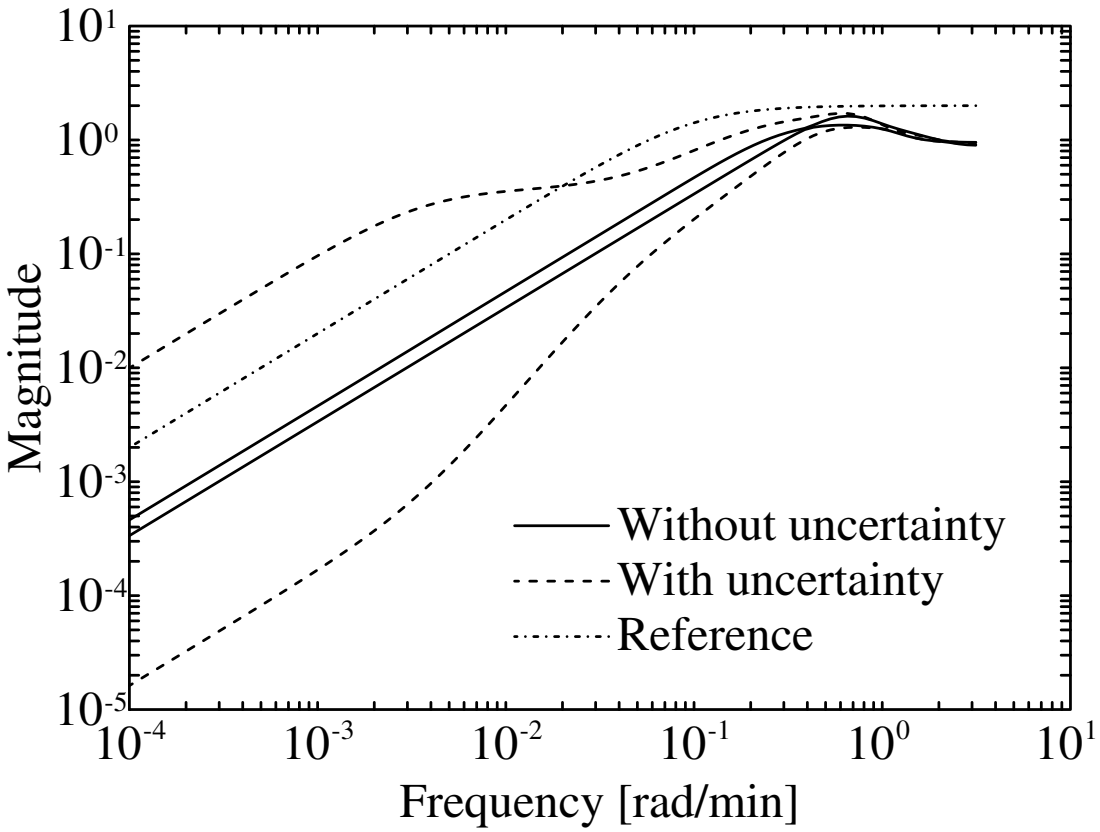

Figure 5.12: Maximum and minimum singular values of the sensitivity function for the distillation column (Eq. 5.49) with DMCss controller C (Table 5.1). Uncertainty as defined in Eq. 5.51.

Fig. 5.13 and 5.14 show responses for OBMPC controllers E and F, respectively, for the same output disturbance as used in Fig. 5.11. The OBMPC controllers perform well despite the uncertainty (Eq. 5.51) and suppress the disturbance much faster than DMCss does (Fig. 5.11). The response of controller E is nearly unaffected of the uncertainty. Controller F yields an almost perfectly decoupled response when there is no uncertainty (*i.e.* x_B is not affected by the disturbance in y_D), while the response with input error clearly demonstrates interaction between the two loops.

In the case of an *input* disturbance the difference between the OBMPC controllers and the DMCss controller would be even larger, because of limitation 2.

The sensitivity plot for controller E is shown in Fig. 5.15. This controller is using a high input weight and a large disturbance-to-noise ratio. The plot shows that this controller does *not* try to invert the plant; the solid curves (no uncertainty) do not lie close to each other. We can also conclude that it is insensitive to uncertainty since the dotted curves (uncertainty defined in Eq. 5.51) lie close to the solid curves.

Fig. 5.16 shows the sensitivity plot for controller F. This controller has no weight on the inputs (dead-beat K_{MPC}) but is tuned for substantial measurement noise ($f_a =$

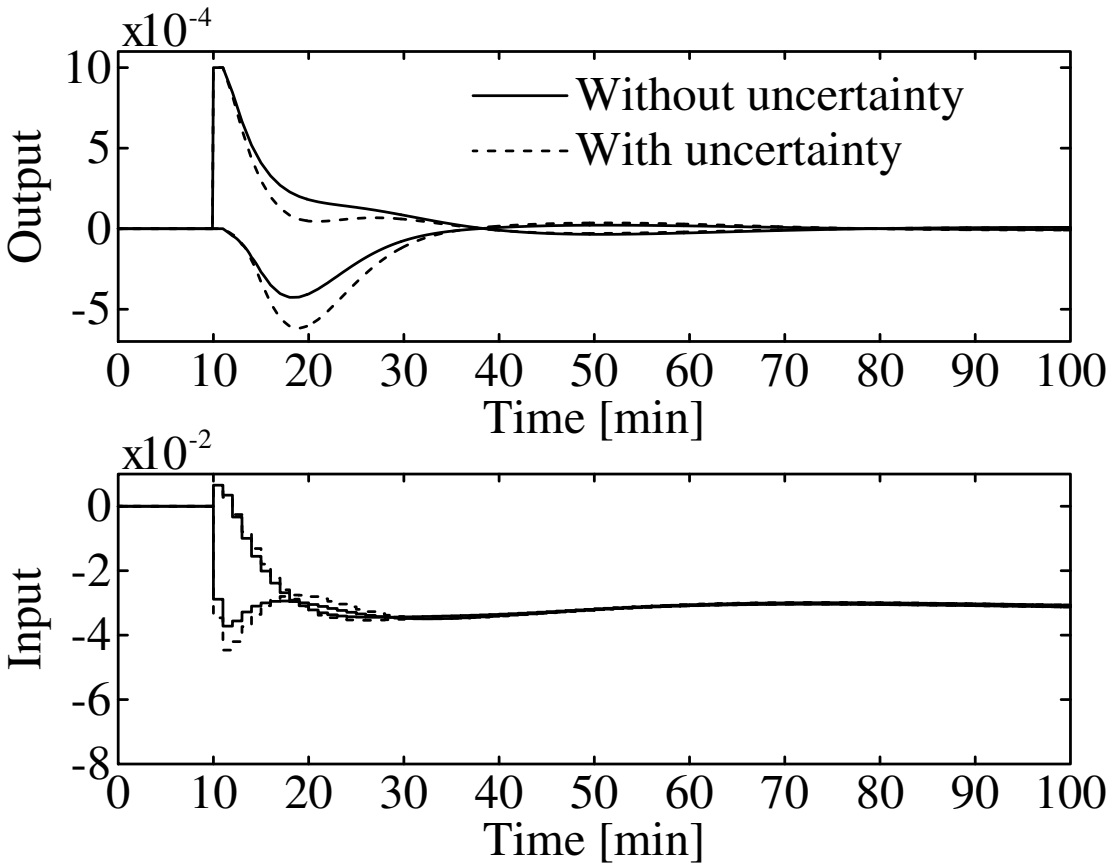

Figure 5.13: Responses for the distillation column (Eq. 5.49) with OBMPC controller E (Table 5.1). A 0.001 step disturbance acts on y_D at $t = 10$. Uncertainty as defined in Eq. 5.51.

0.22). From the plot we see that this controller *is* inverting the plant for frequencies above $\omega \approx 0.01$ rad/min. Below this frequency it is still trying to invert the plant, but it does not succeed, since the true plant and the model with approximated residual dynamics are slightly different. This controller is sensitive to input uncertainty, in the sense that nominal performance and performance with uncertainty are very different. However, the low frequency controller gain is so high that even the performance *with* uncertainty is satisfactory, except over a short frequency range.

Although controller F yields satisfactory performance, we may conclude that the plant is rather sensitive to input uncertainty also at frequencies above the bandwidth. Thus, the best tuning approach for this plant is approach 1 above, used for tuning controller E.

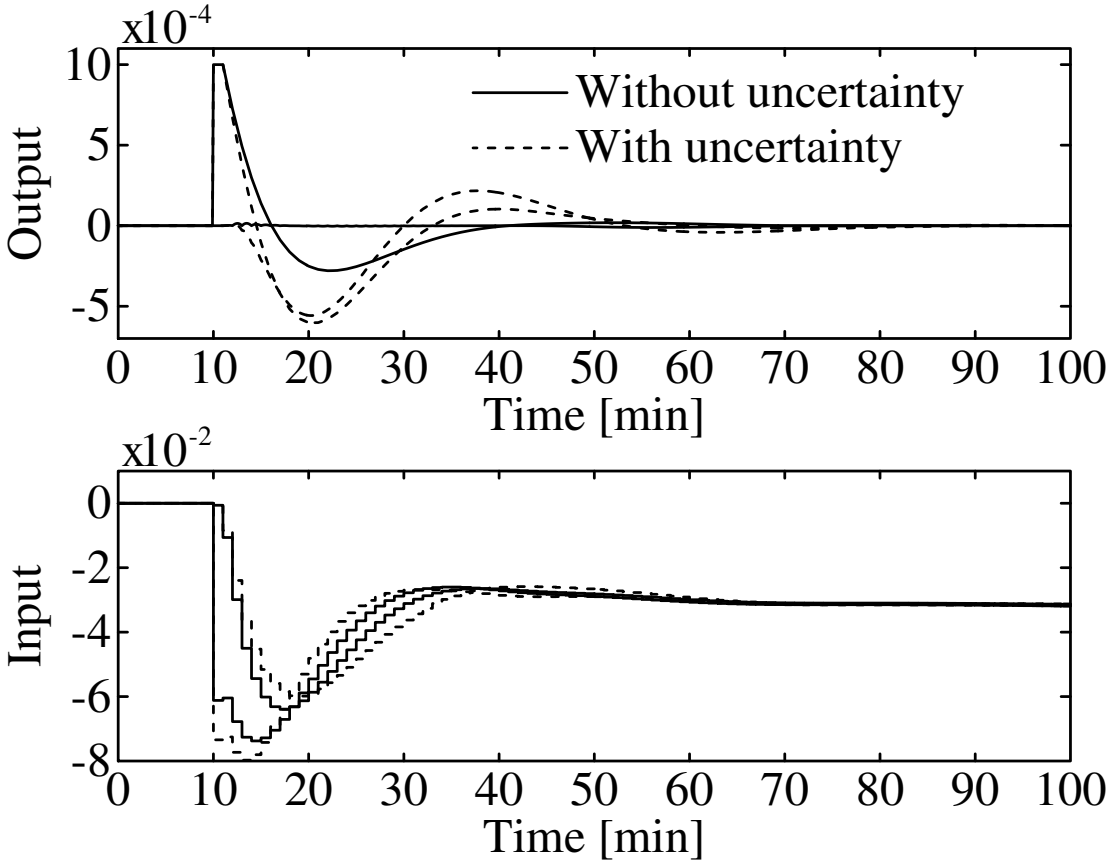

Figure 5.14: Responses for the distillation column (Eq. 5.49) with OBMPC controller F (Table 5.1). A 0.001 step disturbance acts on y_D at $t = 10$. Uncertainty as defined in Eq. 5.51.

5.4 Discussion

We have studied feedback limitations of unconstrained DMC with a quadratic objective function (Eq. 5.13). There are several variants of DMC: "original" DMC (Cutler and Ramaker, 1980), DMC with least squares satisfaction of input constraints (Prett and Gillette, 1980), DMC with constrained linear programming optimization (LDMC) (Morshedi *et al.*, 1985), DMC with constrained quadratic programming optimization (QDMC) (García and Morshedi, 1986). These variants use different optimizers but the predictor is the same for all of them. Both the limiting assumptions (A1 and A2), which we have studied, are implicit in the predictor and will not be avoided by modifying the optimizer, so the results in this paper hold for all of these algorithms. The results also carry over to the general case with constraints, since the issue of constraints only affects the optimizer.

The requirement $S_n \approx S_{n+1}$ of assumption 1, can be avoided within the DMC framework (as defined by Fig. 5.1) by using a general state space model instead of

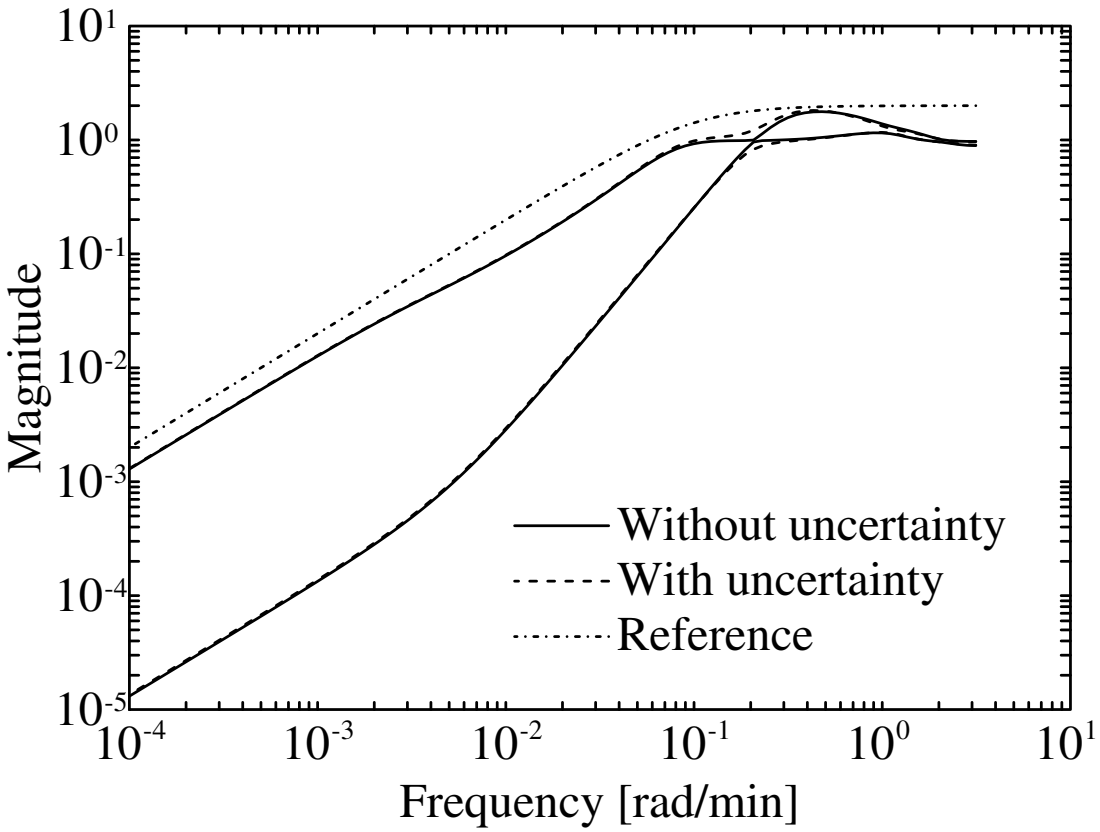

Figure 5.15: Maximum and minimum singular values of the sensitivity function for the distillation column (Eq. 5.49) with OBMPC controller E (Table 5.1). Uncertainty as defined in Eq. 5.51.

a step response model. However, the plant still has to be stable to ensure internal stability. Assumption A2 cannot be avoided unless the *constant* matrix $\mathcal{I}$ is exchanged with a transfer function including *states*. This is most clearly seen in the DMCss algorithm where the input to $\mathcal{I}$ is $\hat{y}(k)$. $\hat{y}(k)$ cannot be "filtered" by $\mathcal{I}$ since it has no states and therefore no knowledge of previous measurements. Using a gain different form 1 in $\mathcal{I}$ would not filter $\hat{y}(k)$, but rather introduce a steady state offset.

In this paper we have excluded the feedforward part of the algorithms, although feedforward control is a standard feature of MPC. It is simple to include feedforward in the algorithms by introducing measured disturbances as inputs to the predictor. However, this does not affect our results, the feedback limitations are still present.

In the following we discuss some of the results and our choice of example processes and controller tunings.

The SISO example (Eq. 5.48) has a time constant much larger than the time delay. This parameter choice is made on purpose to demonstrate limitations L1 and L2, since they are especially important when the time constant of the open-loop plant is large, compared to the desired closed-loop time constant. In the SISO simulations we use

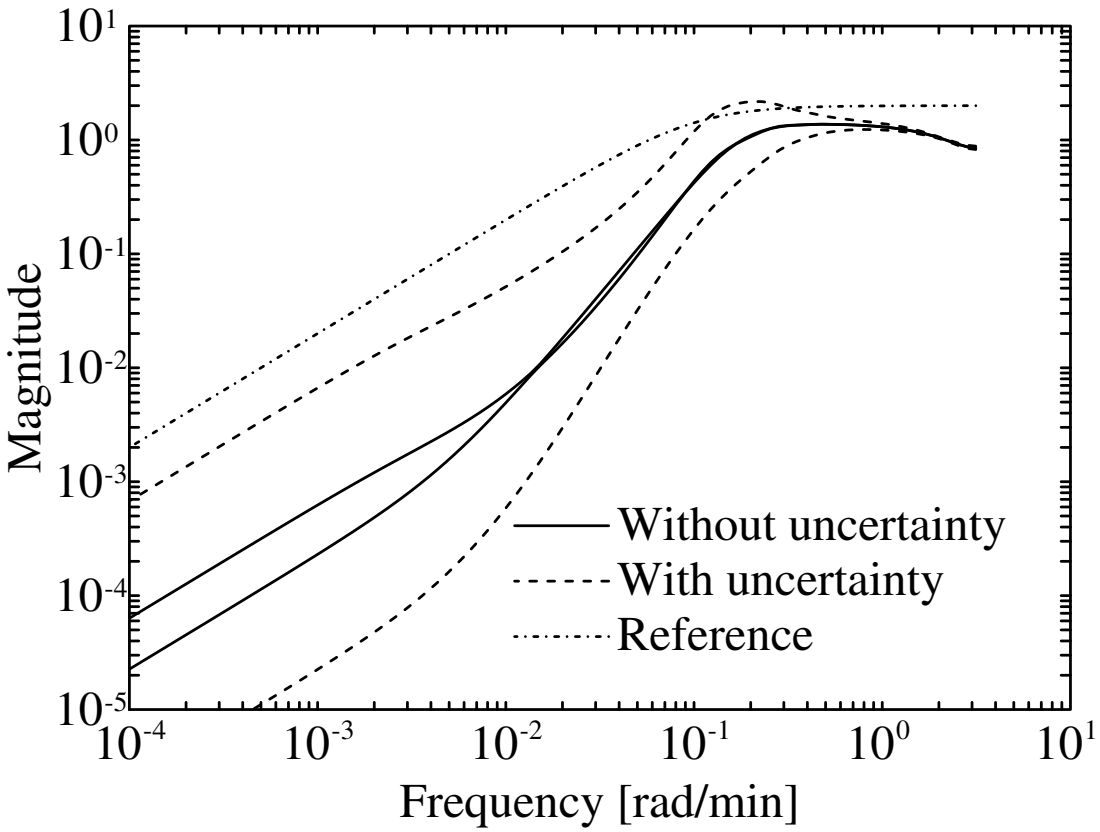

Figure 5.16: Maximum and minimum singular values of the sensitivity function for the distillation column (Eq. 5.49) with OBMPC controller F (Table 5.1). Uncertainty as defined in Eq. 5.51.

controllers where the optimizer is tuned for dead-beat control. The reason for this tuning is that we want to produce clear illustrative simulations where the controller action is easy to understand. In real applications one should always use a non-zero input weight Λ to achieve some robustness to noise and high-frequency model-plant mismatch.

All the simulations presented in this paper are *without* measurement noise. Again the reason is that we want to show clear illustrative simulations. (We have also performed the simulations with noise and it does not change our results.)

We have demonstrated that a truncated step response model may cause severe model-plant mismatch, both at high and low frequencies. Low frequency mismatch is not critical as long as the "sign" of the process is correct, but high frequency mismatch may yield an unstable system (Fig. 5.3). With the OBMPC controller truncation is avoided. In controller D we use a rough approximation of the residual dynamics (an integrator) to show that even this approximation is better than truncation.

The sensitivity plots for the distillation column (Fig. 5.12, 5.15 and 5.16) shows singular values of the sensitivity function for no uncertainty and for *one specific* case

of uncertainty. However, we have used the structural singular value, μ, to check that the controllers will perform well also for other cases of uncertainty (see Skogestad *et al.* 1988, for instance).

We have not put any effort into finding the best approximation of the residual dynamics, although that may have improved the OBMPC responses further, instead the simplest choices of A_u and B_u are used throughout the paper. Hovd *et al.* (1991) discuss how to choose A_u and B_u in an optimal fashion.

5.5 Conclusions

We have shown that there are situations where the feedback performance of DMC is poor irrespectively of tuning. This poor performance is due to the two assumptions (A1 and A2) made in the *predictor* part of the algorithm. This explains why the performance cannot be improved by a different tuning – different tuning only affects the *optimizer* part of the algorithm.

The Observer Based Model Predictive Control (OBMPC) algorithm by Lee *et al.* (1991) allows us to avoid the limitations of DMC and still preserve all the attractive properties of the DMC algorithm.

Nomenclature

A - state matrix
$\mathcal{A}$ - disturbance state matrix, Eq. 5.37
a - element in state matrix
B - input matrix
b - element input matrix
C - output matrix
f_a - tuning parameter in filter gain K
f_b - tuning parameter in filter gain K
$\mathcal{I}$ - Eq. 5.12
K - Kalman filter gain
K_c - PI-controller gain
K_{MPC} - MPC feedback gain
k_{ij} - gain, Eq. 5.49
L - reflux
M - matrix in step response model, Eq. 5.3
m - input horizon
N - matrix in step response model, Eq. 5.4
n - model horizon
n_u - number of inputs
n_y - number of outputs
p - prediction horizon

$\mathcal{R}$ - set point vector
S - step response coefficient matrix, Eq. 5.3
s - step response coefficient
T - disturbance input matrix, Eq. 5.25
ΔT - sampling time
t - time [min]
$\mathcal{U}$ - optimal control sequence
u - manipulated input
V - noise covariance matrix
V_B - boilup
v - measurement noise
W - disturbance covariance matrix
w - disturbance
x - state variable
x_B - bottom composition [kmol/kmol]
Y - output vector
$\tilde{Y}$ - dynamic states of DMC predictor
$\bar{Y}$ - dynamic states of OBMPC predictor
$\mathcal{Y}$ - predicted output vector
y - controlled output
$\hat{y}$ - measured output
y_D - top composition [kmol/kmol]
z - shift operator

Greek symbols

α - parameter in disturbance model, Eq. 5.37
Γ - output weighting matrix, Eq. 5.13
Δ - $\Delta u(k) = u(k) - u(k-1)$
θ - time delay [min]
Λ - input weighting matrix, Eq. 5.13
λ_{11} - (1,1) RGA element
τ_I - PI-controller integral time constant [min]
τ_1, τ_2 - time constant [min], Eq. 5.49
ω - frequency [rad/min]
ω_B - closed-loop bandwidth [rad/min]

Abbreviations

DMC - Dynamic Matrix Control
DMCss - Dynamic Matrix Control with state space model
MIMO - Multi Input Multi Output
MPC - Model Predictive Control
OBMPC - Observer Based Model Predictive Control
QDMC - Quadratic Programming Dynamic Matrix Control
RGA - Relative Gain Array

SISO - Single Input Single Output

References

Bristol, E.H. (1966). "On a New Measure of Interactions for Multivariable Process Control", *IEEE Automat. Control*, **AC-11**, 133-134.

Cutler, C.R. and B.L. Ramaker (1980). "Dynamic Matrix Control - A Computer Control Algorithm", *Proc. Joint Automatic Control Conf.*, San Francisco, California, Paper WP5-B.

García, C.E. and A.M. Morshedi (1986). "Quadratic Programming Solution of Dynamic Matrix Control (QDMC)", *Chem. Eng. Commun.*, **46**, 73-87.

García, C.E., D.M. Prett and M. Morari (1989). "Model Predictive Control: Theory and Practice - a Survey", *Automatica*, **25**, 3, 335-348.

Hovd, M., J.H. Lee and M. Morari (1991). "Model Requirements for Model Predictive Control", *European Control Conference*, Grenoble, France.

Lee, J.H., M. Morari and C.E. García (1991). "State-Space Interpretation of Model Predictive Control", Submitted to *Automatica*.

Li, S., K.Y. Lim and D.G. Fisher (1989). "A State Space Formulation for Model Predictive Control", *AIChE Journal*, **35**, 2, 241-249.

Middleton, R.H. (1991). "Trade-offs in Linear Control System Design", *Automatica*, **27**, 2, 281-292.

Morshedi, A.M., C.R. Cutler and T.A. Skrovanek (1985). "Optimal Solution of Dynamic Matrix Control with Linear Programming Techniques (LDMC)", *Proc. Am. Control Conf.*, Boston, Massachusetts, pp. 199-208.

Prett, D.M. and C.E. García (1988). *Fundamental Process Control*. Butterworths, Stoneham, Massachusetts.

Prett, D.M. and R.D. Gillette (1980). *Proc. Joint Automatic Control Conf.*, San Francisco, California.

Skogestad, S. and M. Morari (1988). "Understanding the Dynamic Behavior of Distillation Columns", *AIChE Journal*, **33**, 10, 1620-1635.

Skogestad, S., M. Morari and J.C. Doyle (1988). "Robust Control of Ill-conditioned Plants: High-purity Distillation", *IEEE Automat. Control*, **33**, 1092-1105.

Skogestad, S., P. Lundström and E.W. Jacobsen (1990). "Selecting the Best Distillation Control Configuration", *AIChE Journal*, **36**, 5, 753-764.

Chapter 6

Opportunities and Difficulties with 5×5 Distillation Control

Petter Lundström and Sigurd Skogestad
Chemical Engineering
University of Trondheim, NTH
N-7034 Trondheim, Norway

Presented at *IFAC-Symposium ADCHEM'94*, Kyoto, Japan

Abstract

Multivariable 5×5 distillation control, *i.e.* control of levels, pressure and compositions by one multivariable controller, provides opportunities to improve the control performance as compared to decentralized control. Multivariable interactions can be counteracted with a 5×5 controller. However, the main advantage is automatic constraint handling which can not be realized by a fixed linear 5×5 controller, but requires a solution based on on-line optimization, for example, using a Model Predictive Control (MPC) strategy. A multivariable control scheme also presents some difficulties. Unconsidered model uncertainty may be a severe problem. It may also be difficult to tune the multivariable controller. In this paper the MPC approach is combined with the $\mathcal{H}_\infty/\mu$ framework in order to obtain a robust design.

6.1 Introduction

A one-feed two-product distillation column, as shown in Fig.6.1, may be viewed as a 5×5 dynamic system. This means that for a fixed design and a given feed the column has 5 (dynamic) degrees of freedom, or in control terms, there are 5 manipulated inputs which may be used to control 5 controlled outputs.

The controlled variables (outputs) are the liquid holdup in reboiler and condenser (M_B, M_D, here assumed on a molar basis), pressure in the condenser (P_D), composition of light component in the top product (distillate) (x_D) and composition of light component in the bottom product (bottoms) (x_B). In this paper all controlled outputs are measured, but measurement errors are included in the analysis. The manipulated variables (inputs) are the flows of reflux, distillate and bottoms (L_T, D and B, here assumed on a molar basis), and the heat duty in reboiler and condenser (Q_R, Q_C). The feed rate (F), composition (z_F) and energy content (defined in terms of the bubble point pressure of a liquid feed, P_F^{sat}) all act as disturbances. In addition, there are disturbances in all the manipulated variables.

In industry most columns are operated by single-input-single-output (SISO) controllers and manual adjustments. Such a decentralized (multiloop) control structure has the advantage of being easy to retune and to understand. However, fixed pairing of outputs and inputs may limit the performance of the overall system, since the SISO controllers do not utilize information from the other loops. Another disadvantage with decentralized control is that the control performance may seriously deteriorate if the

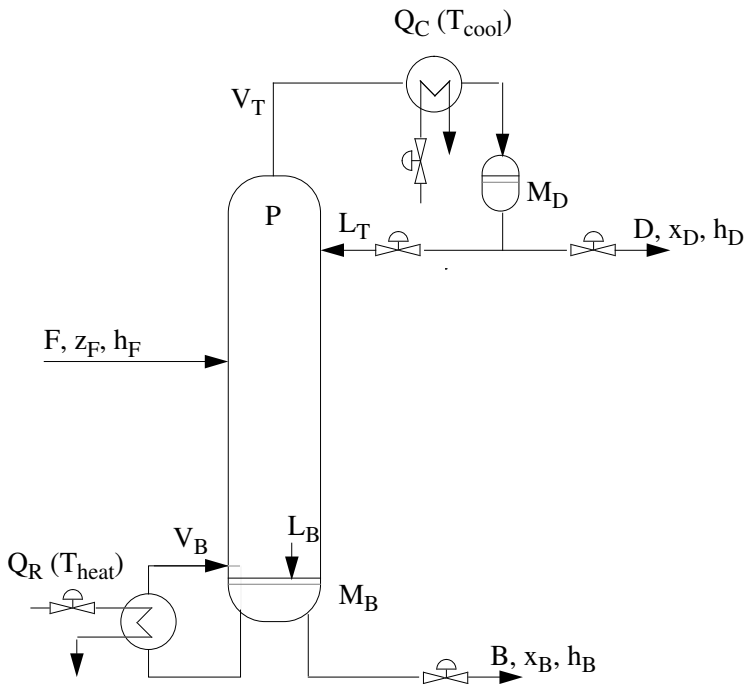

Figure 6.1: One-feed two-product distillation column.

system hits some constraint. For example, if a stabilizing loop saturates, the system goes unstable. To avoid this, the plant has to be operated sufficiently far away from the constraints, or facilities for loop reconfiguration have to be installed "on-top" of the SISO controllers. For example, for a decentralized control scheme where pressure (P_D) is controlled by manipulating the condenser cooling (Q_C) and maximum cooling is reached, the controller has to be reconfigured and use, for example, heat input to the reboiler (Q_R) for pressure control.

From a theoretical point of view it is obvious that the 'optimal' controller should use *all* available information (measurements, plant model, expected model uncertainty, expected disturbances, known future setpoint changes, known constraints, etc.) to manipulate all 5 inputs in order to keep all 5 outputs at their optimal values (5×5 control) (Skogestad, 1989). It is also clear that constraint handling is a very important issue for this 'optimal' control scheme, since, in general, optimality is obtained at some constraint, for example, maximum throughput.

A fundamental difficulty with any optimizing scheme is to define an objective function which yields a mathematically optimal solution in agreement with what is actually desired. Another problem is to obtain sufficiently accurate information (measurements, plant model, uncertainty bounds, etc.) to make the optimization worthwhile.

The purpose of this paper is to evaluate the opportunities and difficulties with applying 5×5 control to a distillation column. The paper is organized as follows. In section 6.2 we present a fairly rigorous non-linear 5×5 model, which, contrary to most other distillation models, does not assume constant pressure (which would yield a 4×4 model). In section 6.3 we perform a controllability study using a linearized model. We also consider a decentralized controller which leads to rather poor performance for the example column in question. In section 6.4 we study the *unconstrained* multivariable problem, using the $\mathcal{H}_\infty$-norm to measure control performance. This norm makes it possible to specify desired responses in terms of closed-loop time constants, allowable steady state offset and acceptable overshoot, and also allows us to address robustness using the structured singular value, μ (Doyle, 1982). In section 6.5 we consider model predictive control using a state observer based MPC algorithm (Morari and Ricker, 1991). To obtain a robust controller, we first attempt to tune the unconstrained MPC controller to mimic the performance of the robust $\mathcal{H}_\infty/\mu$ controller by using μ-analysis and the weights obtained from the $\mathcal{H}_\infty$ design. Of course, this may not be done directly as an MPC controller behaves similar to an $\mathcal{H}_2$-controller, which is not quite the same as an $\mathcal{H}_\infty$-controller (the norms are somewhat different). When the unconstrained performance has been assessed using μ, we use simulations to evaluate the performance for the constrained case.

6.2 5×5 Distillation Model

In this section we briefly present the distillation column which is used as an example process in the rest of the paper. The example column separates a binary mixture into a

Table 6.1: Column data

Feed (d):	F	=	1.0 [kmol/min]
	$z_F(1)$	=	0.5 [kmol/kmol]
	P_F^{sat}	=	0.11 [MPa]
Controlled outputs (y):	$x_D(1)$	=	0.99 [kmol/kmol]
	$x_B(1)$	=	0.01 [kmol/kmol]
	P_D	=	0.1 [MPa]
	M_D	=	32.1 [kmol]
	M_B	=	11.0 [kmol]
Manipulated inputs (u):	L_T	=	2.725 [kmol/min]
	Q_R	=	129.09 [MJ/min]
	Q_C	=	-129.02 [MJ/min]
	D	=	0.5 [kmol/min]
	B	=	0.5 [kmol/min]
Key hydraulic parameters:	$\bar{\tau_L}$	$\approx$	2.4 [sec]
	$\sum \tau_L$	$\approx$	93 [sec]
	$K_{2(Top)}$	$\approx$	0.5
	$K_{2(Bot)}$	$\approx$	0.8

top and a bottom product of relatively high purity (99%). The column closely matches "column A" studied by Skogestad and Morari (1988), but the model used here is much more detailed:

1. Pressure is not assumed constant.

2. Vapor holdup is included.

3. Vapor flow rate from one tray to another is computed from the pressure difference between the trays.

4. Liquid flow rate is computed from the Francis weir formula, including a correlation between vapor flow and froth density (Bennett *et al.*, 1983) such that a change in vapor flow will have an initial effect on the liquid flow (the "K_2"- or "λ-effect", Rademaker *et al.*, 1975).

The column has 39 trays plus a total condenser and a reboiler, and is modelled using 41 control volumes. It is assumed that each control volume contains a perfectly mixed two-phase system in thermal and vapor-liquid equilibrium. An implicit UV-flash calculation is used to obtain liquid and vapor compositions, temperature and pressure on each tray. This yields a model with 3 states (differential equations) per control

Table 6.2: Data used in Fig. 6.2

Input	Perturbation at t=20 min				
L_T	2.724	to	2.729	kmol/min	(0.18%)
Q_R	128.849	to	129.049	kJ/min	(0.16%)
Q_C	−129.018	to	−128.818	kJ/min	(0.16%)
D	0.500	to	0.505	kmol/min	(1.00%)
B	0.500	to	0.505	kmol/min	(1.00%)

Output	Range			
x_D	0.987	to	0.993	kmol/kmol
x_B	0.007	to	0.013	kmol/kmol
P_D	0.099	to	0.107	MPa
M_D	31.000	to	33.500	kmol
M_B	9.500	to	12.000	kmol

volume (the molar holdup of each component and the internal energy), resulting in a total of 123 states for the column with condenser and reboiler.

The nonlinear model has been implemented in the equation oriented simulation package SPEEDUP (Pantelides, 1988). This package has been used to obtain the steady-state solution and to linearize the system. The dynamic open-loop responses presented in this paper (Fig. 6.2) were also obtained by using SPEEDUP, while the closed-loop responses are linear simulations performed in MATLAB.

A summary of the column data is given in Table 6.1. Open-loop time responses are summarized in Fig. 6.2 and Table 6.2. Note that a perturbation of Q_C yields inverse responses in all outputs except in P_D. The heat duties, Q_R and Q_C, are defined positive if heat is *added* to the reboiler and condenser, respectively. Also note that we assume that the heating and cooling duties are adjusted directly, that is, there is no "self-regulation" and Q_C and Q_R are not affected by changes in pressure and temperature in the column. This may be the case, for example, if heat is provided by condensation, and cooling is provided by boiling. This assumption yields a very long time constant for the open-loop pressure response, and it may be estimated to be about $(M_L + 4M_V)/F = 74$ min., where M_L and M_V are the total liquid and vapor molar holdups in the column, condenser and reboiler, and F is the molar feed flow. This formula is derived from an overall heat balance assuming that the temperature change is the same throughout the column. The factor 4 for the vapor holdup is a typical value, and is due to the fact that $c_{PV} > c_{PL}$ and that some energy is needed for evaporation when pressure increases. If we have self-regulation in the condenser, *e.g.*, $Q_C = UA(T_{cool} - T_D)$, then we get $F + UA/c_{PL}$ in the denominator instead of F, and the time constant is much smaller, typically about 2 min.

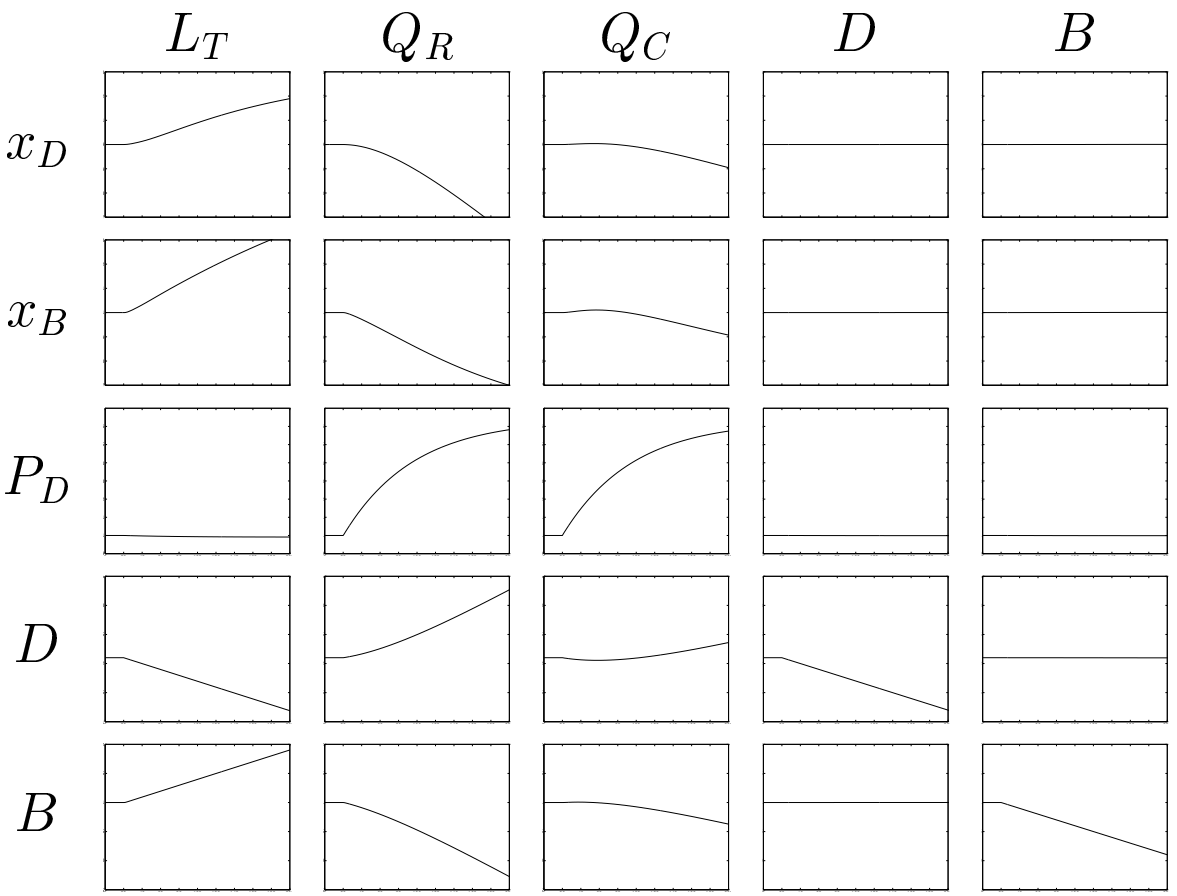

Figure 6.2: Open loop step responses showing the effect of the 5 inputs (u) on the 5 outputs (y). 200 min simulation time. Perturbations and output ranges are displayed in Table. 6.2

6.3 Controllability analysis

In this section simple linear tools (*e.g.*, Wolff *et al.*, 1992) are used to assess the controllability properties of the plant, that is, to evaluate any inherent performance limitations. The results from the controllability analysis are also used to specify realistic requirements for control performance and thereby reduce the need for iterative adjustments of the performance requirements, *i.e.* the 'weights' used to tune the controller.

Conclusions drawn from some of the measures, such as the inputs required for perfect control or the presence of RHP-zeros, are valid independently of the control algorithm, while some other measures (CLDG, PRGA) only apply to decentralized control.

The model used in this section was obtained by linearizing the non-linear model using the linearization package CDI within SPEEDUP and then reduce the number of states from 123 to 15, using 'ohkapp' from Robust Toolbox (Chiang and Safonov, 1992).

Table 6.3: Maximum acceptable deviation (*mad*) for used scaling. (Units and order of elements for these vectors are given in Table 6.1.)

Output error:	y_{mad}	=	$[0.01\ 0.01\ 0.050\ 30.\ 10.]^T$
Setpoints:	r_{mad}	=	$[0.01\ 0.01\ 0.025\ 0.5\ 0.5]^T$
Inputs:	u_{mad}	=	$[2.7\ 130\ 130\ 0.5\ 0.5]^T$
Feed disturbances:	d_{mad}	=	$[0.15\ 0.1\ 0.025]^T$

The open-loop model of the plant has two pure integrators, namely the holdups in reboiler and condenser. These pure integrators may cause numerical problems for CDI and for the model reduction routine. To avoid this problem, the levels are stabilized in the *non-linear* model, before linearization, using very low proportional feedback from the levels to D and B, respectively, thereby placing the eigenvalues at -0.0001 instead of 0.

6.3.1 Scaling

RGA, poles and zeros are independent of scaling, but most other measures depend critically on scaling. Therefore, all results and plots in the following are in terms of scaled variables, *i.e.*, all outputs, setpoints, inputs and disturbances are scaled by "the maximum acceptable deviation" from the desired operating condition of each variable, such that the scaled variables stay within ± 1 if the acceptable deviation limits are not violated. The values used for scaling are tabulated in Table 6.3 For example, the scaled reflux (input) is $u_1 = \Delta L_T / L_{T_{mad}}$, where $L_{T_{mad}}$ is the maximum allowed deviation in reflux. From Table 6.3 $L_{T_{mad}} = 2.7$ kmol/min, and since this is equal to the nominal flow, we get that $u_1 = -1$ corresponds to zero reflux and $u_1 = +1$ corresponds to a reflux of 5.7 kmol/min.

Note that the performance requirement for the levels are very lax, as the allowed error in Table 6.3 (30.0 and 10.0) is much larger than the allowed setpoint change (0.5 and 0.5). This is reasonable since we have no strict requirements for level control, but rather want to use variations in level to avoid sudden changes in the product flows, D and B.

6.3.2 Relative gain array (RGA)

The RGA (Bristol, 1966) was originally introduced as a steady state interaction measure and as a tool for input-output pairing for decentralized control. However, the RGA may be computed frequency-by-frequency and used to assess interaction at frequencies other than zero, and also to analyze sensitivity to input uncertainty for multivariable control (Skogestad and Morari, 1987b). The frequency dependent RGA for a square system G is defined by $RGA(\omega) = G(j\omega) \times (G^{-1}(j\omega))^T$ where the symbol $\times$ denotes element-by-element multiplication.

The steady state RGA for the linearized 5×5 plant is:

	L_T	Q_R	Q_C	D	B
x_D	36.76	−64.65	28.88	0.00	0.00
x_B	−35.72	63.49	−26.76	0.00	0.00
P_D	−0.04	2.16	−1.12	0.00	0.00
M_D	0.00	0.00	0.00	1.00	0.00
M_B	0.00	0.00	0.00	0.00	1.00

(6.1)

The conventional "LV-configuration", which is considered for the decentralized controller in this paper, corresponds to pairing on the diagonal elements.

The first observation from the steady-state RGA is that the 4,4 and 5,5 elements are 1.0 while all other elements in columns 4 and 5 and rows 4 and 5 are zero. Following the conventional pairing rule for decentralized control we should pair on elements close to 1, *i.e.* use D to control M_D and B to control M_B.

The second observation is that the 3,3 element is negative. From the results of Grosdidier *et al.* (1985) we know that a decentralized control scheme with integral action paired on this negative RGA element leads to

1. The overall system is unstable, or
2. The pressure loop is unstable, or
3. The remaining system is unstable if the pressure loop fails.

In practice, this means that using Q_C to control P_D and tuning for a stable pressure loop and a stable overall system leads to instability if the pressure loop fails, *e.g.* if Q_C saturates. Thus, one must be very careful to avoid saturation in the pressure loop if decentralized LV control is used. (Recall that we assume that the heat duties Q_C and Q_R may be manipulated directly. If self regulation is included the negative RGA-element will most likely disappear.)

The third observation is that there is strong two-way interactions in the upper left 3×3 subsystem, while there is no two-way interaction in the rest of the system. The physical explanation for the latter is that manipulation of D affects M_D, and B affects M_B, but has almost no influence on the other outputs. Thus, one of the main advantage with the LV-configuration is that composition control is insensitive to the tuning of the level loops.

The RGA elements (RGA_{ij}) as function of frequency are shown in Fig.6.3 with the diagonal RGA elements ($i = j$) as solid lines. We see that the RGA elements decreases as frequency increases, but there are significant interactions also at frequencies corresponding to the expected closed loop bandwidth ($w \approx 0.1$ [rad/min]).

The 3×3 interaction for the composition and pressure subsystem could in principle (if there was no uncertainty) be corrected for by a multivariable controller, for example a decoupler. However, the large RGA elements (Fig. 6.3) at frequencies around the closed-loop bandwidth signal high sensitivity to diagonal input uncertainty (Skogestad

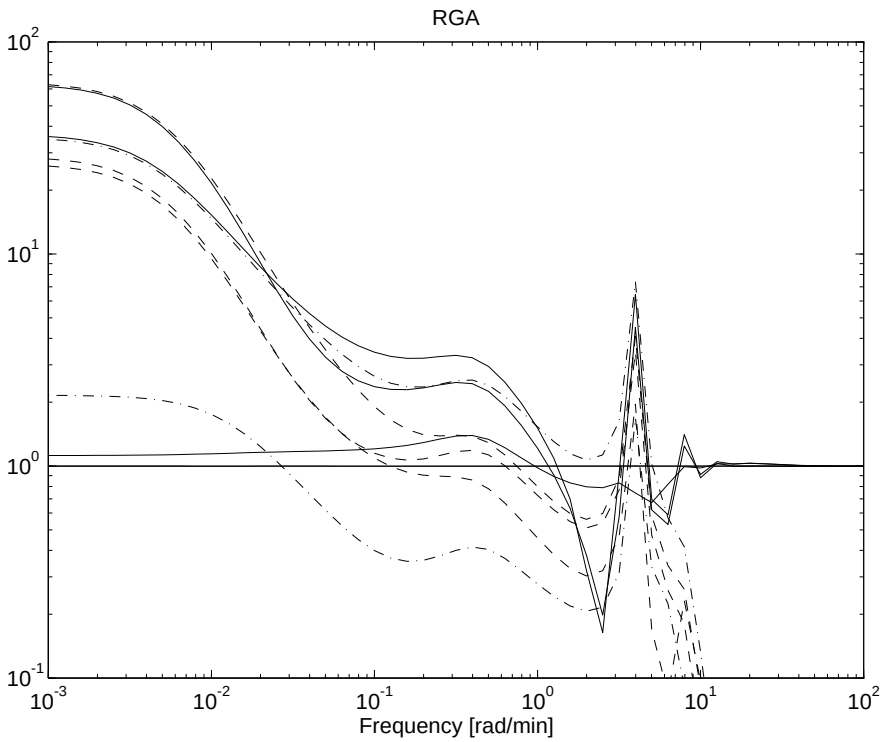

Figure 6.3: Relative Gain Array elements as function of frequency (solid lines: diagonal elements).

and Morari, 1987b) and thereby prevent the use of a decoupler. Thus, we may already at this stage conclude that it is essential to consider input uncertainty when tuning a multivariable controller for this plant.

6.3.3 RHP-zeros

The 5×5 model has no multivariable right half plane (RHP) zeros. However, there are RHP zeros in several elements of the 5×5 model, as shown from the inverse responses in Fig. 6.2. Specifically, a change in cooling duty Q_C yields inverse responses for all outputs, except for the pressure. The main reason behind this is that a change in Q_C, with the other manipulated inputs kept constant, yields an inverse response for the vapor flow V_T entering the condenser: Initially, an increase in cooling yield a fast increase in V_T. However, with increased cooling, Q_C, and constant heating, Q_R, the column temperature starts decreasing, and the heat of vaporization increases leading to a steady state decrease in $V_T = Q_C/H^{vap}$. The inverse responses in the outputs are very slow (zero locations: $z_{13} = 0.0367$; $z_{23} = 0.0264$; $z_{43} = 0.0204$; $z_{53} = 0.0580$ min^{-1}), so for single-loop control the cooling duty can only be used to control the pressure. However, this means pairing on a negative RGA-element and results in the complications described in the previous section. Using the results from Hovd and

Skogestad (1992) we know that the negative RGA (3,3-element) must imply that there is a RHP transmission zero in the remaining subsystem, since there is no RHP zero in the 3,3 SISO-element itself and no 5×5 RHP transmission zeros. Indeed, we find that the upper 2×2 system (from L_T and Q_R to x_D and x_B) has a RHP transmission zero at 0.0129 min^{-1} (the lower 2×2 system is decoupled and does not influence this value). This RHP transmission zero implies that fast control of both compositions (closed loop bandwidth less than about 75 min.) requires that the pressure controller is functioning, if SISO pressure control paired on the 3,3 element is used.

6.3.4 Input saturation

Input saturation imposes a fundamental limitation on the control performance. The inputs required for perfect control are $u = G^{-1}r + G^{-1}G_d d$. Thus, in terms of scaled variables the elements in the matrices G^{-1} and $G^{-1}G_d$ should be less than 1 in the frequency range where control is needed. For our example, with the allowed variations in the inputs as given by u_{mad} in Table 6.3, we find from frequency-dependent plots of the elements of these matrices (not shown) that input saturation is not a serious problem for this plant, not even at relatively high frequencies.

6.3.5 Decentralized control

From the frequency-dependent RGA-plot in Fig.6.3 we note that the diagonal elements are fairly large (about 3) also in the frequency-region important for control, $\omega \approx 0.1$ rad/min. Thus, we can expect interactions at these frequencies when decentralized control is used.

To evaluate decentralized performance for setpoint changes the Performance RGA, which is scaling dependent, is the appropriate tool. This is not shown here, but one main finding is that the worst setpoint change is for top composition, $x_{D,s}$, and in particular that a strong interaction is expected for the pressure.

The closed-loop disturbance gains (CLDG) yield the effect of disturbances under decentralized control. For all outputs the worst disturbance is the feed rate F, and the effect of this disturbance is given in Fig.6.4. The bandwidth requirement for rejecting a 15% disturbance in F is about 14 min for top composition (x_D), 7 min for bottom composition (x_B) and 6 min for top pressure (P_D).

The controllability analysis for decentralized control indicates that $x_{D,s}$ is the most difficult setpoint to track and F is the most difficult disturbance to reject (for this system and with the scalings used here). This has also been confirmed by simulations. All simulations presented in the paper will therefore show responses to changes of $x_{D,s}$ (+0.01 kmol/kmol, *i.e.* +1 in scaled variables), and F (+15% of nominal feed, +1 in scaled variables).

One conclusion from the controllability analysis is that it is difficult to obtain high control performance with decentralized control due to the strong 3×3 interaction. This is confirmed by the simulation in Fig. 6.5. The controller used in the simulation was

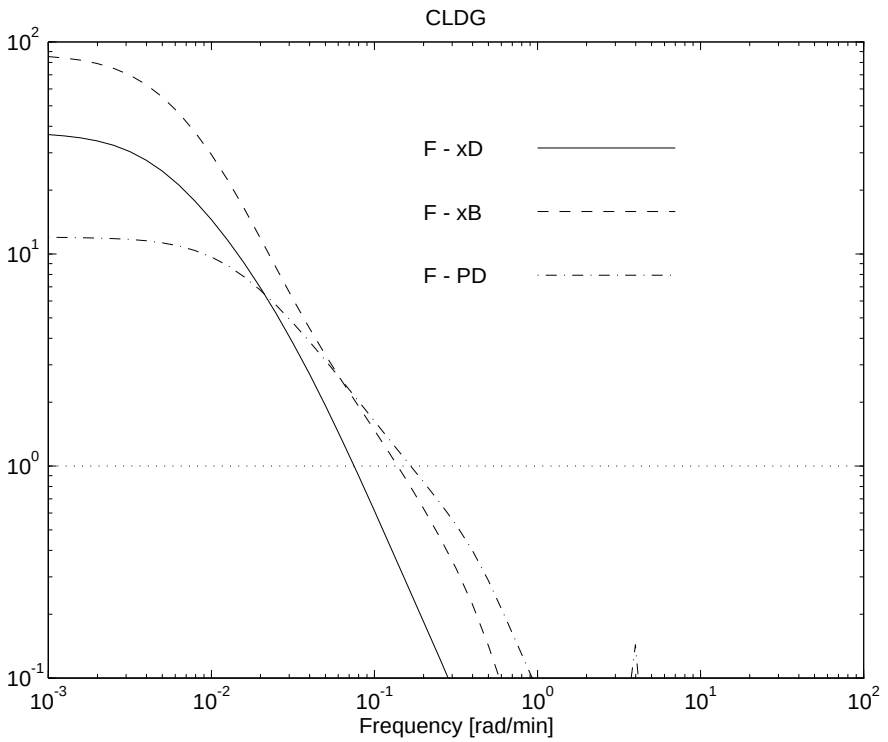

Figure 6.4: Closed Loop Disturbance Gain for decentralized control.

tuned to yield a closed loop time constant of 3 min for the pressure loop, about 15 min for top composition x_D and 8 min for the bottom composition x_B (individually, *i.e.*, without considering interactions). The level loops, which have essentially no effect of the rest of the system, were very loosely tuned to closed loop time constants of 30 min.

Fig. 6.6 demonstrates that the system, with decentralized control, goes unstable if Q_C saturates (the active constraint in the simulation is $Q_C > 0$).

Remarks on decentralized control: Q_C can in practice only be used to control the pressure, since all other outputs yield very slow inverse responses to changes in Q_C. However, this means pairing on a negative RGA element which make the system highly sensitive to pressure control failure.

6.4 $\mathcal{H}_\infty/\mu$ control

6.4.1 Weight selection

In this section we study the *unconstrained* control problem using the $\mathcal{H}_\infty/\mu$ framework. The purpose is to study possible improvements in performance with multivariable control. The $\mathcal{H}_\infty$-norm is used because it is rather straightforward to specify the desired responses in terms of 'classical' measures such as closed-loop time constants, allowable

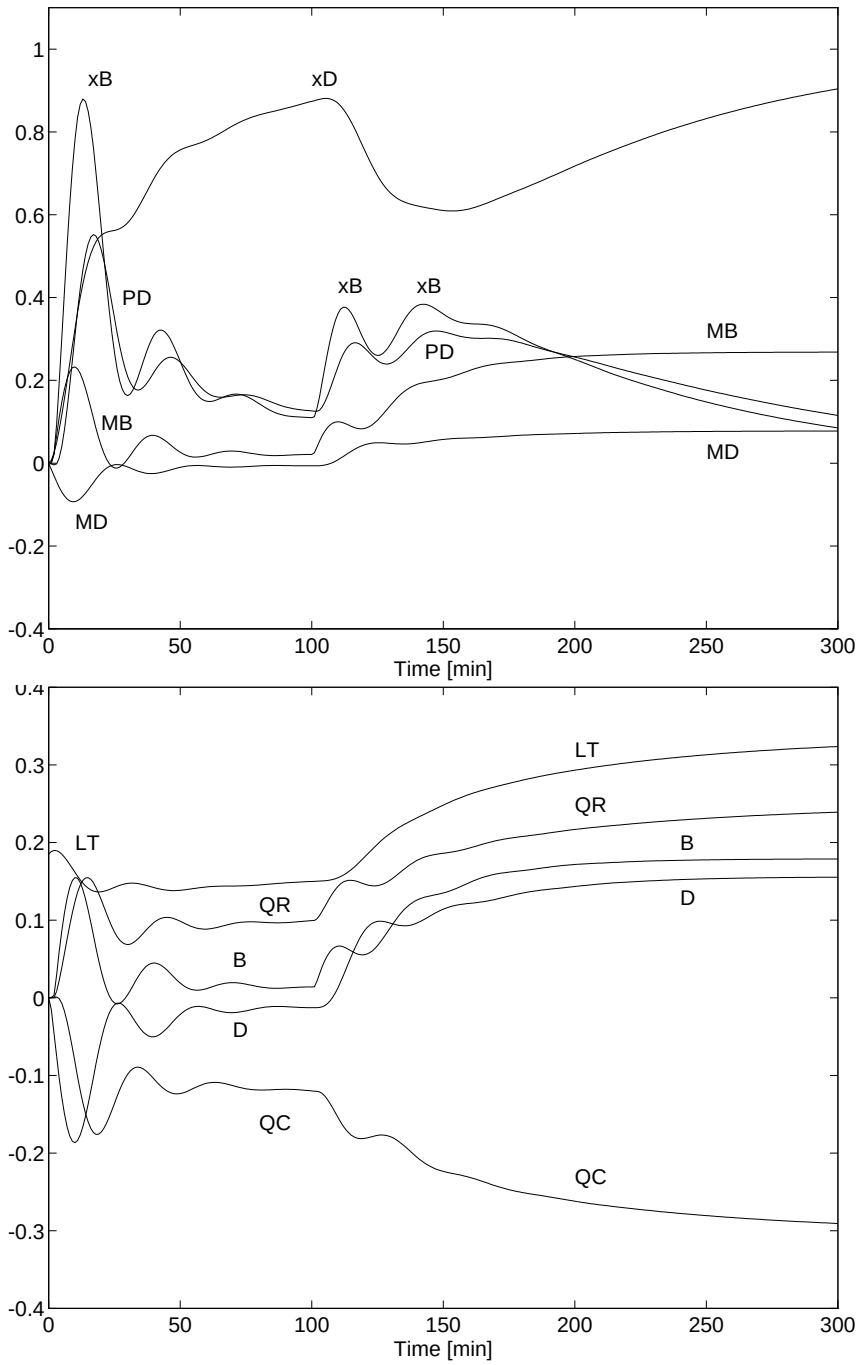

Figure 6.5: Simulated decentralized control performance for setpoint change in x_D at $t = 0$ and 15% feed disturbance at $t = 100$ min. Upper plot: Scaled controlled outputs. Lower plot: Scaled manipulated inputs.

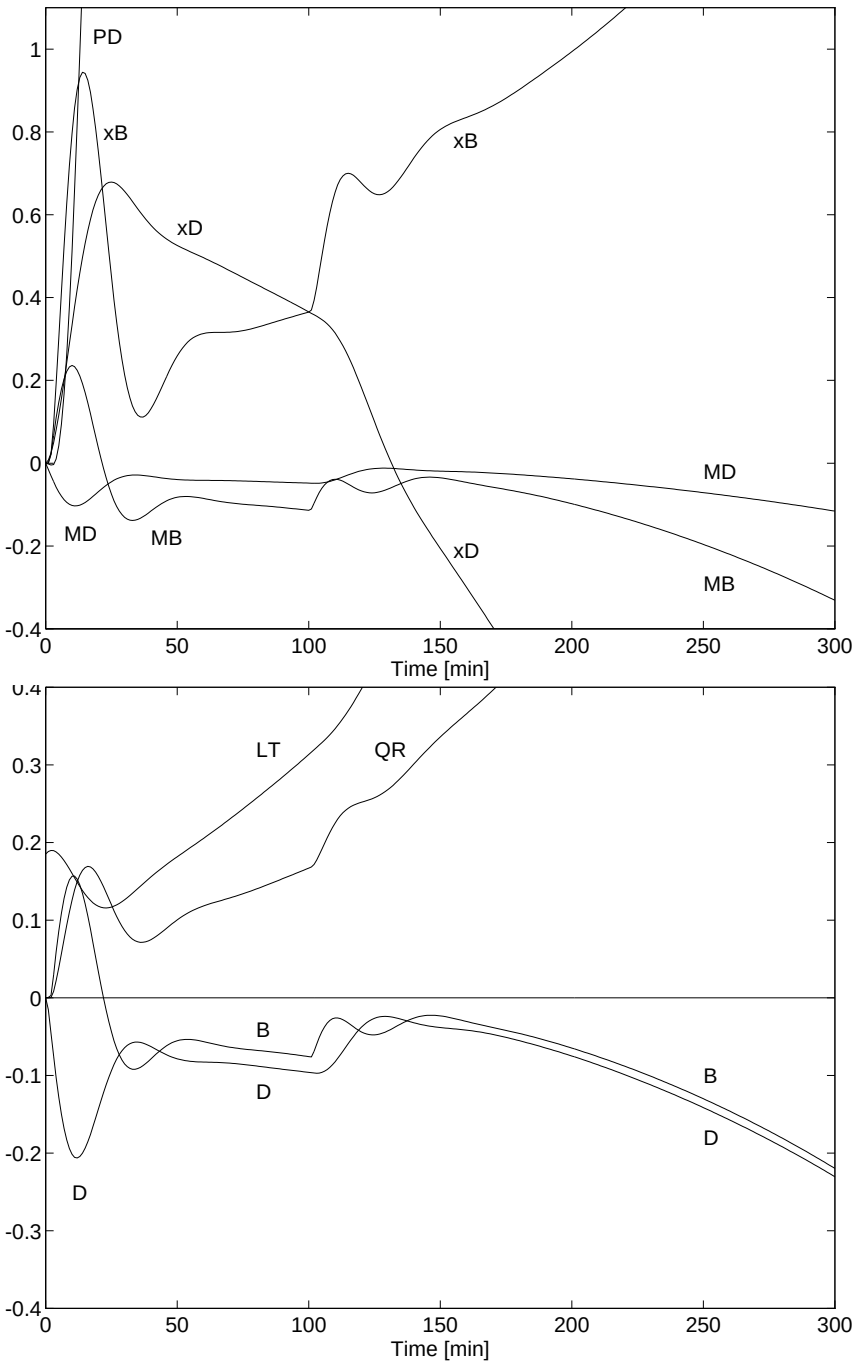

Figure 6.6: Simulated decentralized control performance with constraint $Q_C > 0$, for setpoint change in x_D at $t = 0$ and 15% feed disturbance at $t = 100$ min. Upper plot: Scaled controlled outputs. Lower plot: Scaled manipulated inputs.

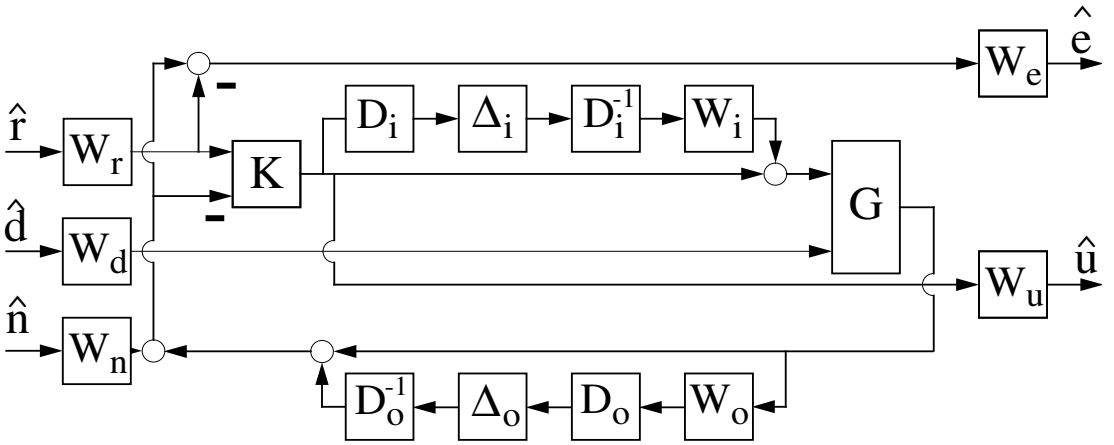

Figure 6.7: Block diagram for robust $\mathcal{H}_\infty$-problem.

steady state offset and acceptable overshoot. Furthermore, one significant advantage with the $\mathcal{H}_\infty$-norm is that it allows worst-case model uncertainty to be included explicitly (using the structured singular value, denoted SSV or μ).

The block diagram in Fig. 6.7 defines the problem studied in this section. K is the controller to be designed. It may be a two-degree-of-freedom (TDF) controller with separated inputs r (setpoint) and y_m (measured outputs) as in the figure, or with a one-degree-of-freedom controller (ODF) with input $r - y_m$.

G is the normalized (scaled) plant model with 8 inputs (5 manipulated inputs u and 3 unmeasured disturbances d) and 5 outputs y. The scalings used for the normalization of G are given in Table 6.3. W_r, W_d and W_n are weight matrices for setpoints r, disturbances d and measurement noise n, respectively. W_e and W_u are weights on deviation from desired setpoint, e, and manipulated inputs, u, respectively. The weighting matrices are diagonal with elements $[W_r] = r_{mad}/y_{mad}, [W_d] = 1, [W_n] = 0.01, [W_u] = 1$ and

$$[W_e](s) = \frac{1}{M_S}\frac{\tau_{cl}s + M_S}{\tau_{cl}s + A}; \quad M_S = 2, A = 0.0001 \tag{6.2}$$

with $\tau_{cl} = [30\ 30\ 30\ 60\ 60]$ min. For the compositions, for which the setpoints r and controlled outputs y have identical scalings, M_S is the maximum allowed peak of the sensitivity function and τ_{cl} is the required closed-loop response time for that output. Note that A is very small so that integral action is in practice required for all outputs.

Model uncertainty is represented by $W_i D_i^{-1}\Delta_i D_i = W_i\Delta_i$ which models input uncertainty, and $D_o^{-1}\Delta_o D_o W_o = \Delta_o W_o$ which models output uncertainty. Δ_i (and Δ_o) is any diagonal matrix with $\mathcal{H}_\infty$-norm less than one, and the D's are scalings for the μ-problem as discussed below. $W_i = 0.1 * I_{5\times 5}$. and $W_o = \frac{\theta s}{(\theta/2)s+1} * I_{5\times 5}$, corresponding to 10% relative gain uncertainty in each input, and a delay of up to approximately $\theta =$ 1 min in each measurement.

We arrived at this problem formulation and these weights through several steps,

starting with a pure $\mathcal{H}_\infty$-problem with only setpoints and no uncertainty and ending up with the overall μ-problem as defined by Fig.6.7. In the following we shall go through some of these steps because it yields some insight.

6.4.2 Setpoint tracking with no uncertainty

This corresponds to the case with $\hat{d} = 0, \Delta_i = 0, \Delta_o = 0$ and yields a pure $\mathcal{H}_\infty$-problem for which synthesis software is readily available (Balas *et al.*, 1991, Chiang and Safonov, 1992). The optimal controller yields a closed-loop $\mathcal{H}_\infty$-norm equal to 0.83. Since this is less than 1 the performance requirement for the worst case direction is achieved with some margin. The $\mathcal{H}_\infty$-controller uses rather high gains at high frequencies; the 'roll-off' frequency is about 10 [rad/min]. This is typical for all the cases we studied and it may be avoided by using a slightly sub-optimal controller with higher $\mathcal{H}_\infty$-norm. This sub-optimal controller yields a blend of $\mathcal{H}_\infty$ and $\mathcal{H}_2$ optimality (which is desirable since our ultimate objective is to use model predictive control which uses the $\mathcal{H}_2$-norm) with 'roll-off' at a lower frequency than the optimal $\mathcal{H}_\infty$-controller, resulting in better robustness with respect to high frequency uncertainty. For this case a sub-optimal controller with $\mathcal{H}_\infty$-norm equal to 1.0 (rather than 0.83) gave approximately the same low-frequency behavior as the optimal controller, but a 'roll-off' frequency of about 0.2 [rad/min].

The obtained suboptimal controller is a 'full' 5×5 controller, however, a more careful analysis of the controller reveals the following two interesting properties:
1) The controller may be decomposed into one 3×3 composition and pressure controller and two single-loop controllers for the levels, corresponding to a multivariable LV-configuration.
2) The 3×3 pressure and composition controller is essentially a decoupler. This may be seen by evaluating the condition number of GK.
These two statements are *not* true when disturbances and/or uncertainty is considered, as discussed below.

Remarks: For setpoint tracking of this system without uncertainty there is 1) No advantage in using the information from M_D (M_B) to compute manipulated inputs other than D (B), and 2) No advantage in computing D (B) based on information from measurements other than M_D (M_B). 3) No advantage with TDF controller, since there are no uncertainties and no disturbances.

6.4.3 Including model uncertainty

Robust performance analysis of the system in Fig.6.7 with model uncertainty, is performed by connecting the scaled outputs $[\hat{e}\hat{u}]^T$ to the scaled inputs $[\hat{r}\hat{d}\hat{n}]^T$ through a "performance perturbation" Δ_P and then rearranging the system into the $M\Delta$-structure shown in Fig.6.8 where $\Delta = diag\{\Delta_i, \Delta_o, \Delta_P\}$. To analyze such a system we must use the structured singular value, μ, instead of the $\mathcal{H}_\infty$-norm. In this paper we use as a tight approximation for μ the scaled $\mathcal{H}_\infty$-norm, $\min_D \|DMD^{-1}\|_\infty$. The structure

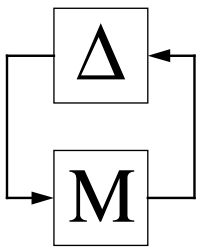

Figure 6.8: $M - \Delta$ structure for μ-analysis.

of the D-scales depend on the model uncertainty. In our case with diagonal uncertainty at the input and the output we get $D = diag\{D_i, D_o, I_5\}$ where D_i and D_o are diagonal matrices each with 5 entries which are "adjusted" to minimize the scaled $\mathcal{H}_\infty$-norm above. The μ-optimal controller is then obtained by DK-iteration (Doyle, 1983) : **1. K-step**. Fix D and obtain K by minimizing the $\mathcal{H}_\infty$-norm ($\min_K \|DM(K)D^{-1}\|_\infty$. **2. D-step.** Obtain D-scales by computing μ using the upper bound, $\min_D \|DMD^{-1}\|_\infty$. These D-scales are frequency-dependent and are fitted to low order transfer functions. One iterates between these two steps until convergence. Note that convergence to the μ-optimal controller is not guaranteed with this procedure, although it usually works well if the problem is reasonably scaled to begin with. Usually only a few iterations are performed such that a sub-optimal μ-controller is obtained.

6.4.4 Setpoint tracking with input uncertainty

To consider the effect of model uncertainty we added input uncertainty (but no disturbances or output uncertainty) and obtained an ODF controller by DK-iteration. Actually we found that the controller obtained by using $D_i = I_{5\times5}$ was almost as good as any other controller. It yields $\mu_{RP} = 0.938$. This value could possibly be reduced a few percent by a more sophisticated higher order D-scale, but after a few DK-iterations with only slightly reduced μ_{RP} we decided to use $D_i = I_{5\times5}$. This choice leads to a low order controller and it also makes it easy to apply the $\mathcal{H}_\infty/\mu$ weights in the MPC design (see section 6.5).

In Table 6.4 the gains of the ODF controller at frequency $\omega = 0.01$ rad/min are given. The main difference between this controller and the controller designed for no uncertainty is that this controller does not invert the plant. Also note that the diagonal elements are the largest elements in each row/column. A second difference is that the level measurements M_D and M_B are not only used to compute D and B, but have a major impact also on the other manipulated variables. However, note that D and B are almost only affected by M_D and M_B. We found that this $\mathcal{H}_\infty$-controller can be reasonably well approximated by a decentralized L/D V/B - configuration (compare with Eq.11 in Skogestad and Morari, 1987a). In this scheme D is computed from M_D, B is computed from M_B, but L_T is computed from both x_D and M_D and V is computed from both x_B and M_B. These results are consistent with earlier findings which found

Table 6.4: Controller element-by-element modulus at $\omega = 0.01$ rad/min.

	e_{x_D}	e_{x_B}	e_{P_D}	e_{M_D}	e_{M_B}
L_T	1.4289	0.3660	0.2290	1.1815	0.7863
Q_R	0.1913	0.9435	0.4865	0.3867	0.4439
Q_C	0.3328	0.7201	0.7358	0.4851	0.0370
D	0.0663	0.0339	0.0193	1.3192	0.1242
B	0.0875	0.0986	0.0376	0.3217	0.7884

that this configuration has much lower RGA-values and is preferable when there is input uncertainty.

Remarks. 1) Here we do not consider any disturbances, and the reason for utilizing the level measurements when computing L_T, Q_R and Q_C must be that the effect of the input uncertainty shows up in these measurements. 2) The required bandwidth for the pressure response is not very high, however, the controller tuned for input uncertainty 'chooses' to use a high pressure bandwidth to reduce the effect of the uncertainty. 3) A two-degree-of-freedom controller improves the performance in this case. It yields $\mu_{RP} = 0.94$ using $D = I_{5\times5}$. Again this is explained by the fact that the uncertainty acts as a disturbance.

6.4.5 Including disturbances and output uncertainty

Including disturbances and output uncertainty to the problem, yields the system shown in Fig. 6.7. This system will after a few DK-iterations yield a controller of rather high order, due to the D-scales. To avoid this high order controller, we use a problem formulation *without* output uncertainty when synthesizing the controller, and then check the performance using μ-analysis on the full problem.

It turns out that the neglected measurement delays (high frequency output uncertainty) can be dealt with by using a sufficiently sub-optimal $\mathcal{H}_\infty$-controller. The finding from the previous section, that $D_i = I_{5\times5}$ is a good D-scale simplifies the design even further to a pure $\mathcal{H}_\infty$-problem.

The controller used for the simulations shown in Fig. 6.9 was obtained by $\mathcal{H}_\infty$-synthesis using a problem with setpoint changes, disturbances, noise and input uncertainty, but *without* output uncertainty. To obtain robustness w.r.t. the neglected measurement delays (high frequency output uncertainty), we synthesized a sub-optimal $\mathcal{H}_\infty$-controller with $\mathcal{H}_\infty$-norm 1.35. Then we computed μ for the full problem. μ_{RP} with output uncertainty is 1.21 and μ_{RS} is 0.99, *i.e.* the performance is not quite as good as required by the weights, but stability is guaranteed for the worst case plant.

The response of this controller is shown by the dashed lines in Fig.6.9. As seen it performs much better than the decentralized controller shown in Fig. 6.5

6.4.6 Final remarks

Some final remarks seem in order. Most of these are in accordance with previous findings.

1) With the scalings used for the plant, the optimal input uncertainty D-scales are close to 1 for all cases. The optimal D-scales for the output uncertainty are about 5.

2) The weights were chosen to yield $\mu \approx 1 \pm 0.2$ for all problems. The reason is that interpretation of μ is difficult if it is too different from 1.

3) A controller designed for setpoint changes only, does not perform well if disturbances are considered.

4) A controller designed without considering input uncertainty performs poorly with input uncertainty.

5) A controller designed without considering output uncertainty performs well if the controller is slightly $\mathcal{H}_\infty$ sub-optimal.

6.5 Model Predictive 5×5 control

In this section we use a Model Predictive Control algorithm which involves constrained on-line optimization over a finite receding horizon to explicitly address input constraints. There are several different variants of these schemes, but they differ mainly in the way that future outputs are predicted. The commonly used QDMC algorithm (García *et al.*, 1986) makes the crude assumption that all disturbances act as steps on the outputs, but as shown by Lundström *et al.* (1991b) this may lead to poor results when both compositions are controlled. Therefore, we use a state observer based MPC algorithm with a steady state Kalman filter gain[1]. The tuning parameters for this MPC controller are: H_p the output prediction horizon, H_c the control horizon, Λ_y output weight, Λ_u input weight and K_f the Kalman filter gain. The filter gain is a function of the disturbance model and the disturbance and noise covariance matrices.

Resently Lee and Yu (1994) presented tuning rules for obtaining robust MPC performance. For the case of diagonal input uncertainty they penalize the input moves using Λ_u in order to obtain robustness. Applying this method to the distillation problem from Skogestad *et al.* (1988) gave $\mu_{RP} = 2.23$, whereas the optimal value is known to be less than 0.978 (Lundström *et al.* 1991a). This is not satisfactory, therefore, in this paper we do not use the input weight Λ_u, but the observer parameters to obtain robustness with respect to input uncertainty.

Our main objective is to use the weights obtained from the rigorous robustness analysis in the previous section as a starting point for weight selection for the MPC controller. There are several difficulties here. First, the MPC scheme uses the $\mathcal{H}_2$-norm rather than the $\mathcal{H}_\infty$-norm. Second, the MPC controller is a finite horizon controller which contains additional tuning parameters. Third, uncertainty can not be included explicitly.

[1]The MPC controller we use here is from the program "scmpc" in the the MPC-toolbox for MATLAB (Morari and Ricker, 1991).

In spite of these difficulties, we were able to tune the MPC controller to mimic the μ-controller very closely. One reason for this success is probably that the $\mathcal{H}_\infty/\mu$-controller is sub-optimal and therefore "$\mathcal{H}_2$-ish" and easier to mimic with MPC. The final tuning of the response time was done by adjusting a single parameter α in the output weight to minimize μ in the robustness problem defined in the previous section. The input uncertainty was in the MPC design represented by opening the loop through Δ_i, which results in a weight (D_i) penalizing the use of u and a disturbance weight $(W_i D_i^{-1})$ acting on the plant inputs. Output uncertainty was not included since the robustness analysis found that this uncertainty was not crucial. The tuning parameters are summarized next.

Optimization part of MPC controller.
Sampling time: 1 min, horizons $H_p = 60$ and $H_c = 3$.

$$\Lambda_y = \alpha W_e; \quad \Lambda_u = |W_u| + |D_i| \tag{6.3}$$

(where W_e and W_u are the $\mathcal{H}_\infty$-weights and D_i the D-scale representing the input uncertainty).

Kalman filter part of MPC controller. Augmented disturbance model to include model uncertainty

$$G_d = C(sI - A)^{-1}B = G \text{ diag}\{W_i D_i^{-1}, W_d\} \tag{6.4}$$

This leads to the Kalman filter gain $K_f = P_f C^T V^{-1}$ where P_f is obtained by solving the Riccati equation $P_f A^T + A P_f - P_f C^T V^{-1} C P_f + B W B^T = 0$ where the covariance matrices for disturbance is $W = I_8$ and for noise is $V = W_n^2$.

For each value of α we obtained the frequency response of the discrete controller and added zero order hold elements at the controller outputs. Using the same problem specification as in the previous section we then minimized μ and obtained a value $\mu = 1.15$ for $\alpha = 0.03$. The linear robust performance was thus in fact somewhat better than the sub-optimal $\mathcal{H}_\infty$-controller obtained in section 6.4.5

The solid lines in Fig.6.9 show the simulated performance of the MPC controller when no constraints are active, that is, when it behaves like a linear controller. The response is seen to be very similar to the μ-optimal controller found previously (dashed lines). The main difference is the speed of response of the levels and the use of inputs D and B.

Fig.6.10 shows the MPC responses when Q_C is constrained to be at its nominal value. As we see, the MPC controller preserves stability, and manages to keep the levels and the pressure close to their desired values. However, the composition control is relatively poor since these can not be maintained at their setpoints when one degree of freedom is lost.

Some final remarks.

1. In the simulations we used a 1 minute delay in each measurement and used -10% input gain error in all inputs except Q_R which has +10% uncertainty.[2]

[2]This input uncertainty was found to be the worst of all ±10% combinations.

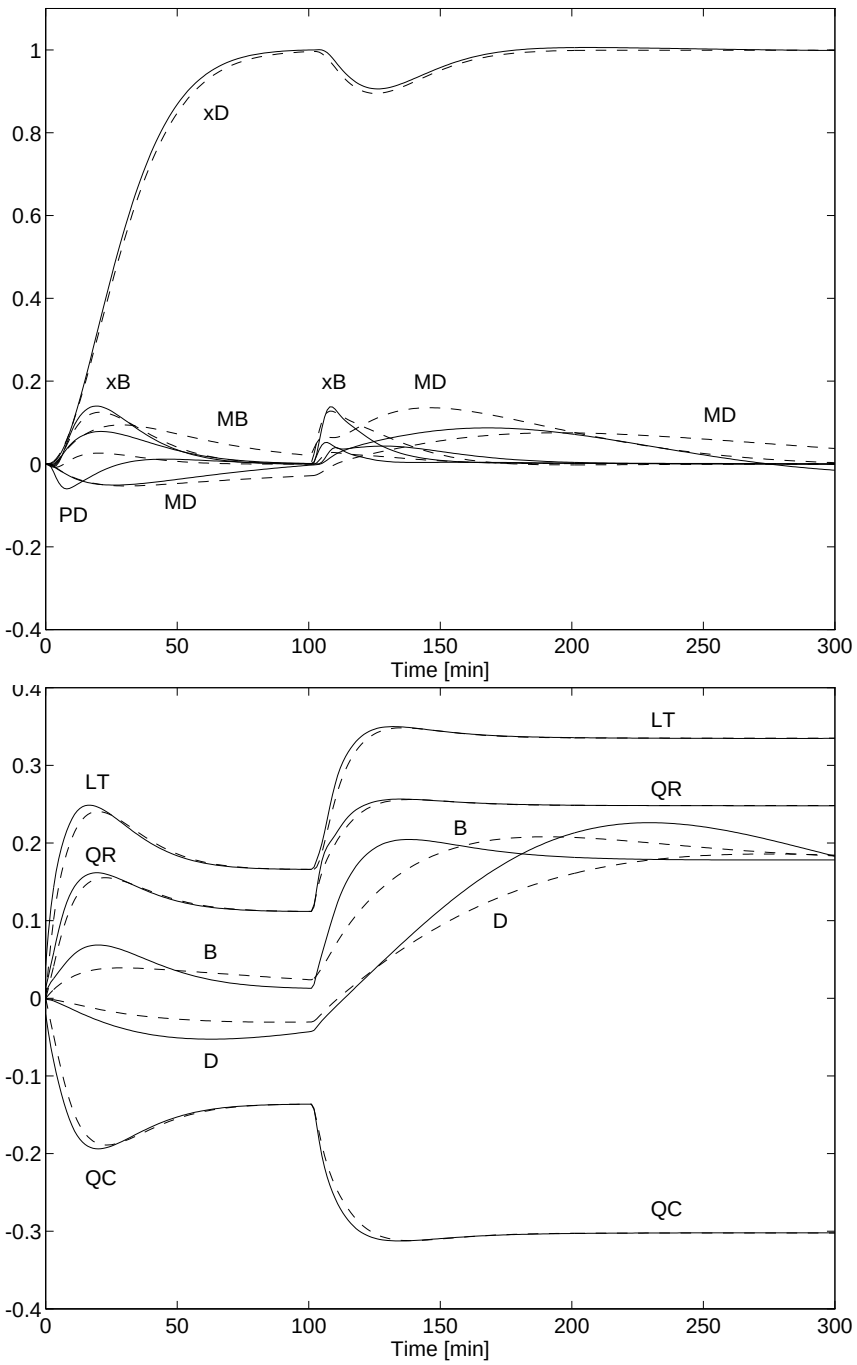

Figure 6.9: Simulated unconstrained control performance for setpoint change in x_D at $t = 0$ and 15% feed disturbance at $t = 100$ min. Solid lines: MPC. Dashed lines: μ-controller Upper plot: Scaled controlled outputs. Lower plot: Scaled manipulated inputs.

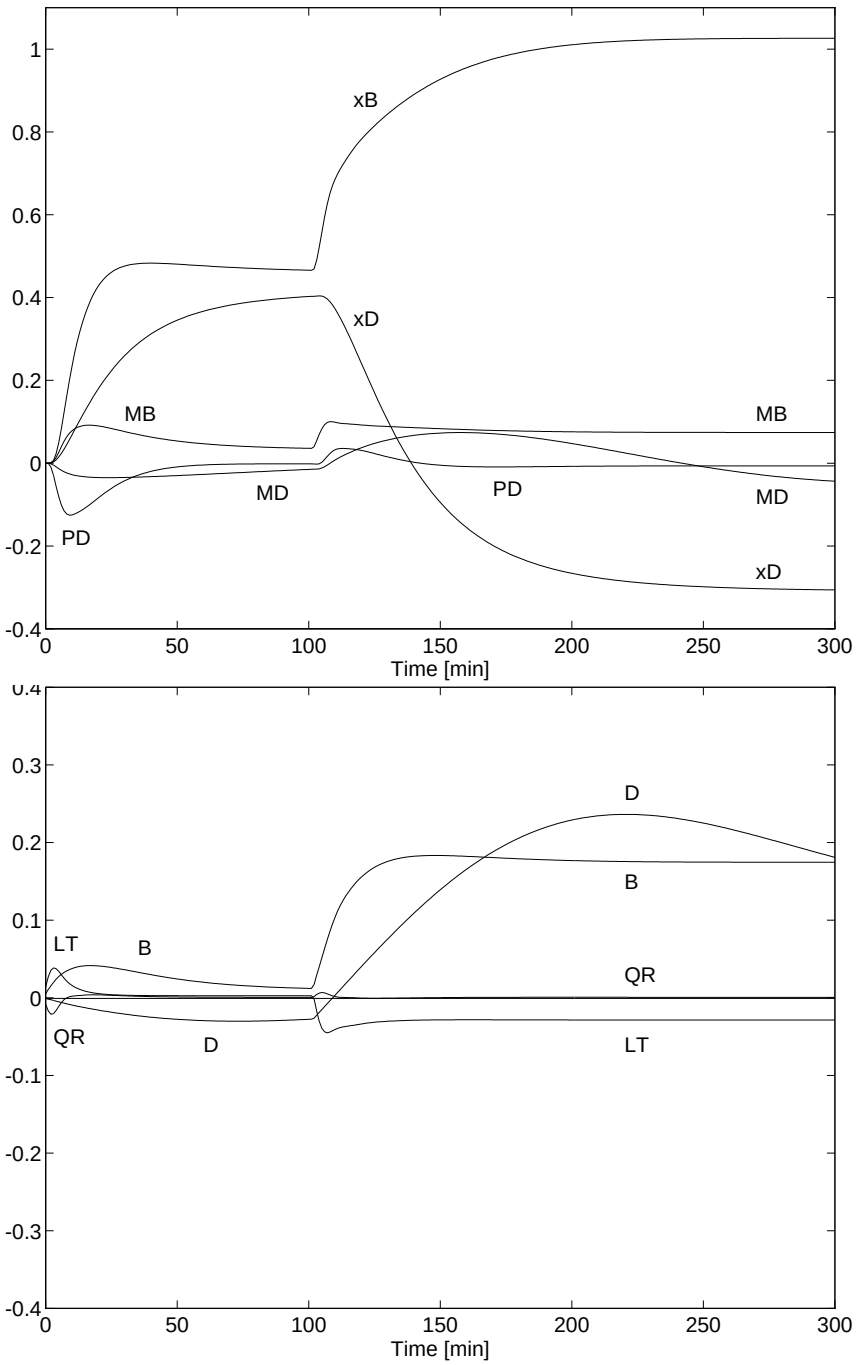

Figure 6.10: Simulated MPC performance with constraint $Q_C > 0$, for setpoint change in x_D at $t = 0$ and 15% feed disturbance at $t = 100$ min. Upper plot: Scaled controlled outputs. Lower plot: Scaled manipulated inputs.

2. The unconstrained simulation shows that the controller performs well both for setpoint tracking and disturbance rejection. No excessive input usage is required. The performance for the outputs in Fig.6.9 is significantly better than for the decentralized scheme shown in Fig.6.5.

3. In the constrained case the use of a MPC scheme avoids the need for complicated logics including overrides and retuning. If the decentralized control scheme from Section 6.3 is used, then the system goes unstable when Q_C is fixed. The multivariable μ-controller does not go unstable, but performs very poorly, and simulations show that it goes unstable when Q_R is fixed.

4. In the simulations there was given no forewarning about the desired setpoint change at $t = 0$. Most controllers are causal and would not be able to make use of this information, but in many MPC implementations such information may be used. For example, if at $t = -100$ min the MPC optimizer was told that a setpoint change is desired at $t = 0$, then it would immediately start changing the inputs to make the transition as fast as possible.

6.6 Discussion

It is often desirable to use a compensator-based controller which retains some of the simplicity of a decentralized controller, that is, $K = C_1 K_{diag}(s) C_2$ where C_1 and C_2 are fixed matrices (or at least contain very simple dynamics) which take care of the interactions whereas K_{diag} consists of simple single-loop controllers to take care of the dynamic effects. One insight from analyzing the optimal multivariable controllers is that a precompensator C_2 (mixing of measurements, that is use level measurement also for composition control) is useful, while a postcompensator C_1 (mixing of inputs) is less useful due to the presence of input uncertainty. A pure precompensator scheme is sometimes implemented as a regular decentralized control scheme, but with a "feedforward" action from the disturbances, where disturbances are estimated from level and pressure measurements. Another insight is that a multivariable prefilter (two degree of freedom controller) may reduce the interactions for setpoint changes. Although such schemes may improve the multivariable properties of the controller, they will still need special logics to handle constraints.

The reboiler and condenser holdups of a distillation column (and to some extent also the pressure) do not have to be tightly controlled, but may be considered 'slack' output specifications. The slackness of these specifications yields a system which may be viewed as a temporarily non-square system with access of inputs. That is, as long as the levels M_D and M_B are within their upper and lower limits we may use all five inputs L_T, Q_R, Q_C, D and B to control three outputs x_D, x_B and P_D. At first we thought this may be used to improve performance. However, in the case of a distillation column, the 'freed' variables D and B are not effective for controlling x_D, x_B or P_D, so the slack level requirements cannot be used to improve the composition or pressure control, however the slack specifications are often used to eliminate fast variations of the inputs D and

B.

6.7 Conclusions

The results in this paper indicate that the main advantages with 5×5 distillation control are the improved disturbance detection by indirect use of the level and pressure measurements, and the explicit input constraint handling. One difficulty is the tuning of the controller, but in our example we were able to tune the MPC scheme quite easily to get acceptable robustness. The following procedure was used: 1) Define a robust $\mathcal{H}_\infty$-problem with an optimal μ-value close to 1. 2) Use the weights and scaling found for this problem to derive MPC tuning parameters. The critical uncertainty, in this case at the inputs, is represented as fictitious disturbances. 3) One adjustable parameter in the MPC controller is used to minimize μ. 4) Time simulations are used to check the results and possible adjust some weights. The resulting controller is not 'optimal' in any mathematical sense, but was found to perform very well.

References

[1] Balas, G.J, Doyle, J.C., Glover, K., Packard, A.K. and Smith, R. (1991). "The μ-Analysis and Synthesis Toolbox", The MathWorks Inc., Natick, MA.

[2] Bennett, D.L., Agrawal, R. and Cook, P.J. (1983), "New pressure drop correlations for sieve tray distillation columns", *AIChE Journal*, **29**, 3, 434-442.

[3] Bristol, E.H. (1966). "On a New Measure of Interactions for Multivariable Process Control", *IEEE Trans. Autom. Control*,

[4] Chiang, R.Y. and Safonov, M.G. (1992). "Robust-control toolbox for MATLAB. User's guide", The MathWorks Inc., Natick, MA.

[5] Doyle, J.C. (1982). "Analysis of Feedback Systems with Structured Uncertainties", *IEE Proc.*, **129**, Part D, 242-250.

[6] Doyle, J.C. (1983). "Synthesis of robust controllers and filters", *Proc. IEEE Conf. Decision Contr.*, San Antonio, TX.

[7] García, C.E. and Morshedi, A.M. (1986). "Quadratic Programming Solution of Dynamic Matrix Control (QDMC)", *Chem. Eng. Commun.*, **46**, 73-87.

[8] Grosdidier, P., Morari, M. and Holt, B.R. (1985). "Closed-Loop Properties from Steady-State Gain Information", *Ind. Eng. Chem. Fundam.*, **24**, 221-235.

[9] Hovd, M. and Skogestad, S. (1992). "Simple frequency-dependent tools for control system analysis, structure selection and design", *Automatica*, **28**, 989-996.

[10] Lee, J.H. and Yu, Z.H. (1994). "Tuning of model predictive controllers for robust performance", *Comp.Chem.Engng.*, **18**, 15-37.

[11] Lundström, P., Skogestad, S. and Wang, Z.-Q. (1991a). "Performance weight selection for H-infinity and μ-control methods", *Trans. Inst. MC*, **13**, 5, 241-252.

[12] Lundström, P., Lee, J.H., Morari, M. and Skogestad, S. (1991b). "Limitations of Dynamic Matrix Control", *Proc. European Control Conference*, 1839-1844, Grenoble, France.

[13] Morari, M. and Ricker, N.L. (1991). "MPC toolbox for MATLAB".

[14] Pantelides, C.C. (1988). "Speedup - Recent Advances in Process Simulation", *Comput. chem. Engng*, **12**, 7, 745-755.

[15] Rademaker, O., Rijnsdorp, J.E. and Maarleveld, A. (1975). "Dynamics and control of continuous distillation units", Elsevier, Amsterdam.

[16] Skogestad, S. (1989). "Modelling and Control of Distillation Columns as a 5×5 System", *DECHEMA Monographs*, **116**, R. Eckermann (Ed.), 403-411. (From 20th Europ. Symp. on Computer Applications in the Chemical Industry (CACHI 89), Erlangen, Germany, April 1989).

[17] Skogestad, S. and Morari, M. (1987a). "Control configuration selection for distillation columns", *AIChE Journal*, **33**, 1620-1635.

[18] Skogestad, S. and Morari, M. (1987b). "Implication of Large RGA-Elements on Control Performance", *Ind. Eng. Chem. Res.*, **26**, 11, 2323-2330. (Also see *correction* to Eq. 13 in **27**, 5, 898 (1988).

[19] Skogestad, S. and Morari, M. (1988). "Understanding the Dynamic Behavior of Distillation Columns", *Ind. Eng. Chem. Res.*, **27**, 10, 1848-1862.

[20] Skogestad, S., Morari, M. and Doyle, J.C (1988). "Robust Control of Ill-conditioned Plants: High-purity Distillation", *IEEE Trans. Autom. Control*, **33**, 12, 1092-1105. (Also see correction to μ-optimal controller in **34**, 6, 672).

[21] Wolff, E.A., Skogestad, S., Hovd. M and Mathisen, K.W. (1992) "A procedure for controllability analysis", *Preprints IFAC workshop on Interactions between process design and process control, London, Sept. 1992*, J. Perkins (Ed.), Pergamon Press, 123-132.

Chapter 7

Final Discussion and Conclusions

7.1 Discussion

This thesis deals with robust multivariable distillation control, using the structured singular value (SSV, μ) as a robustness measure. Multivariable controllers are designed both by DK-iteration (μ-synthesis) and by use of a Model Predictive Control (MPC) technique. The purpose with the thesis is to derive and present guidelines for how to deal with uncertainties and constraints using the structured singular value framework and MPC.

The thesis starts with a study on performance weight selection, *i.e.* how to choose control objectives in the μ-framework. Then uncertainty weight selection is considered, *i.e.* how to model the mismatch between the plant and a nominal model. The results from these two steps are then applied in the design of a two degree of freedom controller. Limitation of one of the most common MPC algoritms is then studied, and finally μ and an improved MPC algorithm are used to design a 5×5 multivariable controller for a distillation column.

Through the work with this thesis it has become clear (in the authors opinion) that μ is an excellent tool for *analysis* of uncertain systems. The μ-framework is also useful for controller *synthesis*, althoght it is not very likely that μ-optimal controllers will be implemented for process control applications. Instead, the main reason for synthezising a μ-optimal controller is to assess the limits for achievable control with an unconstrained linear controller.

The paper on which chapter 2 of this thesis is based (Lundström *et al.*, 1991) has had some impact on the use of μ, for example, Craig (1993) uses and refers to Eq. 2.13 in a controller design study for a run-of-mine milling circuit.

A second effect of this paper is based on the presented 'μ-optimal' controller. This controller is very close to the 'true' μ-optimal controller, and due to this, it has 'μ-optimal' properties which may be studied. Engstad (1991) examined this controller and showed that it could be decomposed into an "SVD"-controller, *i.e.* a diagonal controller with pre- and post-compensators obtained from a singular value decomposition of the plant. Later, Hovd *et al.* (1993) refined these findings and proved that the true μ-

optimal controller for this problem is indeed an SVD-controller. Hovd *et al.* also showed that the structure of the uncertainty is unimportant for this example.

Previously in this section it is stated that it is not very likely that μ-optimal controllers will be used for process control applications. However, there are other applications where μ-controllers seem to be ideal for implementation. Consider a technical device, produced in a large number, which requires rather complicated feedback control in order to function properly. In such a situation it may be very expensive to tune each controller individually. Instead one may use μ and specify a nominal model of the device and an uncertainty set which covers the normal differences between the produced devices, and then design one μ-controller which performs well for the entire set of possible devices.

The theorectical foundation for Model Predictive Control has improved during the last years. In particular it seems clear that the receding horizon approach does not provide any advantages to an infinite horizon approach. This means that the observer based MPC algorithm used in this thesis can be further improved. The tuning approach used in chapter 6 is valid also for an infinite horizon algorithm.

7.2 Conclusions

The main contributions of this thesis are summarized below:

Chapter 2. The chapter exemplifies different approaches to performance weight selection when using $\mathcal{H}_\infty$-objectives. The approaches presented here have been used by other researchers, as discussed in the introduction of the chapter. The contribution of this chapter is the discussion, comparision and exemplification of the approaches. A second contribution is the improved controller presented for the problem proposed in Skogestad *et al.* (1988).

Chapter 3. This chapter presents tight approximations of gain and delay uncertainty on linear fractional form, suitable for the μ-framework. Two of the presented approximating sets are special cases of the uncertainty model studied by Laughlin *et al.* (1986, 1987), but the other approximations are new. These new approximations are contributions on there own;
Set Π_{CI3} yields an analytical expression for the smallest complex perturbation that covers a gain-delay uncertainty,
Set Π_{CR} yields a rational low order outer approximation recommended for μ-synthesis,
Set Π_{MI2} yields a non-conservative and non-optimistic approximation using mixed real/complex perturbations,
Set Π_{MR} yields an arbitrary tight approximation which should be suitable for synthesis when synthesis methods for mixed perturbations becomes available.

The paper also demonstrates that tightness obtained from tight modelling with real valued perturbations may be lost when computing μ, due to the looser upper and lower bounds obtained from mixed-μ problems as compared to pure complex problems.

Chapter 4. A detailed Two-Degree-of-Freedom controller design using the μ-

framework is presented. The paper demonstrates how a given set of specifications may be transformed/approximated into frequency dependent weights which specifies a μ-problem. Gradual refinements of μ-specifications are also shown, and the effects of such refinements are illustrated. The controller presented in this chapter demonstrates that all performance requirements in Limebeer's CDC problem (1991) are obtainable.

Chapter 5. It is shown that there are situations where the feedback performance of Dynamic Matrix Control is poor irrespectively of tuning. The poor performance is due to two essential assumptions made in the predictor part of the algorithm. This explains why the performance cannot be improved by a different tuning, since this only affects the optimizer part of the algorithm. It is also shown that a new MPC algorithm, which includes an observer, does not suffer from the limitations of DMC, but preserves all attractive properties with DMC.

Chapter 6. An ad hoc method for robust tuning of an observer based MPC algorithm is proposed. With this method a μ-controller is first synthesized and then the weights and D-scales (obtained from the μ-synthesis) are used to tune the MPC controller. Only the unconstrained performance of the MPC controller is considered.

The paper also demonstrates severe problems for decentralized control of a distillation column where heat duties in reboiler and condenser are directly manipulated. The decentralized system goes unstable if the pressure control loop is lost, for example due to condenser cooling saturation. The MPC controller handels this saturation without going unstable.

7.3 Directions for Future Work

7.3.1 Tuning of MPC

The tuning procedure presented in chapter 6 is ad hoc but yields reasonably tuned controllers for the problems we have studied.x However, further work on robust tuning of MPC controllers is needed, also for the unconstrained case.

7.3.2 μ synthesis

The controller designs by DK-iteration presented in this thesis (chapters 2, 4 and 6) have demonstarted that the choice of initial D-scales are important. This is not surprising, since DK-iteration is not guaranteed to converge to the optimal solution. However, it shows that it would be useful to have guidelines for how to choose the initial D-scales. The results in this thesis indicates that physically based scaling of inputs and outputs, like in chapter 6, makes $D = I$ a reasonable choice. However, more research could give a better understanding of the importance of the initial D-scales.

Another issue related to the one above is the following: The two uncertainty perturbations $W_i\Delta_U$ and $\Delta_U W_i$ are equivalent from a modelling point of view, but yield different optimal D-scales. Is it possible to say when one of the two alternatives is likely to yield a better result than the other when used for DK-iteration?

7.3.3 Implementation of μ-controller

Practical problems with implementation of μ-optimal controllers should be studied. For example, how do one handle anti-windup?

7.3.4 5×5 control

The study on 5×5 control presented in chapter 6 should be continued. For example, a study where different condensers and reboilers are used (and the heat duties are not directly manipulated variables) would be interesting. The main difference between studying a 5×5 model and a 2×2 model is that in the first case we do not have to assume any pairing and therefore the obtained results are more general, *i.e.* all possible 2×2 cases are coverd. The insights obtained from such a study could be used to determine
1) For what kind of columns is multivariable control substantially better than decentralized control?
2) How much performnce (measured in terms of μ or another measure) is lost when decentralized control is used?
3) What effect does different designs, for example differnt reboilers and condensers, have on controllability?

References

[1] Craig, I.K. (1993). "Robust Controller Specification and Design for a Run-of-Mine Milling Circuit", Ph.D. Thesis, Univ. of the Witwatersrand, Johannesburg, South Africa.

[2] Engstad, P.K. (1991). "Comparison of Robustness Between Different Control Algorithms". *Diploma Thesis*, Dept. of Eningeering Cybernetics, University of Trondheim-NTH, Norway.

[3] Hovd, M., Braatz R.D. and Skogestad S. (1993). "On the structure of the robust optimal controller for a class of problems", *Preprints IFAC World Congress on Automatic Control*, Sydney, Australia.

[4] Laughlin, D.L, Jordan, K.G. and Morari, M. (1986). "Internal Model Control and Process Uncertainty: Mapping Uncertainty Regions for SISO Controller Design", *Int. J. Control*, **44**, 1675-1698.

[5] Laughlin, D.L., Rivera, D.E. and Morari M. (1987). "Smith predictor design for robust performance", *Int. J. Control*, **46**(2), 477-504.

[6] Limebeer, D.J.N. (1991). "The specification and purpose of a controller design case study", *Proc. IEEE Conf. Decision Contr.*, Brighton, England, 1579-1580.

[7] Lundström, P., Skogestad, S. and Wang, Z.-Q. (1991). "Performance weight selection for H-infinity and μ-control methods", *Trans. Inst. MC*, **13**, 5, 241-252.

[8] Skogestad, S., Morari, M. and Doyle, J.C (1988). "Robust Control of Ill-conditioned Plants: High-purity Distillation", *IEEE Trans. Autom. Control*, **33**, 12, 1092-1105. (Also see correction to μ-optimal controller in **34**, 6, 672).